BINDING ACTIVITY OF DUFFY BINDING PROTEIN (PKDBPαII) OF *PLASMODIUM KNOWLESI* CLINICAL ISOLATES FROM PENINSULAR MALAYSIA AND MALAYSIAN BORNEO

LIM KHAI LONE

FACULTY OF MEDICINE
UNIVERSITY OF MALAYA
KUALA LUMPUR

2018

BINDING ACTIVITY OF DUFFY BINDING PROTEIN (PKDBPαII) OF *PLASMODIUM KNOWLESI* CLINICAL ISOLATES FROM PENINSULAR MALAYSIA AND MALAYSIAN BORNEO

LIM KHAI LONE

DISSERTATION SUBMITTED IN FULFILMENT OF THE REQUIREMENTS FOR THE DEGREE OF MASTER OF MEDICAL SCIENCE

FACULTY OF MEDICINE
UNIVERSITY OF MALAYA
KUALA LUMPUR

2018

UNIVERSITY OF MALAYA

ORIGINAL LITERARY WORK DECLARATION

Name of Candidate: **Lim Khai Lone**

Matric No: **MGN 150043**

Name of Degree: **Master of Medical Science**

Title of Project Paper/Research Report/Dissertation/Thesis ("this Work"):

Binding activity of Duffy binding protein (PkDBPαII) of *Plasmodium knowlesi* clinical isolates from Peninsular Malaysia and Malaysian Borneo

Field of Study: **Parasitology**

I do solemnly and sincerely declare that:

(1) I am the sole author/writer of this Work;
(2) This Work is original;
(3) Any use of any work in which copyright exists was done by way of fair dealing and for permitted purposes and any excerpt or extract from, or reference to or reproduction of any copyright work has been disclosed expressly and sufficiently and the title of the Work and its authorship have been acknowledged in this Work;
(4) I do not have any actual knowledge nor do I ought reasonably to know that the making of this work constitutes an infringement of any copyright work;
(5) I hereby assign all and every rights in the copyright to this Work to the University of Malaya ("UM"), who henceforth shall be owner of the copyright in this Work and that any reproduction or use in any form or by any means whatsoever is prohibited without the written consent of UM having been first had and obtained;
(6) I am fully aware that if in the course of making this Work I have infringed any copyright whether intentionally or otherwise, I may be subject to legal action or any other action as may be determined by UM.

Candidate's Signature Date:

Subscribed and solemnly declared before,

Witness's Signature Date:

Name:

Designation:

BINDING ACTIVITY OF DUFFY BINDING PROTEIN (PKDBPαII) OF *PLASMODIUM KNOWLESI* CLINICAL ISOLATES FROM PENINSULAR MALAYSIA AND MALAYSIAN BORNEO

ABSTRACT

The zoonotic *Plasmodium knowlesi* is a major cause of human malaria in Malaysia. This parasite uses the Duffy binding protein (PkDBPαII) to interact with the Duffy antigen receptor for chemokines (DARC) receptor on human and macaque erythrocytes to initiate invasion. Previous studies on *P. knowlesi* have reported distinct Peninsular Malaysia and Malaysian Borneo PkDBPαII haplotypes. Notably, patients with knowlesi malaria in Malaysian Borneo often present with hyperparasitemia and more severe disease compared to patients in Peninsular Malaysia. Therefore, it is our interest to determine the implication of the genetic variation of PkDBPαII from Peninsular Malaysia and Malaysian Borneo on binding activity and affinity to erythrocytes. In this study, the differential binding activity of these haplotypes with human and macaque (*Macaca fascicularis*) erythrocytes was investigated through Erythrocyte-binding assays (rosettes formation assays) and their binding affinities (K_D) were determined using Isothermal Titration Calorimetry (ITC) analysis. The PkDBPαII of Peninsular Malaysia and Malaysian Borneo were expressed on the surface of COS-7 cells and tested with human and monkey erythrocytes, with and without anti-Fy6 (anti-Duffy) monoclonal antibody treatment. Binding activity level was determined by counting the number of rosettes formed between the transfected COS-7 cells and the erythrocytes. Anti-Fy6 treatment was shown to completely block the binding of human erythrocytes with the transfected COS-7 cells, thus verifying the specific binding of human DARC with PkDBPαII. Interestingly, the PkDBPαII of Peninsular Malaysia displayed a higher binding activity with human erythrocytes when compared to the Malaysian Borneo PkDBPαII haplotype (mean number of rosettes formed = 156.89 ± 6.62 and 46.00 ± 3.57, respectively; $P < 0.0001$).

However, no difference in binding activity level was seen in the binding assay using *Macaca fascicularis* erythrocytes. This finding was further supported by ITC, whereby the PkDBPαII of Peninsular Malaysia and Malaysian Borneo were expressed as recombinant proteins using *Escherichia coli* expression system. The expressed PkDBPαII recombinant proteins were affinity purified and refolded back to native state prior to the biomolecular interaction analysis with human erythrocytes. The result showed that the binding affinity of PkDBPαII-Peninsular Malaysia (K_D value = 7.75 μM) was higher than PkDBPαII in Malaysian Borneo (K_D value = 74.1 μM). This study is the first report of phenotypic difference between PkDBPαII haplotypes. The biological implication of this finding is yet to be determined. Therefore, further studies need to be carried out to determine whether this differential binding level is associated with disease severity of knowlesi malaria in humans.

Keywords: *Plasmodium knowlesi*, Malaysia, Duffy binding protein, DARC, ligand-receptor interaction

AKTIVITI PENGIKATAN

PROTEIN PENGIKATAN DUFFY *PLASMODIUM KNOWLESI* (PKDBPαII)

DARIPADA ISOLAT KLINIKAL DI SEMENANJUNG MALAYSIA DAN

BORNEO MALAYSIA

ABSTRAK

Plasmodium knowlesi merupakan punca utama penyakit malaria manusia di Malaysia. Parasit ini memulakan serangan terhadap eritrosit manusia dan kera melalui interaksi antara protein pengikatan Duffy (PkDBPαII) dengan reseptor antigen, Duffy untuk kemokin (DARC). Penyelidikan terhadap *P. knowlesi* sebelum ini telah melaporkan perbezaan antara haplotip PkDBPαII dari Semenanjung Malaysia dan Borneo Malaysia. Kebiasaannya, pesakit malaria knowlesi di Borneo Malaysia sering mendapat simptom hiperparasitemia dan lebih berisiko berbanding pesakit di Semenanjung Malaysia. Oleh itu, kami berminat untuk mengkaji implikasi variasi genetik PkDBPαII dari Semenanjung Malaysia dan Borneo Malaysia terhadap aktiviti pengikatan dan afiniti pengikatan kepada eritrosit. Dalam kajian ini, aktiviti pengikatan haplotip PkDBPαII terhadap eritrosit manusia dan kera *(Macaca fascicularis)* telah dikaji menggunakan kaedah pengikatan eritrosit asai (pembentukan Roset asai) dan pengikatan afiniti (K_D) ditentukan dengan analisis Isoterma Titratan Kalorimetri (ITC). PkDBPαII dari Semenanjung Malaysia dan Borneo Malaysia telah diekspres pada permukaan sel COS-7 dan diuji menggunakan eritrosit manusia dan kera, dirawat dengan anti-Fy6 (anti-Duffy) antibodi monoklon dan juga tanpa rawatan anti-Fy6 (anti-Duffy) antibodi monoklon. Paras aktiviti pengikatan telah dikira sebagai bilangan roset yang terbentuk antara COS-7 (sel yang telah ditransfek) dan eritrosit. Rawatan anti-Fy6 menunjukkan perencatan sepenuhnya terhadap pengikatan eritrosit manusia pada sel COS-7, dengan ini pengikatan oleh DARC manusia bersama rekombinan PkDBPαII adalah spesifik. Selain itu, PkDBPαII dari Semenanjung Malaysia telah menunjukkan aktiviti pengikatan yang lebih tinggi terhadap

eritrosit manusia apabila dibandingkan dengan haplotip PkDBPαII dari Borneo Malaysia (bilangan mean pembentukan roset = 156.89 ± 6.62 and 46.00 ± 3.57, $P < 0.0001$). Akan tetapi, pengikatan asai menggunakan eritrosit *M. fascicularis* tidak menunjukkan perbezaan dalam paras aktiviti pengikatan. Penemuan ini juga disokong oleh ITC, di mana PkDBPαII dari Semenanjung Malaysia dan Borneo Malaysia diekspress sebagai protein rekombinan menggunakan sistem ekspressi *Escherichia coli*. Protein rekombinan PkDBPαII yang diekspress telah melalui penulenan afiniti dan terlipat kepada keadaan asal sebelum analisis biomolekular interaksi terhadap eritrosit manusia. Keputusan telah menunjukkan aktiviti pengikatan afiniti PkDBPαII Semenanjung Malaysia (nilai K_D = 7.75 μM) lebih tinggi daripada PkDBPαII Borneo Malaysia (nilai K_D = 74.1 μM). Penyelidikan ini adalah kajian pertama yang melaporkan perbezaan fenotip antara PkDBPαII haplotip. Implikasi biologi ke atas penyelidikan ini masih belum dikenal pasti. Justeru, kajian yang selanjutnya harus dijalankan untuk menentukan sama ada perbezaan paras pengikatan berkait dengan keparahan penyakit malaria knowlesi terhadap manusia.

Kata kunci: *Plasmodium knowlesi*, Malaysia, Duffy binding protein, DARC, interaksi ligand-reseptor

ACKNOWLEDGEMENTS

After one and a half years of learning and studying, finally, this study is approaching its finish line. This project would never be successfully accomplished without the guidance, support and caring from various people, whom I ought to acknowledge and express my gratitude.

Firstly, I would like to express my deepest gratitude to three impressive supervisors of mine, Professor Dr. Fong Mun Yik, Associate Professor Dr. Lau Yee Ling and Dr. Amirah binti Amir. I am so grateful to have them supporting me, guiding me and helping me throughout this journey. The door to their office was always open whenever I ran into a trouble or difficulty about my research. I sincerely thank you for your guidance, motivation, and trust. Without your encouragement and immerse knowledge in the field, this Master project would be unbelievably difficult to be accomplished.

Besides, I would also like to express my gratitude to members of Department of Parasitology: head of department, department staffs, lecturers, postgraduates and my lab mates for continuous encouragement through the process of researching. I am gratefully indebted to Dr. Cheong Fei Wen, Dr. Jonathan Liew Wee Kent, Dr. Wong Meng Li and Mr. Ng Yit Han, for their valuable ideas and comments on this thesis. Nonetheless, I would also like to acknowledge University Malaya Research Fund Assistance (BKP) grant (BK013-2016) and Ministry of Higher Education FRGS grant (FP036-2015A) for providing me the opportunities and funding for this research.

Finally, I must express my very profound gratitude to my dearest mom (Mdm. Catherine Chong Siew Chin), my guardian (Mr. Chan Dark Wan) and my partner for life (Ms. Winnie Cheah Win Nee) for providing me with unfailing support and continuous encouragement throughout my years of study and through the process of writing this thesis. This accomplishment would not have been possible without them. Thank you.

TABLE OF CONTENTS

LIST OF FIGURES

LIST OF TABLES

LIST OF SYMBOLS AND ABBREVIATIONS

Abbreviation	Indication
%	percent
°C	degree Celsius
et al.	et alia (and others)
µg	microgram
ng	nanogram
mg	milligram
g	gram
µL	microliter
mL	milliliter
L	liter
µM	micromolar
mM	millimolar
M	molar
min	minute
rpm	revolutions per minute
V	volt
s	second
U	Unit
bp	base pair
UV	ultraviolet
in vivo	biological interactions or experiments performed within a living organism.
in vitro	experiment performed in artificial environments which is outside the living organism.

spp.	*species pluralis*
e.g.	*exempli gratia*
PkDBPαII	*Plasmodium knowlesi* Duffy binding protein alpha region II
AcGFP1	green fluorescent protein from *Aequorea coerulescens*
ITC	Isothermal Titration Calorimetry
EBAs	Erythrocyte-binding assays
HAN	clinical isolate Hanafiah
SBH31	clinical isolate Sabah 31
PCR	polymerase chain reaction
dNTPs	deoxyribonucleotide triphosphates
DNA	deoxyribonucleic acid
RE	restriction enzyme
CIAP	calf intestinal alkaline phosphatase
PBS	phosphate buffered saline
DMEM	Dulbecco's modified eagle medium
RPMI 1640	Roswell Park Memorial Institute 1640 medium
FBS	fetal bovine serum
EDTA	ethylenediaminetetraacetic acid
IPTG	isopropyl β-D-1-thiogalactopyranoside
SDS-PAGE	sodium dodecyl sulfate polyacrylamide gel electrophoresis
TEMED	tetramethylethylenediamine
CBB	coomassie brilliant blue
PVDF	polyvinylidene difluoride
BCIP/NBT	5-bromo-4-chloro-3-indolyl phosphate/nitro blue tetrazolium
BSA	bovine serum albumin
MWCO	molecular weight cut-off

LIST OF APPENDICES

CHAPTER 1: INTRODUCTION

Malaria is one of the important parasitic diseases that is responsible for high global morbidity and mortality, especially in Africa, Asia and South and Central America. Nearly half of the world population is at risk of getting infected with malarial parasites. In 2016, 216 million cases of malaria were reported globally, causing nearly 445000 deaths (WHO, 2017b). This mosquito-borne infectious disease is caused by the blood protozoa belonging to the genus *Plasmodium*. Four species, *Plasmodium falciparum*, *Plasmodium vivax, Plasmodium malariae* and *Plasmodium ovale* (now comprises of *P. ovale wallikeri* and *P. ovale curtisi*) are known to cause human malaria (Hay *et al.*, 2004; Sutherland *et al.*, 2010). However, human cases of *Plasmodium knowlesi* (a simian malaria parasite) infection were reported in parts of Southeast Asia and is now acknowledged as the fifth human malaria parasite (Jongwutiwes *et al.*, 2004; Cox-Singh & Singh, 2008; Luchavez *et al.*, 2008; White, 2008; Bronner *et al.*, 2009; Galinski & Barnwell, 2009; Jiang *et al.*, 2010; Jeslyn *et al.*, 2011; Jongwutiwes *et al.*, 2011; Khim *et al.*, 2011; WHO, 2011). *Plasmodium knowlesi* has a unique 24 h erythrocytic cycle which is the shortest among other human *Plasmodium* species, and therefore capable of causing severe complications due to hyperparasitemia and even death if untreated (Daneshvar *et al.*, 2009). Currently, knowlesi malaria is the most common cause of human malaria in Malaysia especially in Malaysian Borneo (Singh & Daneshvar, 2010; Barber *et al.*, 2011; WHO, 2011; Yusof *et al.*, 2014; Ooi *et al.*, 2017; Rahim *et al.*, 2017).

The invasion of *Plasmodium* merozoites into erythrocytes is a multi-step process which involves initial attachment of the merozoite, reorientation of apical end, tight-junction formation and entry of whole merozoite into a parasitophorous vacuole (Dvorak *et al.*, 1975; Aikawa *et al.*, 1978). These complex processes are mediated by specific interaction between the parasite's ligand and its corresponding receptor on the surface

membrane of erythrocyte (Cowman & Crabb, 2006). Erythrocytes expressing Duffy antigen receptor for chemokines (DARC) are also known as Duffy-positive human erythrocytes, and they are known to be susceptible to invasion by merozoites of *P. vivax* and *P. knowlesi*. During merozoite invasion, *P. vivax* Duffy binding protein (PvDBP) binds to the DARC on the surface of erythrocyte (Miller *et al.*, 1975; Miller *et al.*, 1976; Mason *et al.*, 1977). *Plasmodium knowlesi* has three major erythrocyte binding proteins which are homologous to PvDBP, known as the α, β, and γ proteins. Among the three proteins, only the α protein has been shown to bind Duffy-positive human and macaque erythrocytes, thus is more specifically known as *P. knowlesi* Duffy binding protein (PkDBPα) (Adams *et al.*, 1992; Chitnis & Miller, 1994; Singh *et al.*, 2002; Singh *et al.*, 2003; Singh *et al.*, 2006; Fong *et al.*, 2014). These are large proteins and can be further divided into seven regions (I-VII) (Chitnis & Miller, 1994). Region II of *P. knowlesi* α protein (PkDBPαII) contains cysteine-rich Duffy binding-like (DBL) domain that is crucial for binding to human DARC (Chitnis & Miller, 1994; Sim *et al.*, 1994; Singh *et al.*, 2002; Singh *et al.*, 2003). Whereas, region II of *P. knowlesi* β and γ proteins, bind only to macaque erythrocytes via the Duffy-independent pathway (Adams *et al.*, 1992; Chitnis & Miller, 1994). From previous studies, it was noticed that the PkDBPαII preferentially bound to Duffy-positive Fy(a–b+) human erythrocytes compared to Duffy-positive Fy(a+b–), and the exact reason for this is still unknown (Mason *et al.*, 1977; Haynes *et al.*, 1988; Chitnis & Miller, 1994; Chitnis *et al.*, 1996; King *et al.*, 2011).

Although knowlesi malaria is seen in both Peninsular Malaysia and Malaysian Borneo, cases of severe knowlesi infection with hyperparasitemia were frequently reported in Malaysian Borneo (Cox-Singh *et al.*, 2008; Daneshvar *et al.*, 2009; Cox-Singh *et al.*, 2010; Singh & Daneshvar, 2010; William *et al.*, 2011; Fatih *et al.*, 2012; Rajahram *et al.*, 2012; Barber *et al.*, 2013a; William *et al.*, 2014). A recent study performed on the PkDBPαII has shown that there are distinct genetic differences between the PkDBPαII of

P. knowlesi clinical isolates from Peninsular Malaysia and Malaysian Borneo (Fong *et al.*, 2014; Fong *et al.*, 2015). Two distinct haplotypes were identified in Peninsular Malaysia and Malaysian Borneo, which are haplotype H2 and H47 respectively. Since PkDBPαII is the crucial protein for the invasion of *P. knowlesi* merozoite into human erythrocytes, mutation in the functional regions of the protein may influence its ability as a competent ligand to DARC of human erythrocytes. As for now, studies on the binding specificity of PkDBPαII have been well characterized but comparative studies on the binding activity of PkDBPαII haplotypes are lacking at the moment. Therefore, it is interesting to find out whether these haplotypic differences in PkDBPαII reveal disparity in term of binding activity or affinity to human erythrocytes. This study is important to be carried out in order to provide insights into the pathogenesis of *P. knowlesi* in humans.

Objectives of this research are as follows:

1. To generate recombinant PkDBPαII from clinical isolates of Peninsular Malaysia and Malaysian Borneo in mammalian and prokaryotic expression systems.
2. To investigate and compare the binding activity and affinity of Peninsular Malaysia and Malaysian Borneo PkDBPαII to human and macaque (*Macaca fascicularis*) erythrocytes

CHAPTER 2: LITERATURE REVIEW

2.1 Malaria

Malaria is a mosquito-borne disease caused by protozoan parasites of the genus *Plasmodium* that infects over hundreds of animal species such as reptiles, birds and various mammals (Garnham, 1966). To date, a total of 6 *Plasmodium* species are acknowledged and known for human malaria transmission, namely *Plasmodium falciparum, P. ovale wallikeri, P. ovale curtisi, P. malariae, P. vivax* and *P. knowlesi*. Malaria patient often presents with symptoms such as fever paroxysm, nausea, shivering and sweats as a result of repeated rounds of invasion and multiplication by the parasite in the host's erythrocytes. If the disease prolongs without immediate medical attention, the patient may develop severe complication with serious organ failures and eventually death. In the recently released World Malaria Report 2017, a total of 91 countries and areas have ongoing malaria transmission with approximately 216 million cases, resulting in 445000 deaths (WHO, 2017b). In 2016, the African region has accounted for the highest malaria cases (90%), followed by Southeast Asia region (7%) and Eastern Mediterranean region (2%). Since 2010, the incidence rate of malaria has declined by 18% globally. Among other regions, the Southeast Asia region has the highest reduction (48%) followed by America region (22%), African region (20%) and Western Pacific Region (12%) (WHO, 2017b). Although a decline in the incidence rates of malaria globally was seen, the mortality rates of malaria remained virtually unchanged in the regions of Southeast, Western Pacific, and Africa. Between 2015 and 2016, 18 countries were reported to have attained zero indigenous cases for 3 years or more, and only 6 of the 18 countries were certified as free of malaria by WHO (WHO, 2017b). Despite this progress, challenges in malaria control and elimination remain. Until now, there are no effective vaccines available for malaria and it contributes to poverty in countries like Africa due to the cost

of illness and treatment of at least US$12 billion per annum (WHO, 2017a). On top of that, the emergence of zoonotic malaria species, such as *P. knowlesi* in the Southeast Asia countries, poses an additional challenge towards malaria elimination.

2.2 Life cycle of *Plasmodium* spp.

The life cycle of a *Plasmodium* parasite in human (Figure 2.1) begins when a *Plasmodium*-infected female *Anopheles* mosquito injects sporozoites into the human host during a blood meal (Garnham, 1966). These are transported by the blood circulatory system to the liver. In the liver, the parasites invade the hepatocytes, undergo asexual multiplication (exo-erythrocytic cycle) and mature into schizonts (Meibalan & Marti, 2017). These mature hepatic schizonts will then rupture and release merozoites that infect erythrocytes in the bloodstream to continue their development in the erythrocytic cycle. During this erythrocytic cycle, the merozoite develops into trophozoites and mature to form schizonts containing numerous merozoites. Upon maturation, the schizont ruptures, releasing invasive merozoites to infect new erythrocytes, thus completing the erythrocytic cycle.

Some of the merozoites undergo gametogenesis in erythrocytes and differentiate into microgametocytes (male) and macrogametocytes (female). These gametocytes are then taken up by the female *Anopheles* mosquito during a blood meal. In the mosquito, microgamete and macrogamete fuse to form a zygote. Within a day, the zygote differentiates into an ookinete, which penetrates the midgut wall and further develops into an oocyst containing thousands of sporozoites. Upon maturation, sporozoites will be released from the oocyst, where they will migrate and invade salivary glands. During the next blood meal, the infected female *Anopheles* mosquito inoculates the sporozoites into another human host, thereby repeating the life cycle of *Plasmodium* parasite.

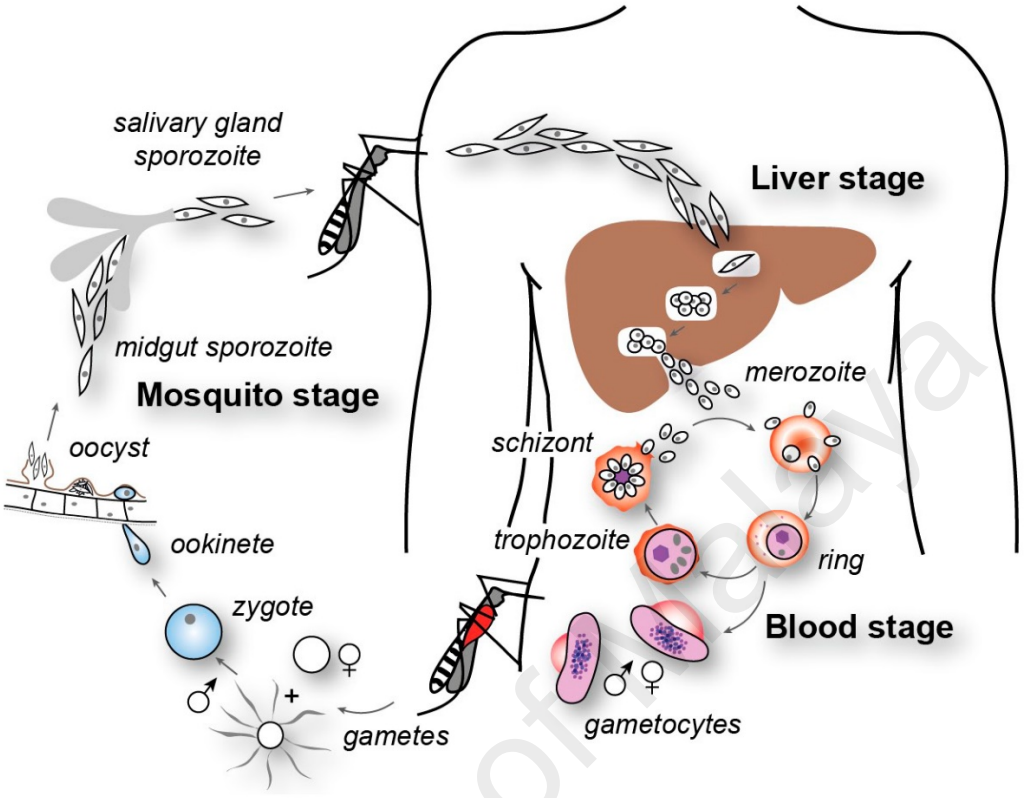

Figure 2.1: Life cycle of *Plasmodium* spp. The asexual cycle of *Plasmodium* sp. begins with the entry of the sporozoites into human host via the bite of an infected female *Anopheles* mosquito. These sporozoites invade hepatocytes, in which they develop to produce merozoites that are released into the bloodstream. These invasive merozoites invade erythrocytes, develop into trophozoites, then into schizonts. When these mature schizonts rupture, more merozoites are released that will further invade new erythrocytes. The sexual cycle begins when the gametocytes (microgametocytes and macrogametocytes) are taken up by a feeding mosquito into its gut. From there, the gametocytes mature to form gametes and then fertilized to form a zygote. The zygote develops into an ookinete and then into oocyst containing numerous sporozoites. Rupture of oocyst releases sporozoites that migrate to the salivary glands of the mosquito. The life cycle starts anew when the mosquito bites another human host and inoculates sporozoites during a blood meal. Adapted from Cowman *et al.* (2012).

Clinical manifestation of malaria is usually associated with the development of blood stage parasites. Therefore, during their liver stage development, it is hard to diagnose whether a person is in fact infected with malaria parasite. In *P. vivax* and *P. ovale* infections, patients who have recovered from previous malaria infection may suffer several additional relapses. These relapses occur because *P. vivax* and *P. ovale* have a dormant liver stage (hypnozoites) that may be reactivated leading to blood stage infection. The duration of the erythrocytic cycle varies among *Plasmodium* species. *Plasmodium knowlesi* has a quotidian cycle (approximately 24 h), and *P. falciparum*, *P. vivax*, and *P. ovale* have tertian cycles (approximately 48 h). *Plasmodium malariae* has a quartan cycle (approximately 72 h) (Garnham, 1966).

2.3 Clinical symptoms and signs of malaria

In general, the clinical manifestations and severity of malaria depend on the infecting *Plasmodium* species, human host's genetics, immune status, previous exposure to malarial infection and prophylactic status of the individual (Boström *et al.*, 2012). Symptoms in humans are often non-specific such as high fever, headache, chills, cough, abdominal pain, anemia, nausea, diarrhea, vomiting and profuse sweating (Singh *et al.*, 2004; Bronner *et al.*, 2009; WHO, 2017a). Symptoms of malaria typically begin with a period of shivering, chills and are accompanied by high fever. The febrile paroxysm occurs during the lysis of parasitized erythrocytes and release of merozoites into the bloodstream at the completion of each erythrocytic cycle (Schumacher & Spinelli, 2012). The fever pattern represents the time required for the development and completion of each erythrocytic cycle, from invasion into the erythrocyte to the release of new merozoites. Common signs and laboratory findings in malaria infection often include jaundice, pallor, thrombocytopenia, anemia, hepatosplenomegaly, elevated total bilirubin, and aminotransferase level (Daneshvar *et al.*, 2009; Barber *et al.*, 2012).

In general, the severity of malaria disease and risk of death increase with high parasite counts (parasitemia). *Plasmodium falciparum* is the most pathogenic species since it can infect all types of erythrocyte and is capable of causing intense parasitemia of 60% or more (Schumacher & Spinelli, 2012). In contrast, an infection caused by other human *Plasmodium* species usually have lower parasitemia of 2% or less; with the reason being *P. vivax* and *P. ovale* show preference to infect reticulocytes and *P. malariae* infects mostly senescent or aging normocytes. However, severe malaria infection and fatalities have been observed in the case of *P. knowlesi* infection (Cox-Singh *et al.*, 2008; Cox-Singh *et al.*, 2010; William *et al.*, 2011; Willmann *et al.*, 2012). *Plasmodium knowlesi* has a short erythrocytic cycle of 24 h, therefore it is capable of causing hyperparasitemia in short period of time which may lead to severe malaria complications (e.g. kidney failure, abnormal liver function, and acute respiratory distress) and even deaths (Bronner *et al.*, 2009). A retrospective study in Sabah, Malaysia, found that approximately 22% of malaria incidences were severe knowlesi infection (William *et al.*, 2011).

2.4 Treatment of malaria

Many factors have to be considered when treating a patient with antimalarial drugs and these include the clinical status of the patient, species of the infecting parasite, pregnancy status, area where the infection takes place and the drug-resistance status of the parasite. Malaria is a potentially lethal disease especially in the cases of *P. falciparum* and *P. knowlesi* infections, thus, effective treatment should be initiated as soon as possible. Most drugs used in malaria treatment are effective against the blood stage parasite (merozoites, trophozoites, and schizonts) and these include chloroquine, artemether-lumefantrine, mefloquine, doxycycline, artesunate, atovaquone-proguanil and quinine. Primaquine must be given in *P. vivax* and *P. ovale* infection to prevent relapse as it is effective against hypnozoite stage of these parasites. Despite its effectiveness, primaquine is

contraindicated in pregnancy. Similarly, lower dose over a long period of time is highly recommended for G6PD (glucose-6-phosphate dehydrogenase) deficient patient.

2.5 Diagnosis of malaria

Malaria diagnosis relies on microscopy examination of Giemsa stained thick and thin blood smears. Microscopic examination of blood smears is still acknowledged as the gold standard diagnostic method for human malaria. The infecting *Plasmodium* species can be detected and identified by examining and comparing the morphological characteristics of each species under light microscopy. However, *P. knowlesi* can be misdiagnosed as *P. falciparum* and *P. malariae* infection due to their morphological similarities. *Plasmodium knowlesi* resembles *P. falciparum* in its early trophozoite stage as they both appear as ring forms with double chromatin dots, multiple-infected erythrocytes and appliqué form in the infected erythrocyte (Coatney *et al.*, 1971; Lee *et al.*, 2009b). Whereas, the late trophozoites stage, schizonts, and gametocytes of *P. knowlesi* are generally indistinguishable from *P. malariae*. Most remarkably, the elongated trophozoites (band-form) which is the unique morphological feature of *P. malariae* is also seen in the blood smears of *P. knowlesi* under microscopy examination (Lee *et al.*, 2009b; Figtree *et al.*, 2010; Lee *et al.*, 2013). Therefore, laboratory misdiagnosis of knowlesi infection as malariae or falciparum by microscopy is likely, and may lead to underestimation of the incidence of knowlesi infection especially in endemic countries (Singh *et al.*, 2004; Barber *et al.*, 2013b). Additionally, patients with *P. knowlesi* infections can be symptomatic at low parasitemia and even remain undetectable with thick film microscopy inspection (Daneshvar *et al.*, 2009). Therefore, diagnosis with only microscopic examination will limit the accuracy for identifying the infecting *Plasmodium* species.

Another technique for laboratory diagnosis of malaria is the rapid diagnostic immunochromatographic test (RDT), which utilizes antibodies for the detection of malaria antigens. This detection method is much simpler and is a useful alternative to microscopy in circumstances where the reliable microscopic diagnosis is not available. Unfortunately, RDTs such as BinaxNOW Malaria, Entebe Malaria Cassette (MC), First Response Malaria (HRP2) and OptiMAL-IT have failed to detect *P. knowlesi* infection. Most of these RDTs can only differentiate between non-falciparum and *P. falciparum* infection (McCutchan *et al.*, 2008; Kawai *et al.*, 2009; van Hellemond *et al.*, 2009; Wilson, 2012; Tanizaki *et al.*, 2013; Daniels *et al.*, 2017). Thus, commercial RDTs for malaria diagnosis should be used with great caution, particularly in the suspected case of *P. knowlesi* infection.

Identification of *P. knowlesi* infection using microscopy or RDTs alone can be challenging due to morphological similarities and cross-reactivity. As alternatives, various molecular detection methods have been developed to provide more reliable and accurate results. These include nested polymerase chain reaction (PCR), real-time PCR and loop-mediated isothermal amplification (LAMP) assays (Singh *et al.*, 2004; Wang *et al.*, 2014; Lau *et al.*, 2016). Nested PCR is recognized as the molecular gold standard in malaria diagnosis (Jeremiah *et al.*, 2014). Thus, nested PCR targeting the 18s small subunit ribosomal RNA (SSU rRNA) gene in *Plasmodium* species is extensively used in many studies (Singh *et al.*, 2004; Vythilingam *et al.*, 2008; Yusof *et al.*, 2014). Diagnosis using PCR-based techniques have several advantages over microscopy and RDTs as they are highly sensitive and specific particularly in cases with low parasitemia or mixed infections (Snounou *et al.*, 1993; Kimura *et al.*, 1997; Kain *et al.*, 1998; Zakeri *et al.*, 2010; Sri *et al.*, 2015; Yentur *et al.*, 2016). Nonetheless, PCR has its drawbacks because the procedures are often complicated, time consuming, laborious and require high-

precision thermal cycler which can be expensive for many poor endemic countries for routine diagnosis (Singh *et al.*, 2004).

2.6 *Plasmodium knowlesi*

Plasmodium knowlesi is found naturally throughout Southeast Asia and causes malaria in long-tailed (*Macaca fascicularis*) and the pig-tailed (*Macaca nemestrina*) macaques. Naturally acquired *P. knowlesi* infection in humans was believed to be rare until the discovery of a high number of knowlesi infection in the human population of Sarawak, Malaysian Borneo (Singh *et al.*, 2004; Barber *et al.*, 2017). This zoonotic malaria has a 24-hour replication cycle; hence, it multiplies rapidly and may progress from an uncomplicated infection to a severe infection and even death if left untreated.

It was first described in 1931 in a long-tailed macaque (*M. fascicularis*), and later in pig-tailed (*M. nemestrina*) macaques and the mitred leaf monkey (*Presbytis melalophos*) (Coatney *et al.*, 2003). Experimentally, *P. knowlesi* is also capable of infecting the rhesus macaque (*Macaca mulatta*), producing a fulminating infection. In 1932, Knowles and Das Gupta described the erythrocytic stages of *P. knowlesi* and for the first time, they demonstrated that it could be transmitted to human (Knowles & Gupta, 1932; Napier & Campbell, 1932). Later in 1933, Sinton and Mulligan confirmed that the parasite which Knowles and Das Gupta described was actually a new species, and named the parasite as *P. knowlesi* in honor of Knowles (Sinton & Mulligan, 1933). In the early 1930s, *P. knowlesi* infection was initially considered to be less virulent and therefore preferred over *P. vivax* as a pyretic agent for the treatment of neurosyphilis (Wagner-Jauregg, 1918; Van Rooyen & Pile, 1935). However, this practice was discontinued as a result of severe complications and deaths (Coatney *et al.*, 1971).

Although *P. knowlesi* has been shown to be capable of infecting human via blood passage in the early 1930s, there was no record of natural case of *P. knowlesi* infection in

humans, at least not until 1965, where an American traveler acquired the infection while working in the Peninsular Malaysia (Chin *et al.*, 1965). This was followed by another suspected case of naturally acquired *P. knowlesi* infection in Peninsular Malaysia in 1971 (Fong *et al.*, 1971). In 2004, a large focus of naturally acquired *P. knowlesi* infection in humans was documented in Malaysian Borneo (Singh *et al.*, 2004). Due to negative result from PCR assays of microscopy-confirmed cases of *P. malariae*, Singh and his team were driven to investigate these cases in the Kapit Division of Sarawak (Singh *et al.*, 2004). By developing *P. knowlesi*-specific PCR primers, they discovered that *P. knowlesi* is responsible for a total of 120 out of 208 malaria cases at Kapit Hospital, out of which 112 were identified as single *P. knowlesi* infections and 8 were mixed infections of *P. knowlesi* with other human *Plasmodium* species (Singh *et al.*, 2004; Singh & Daneshvar, 2013). Since this finding, many reports of human knowlesi malaria have been documented and it was later discovered that *P. knowlesi* have been around to cause malaria in humans since 1996 (Lee *et al.*, 2009a).

On its own, *P. knowlesi* accounts for up to 70% of malaria cases in Malaysia Borneo (Daneshvar *et al.*, 2009). Since 2012, *P. knowlesi* surpasses *P. vivax* as the primary causative agent of human malaria in Malaysia (Figure 2.2), and contributed 69% of total reported cases in the year 2016 alone (William *et al.*, 2013; William & Menon, 2014; Yusof *et al.*, 2014; Abeyasinghe, 2017; Barber *et al.*, 2017). Currently *P. knowlesi* infection has been reported from all countries in Southeast Asia except Laos (Jongwutiwes *et al.*, 2004; Zhu *et al.*, 2006; Cox-Singh *et al.*, 2008; Luchavez *et al.*, 2008; Vythilingam *et al.*, 2008; Eede *et al.*, 2009; Sulistyaningsih *et al.*, 2010; Khim *et al.*, 2011).

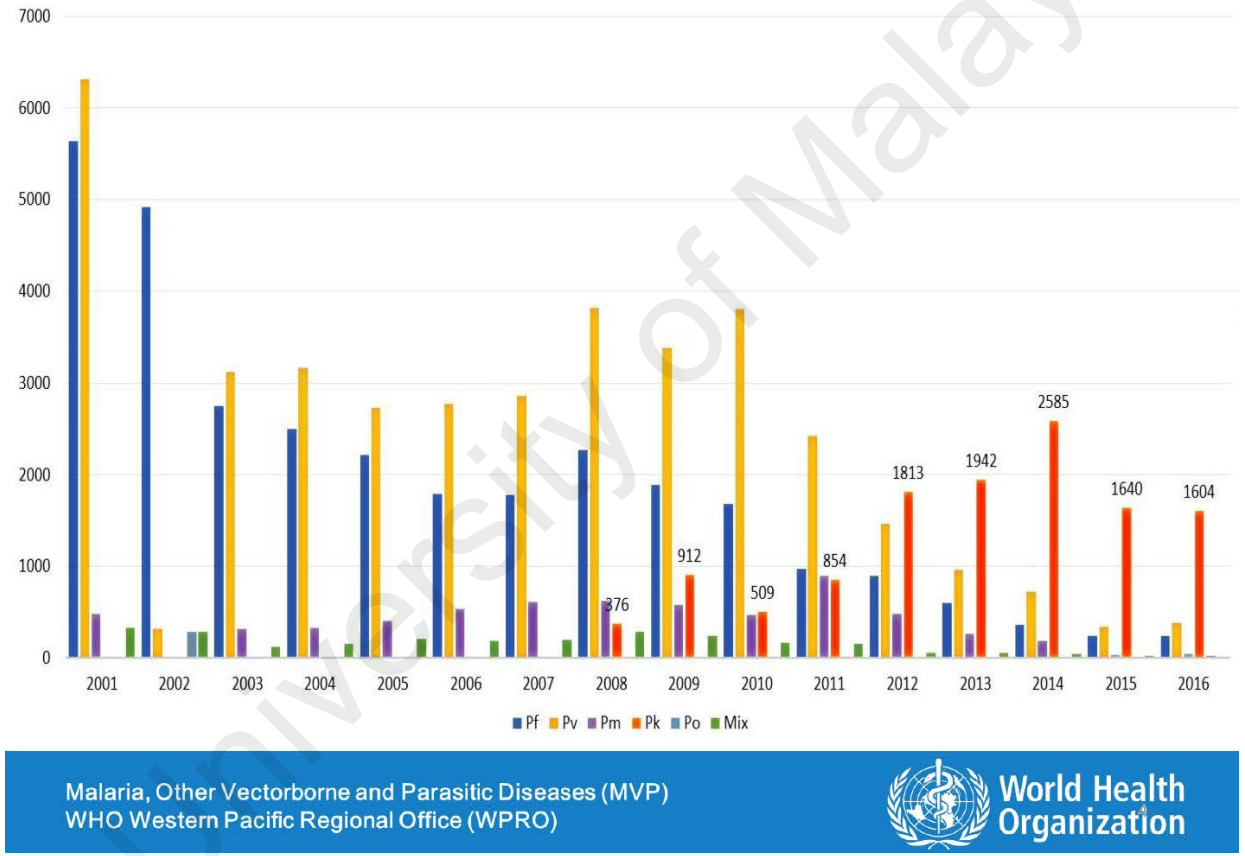

Figure 2.2: Distribution of malaria cases by species in Malaysia from 2001 – 2016. Figure legend: "Pf", "Pv", "Pm", "Pk", "Po" and "Mix" represent *P. falciparum*, *P. vivax*, *P. malariae*, *P. knowlesi*, *P. ovale* and mixed infections, respectively. Adapted from Abeyasinghe (2017).

2.7 Invasion of erythrocytes by *P. knowlesi*

Invasion of erythrocyte by *P. knowlesi* begins with recognition and penetration of the host red blood cell (RBC) by the merozoite. The invasion process is accomplished in four main steps (Figure 2.3): (A) initial attachment, (B) apical reorientation, (C – D) tight-junction formation, and (E) entry of parasite (Dvorak *et al.*, 1975).

The initial interaction or attachment between a free merozoite and erythrocyte is a crucial step for the parasite to recognize erythrocyte competence for invasion. This recognition is often reversible and with low affinity (Cowman & Crabb, 2006). Since the primary interaction occurs by random collision, the apical end of a merozoite would also be in a random orientation. To ensure a closer interaction with the erythrocyte, a reorientation event occurs to juxtapose the apical end of the merozoite with the erythrocyte membrane. As for the entry of the parasite, a tight-junction is formed between the membrane of the merozoite and erythrocyte. This process is powered by the parasite actin-myosin motor and this enhances the penetration into the erythrocyte membrane forming parasitophorous vacuole (Keeley & Soldati, 2004). The parasitophorous vacuole is a protective vacuole that isolates the parasite from the host-cell cytoplasm, forming an ideal environment for the parasite development.

2.7.1 Host cell recognition by *P. knowlesi*

In normal peripheral blood, there are two principal erythrocyte populations, the reticulocytes (premature RBC) which represent less than 1% of the erythrocyte population and the normocyte (mature RBC). Different *Plasmodium* species have been shown to have distinct preferences over the erythrocyte type they invade. This can be clearly seen in the case of *P. vivax* which invades only reticulocytes that are Duffy-positive. *Plasmodium knowlesi* was known to invade normocytes but recently it was found that it may have a slight preference for reticulocytes as well

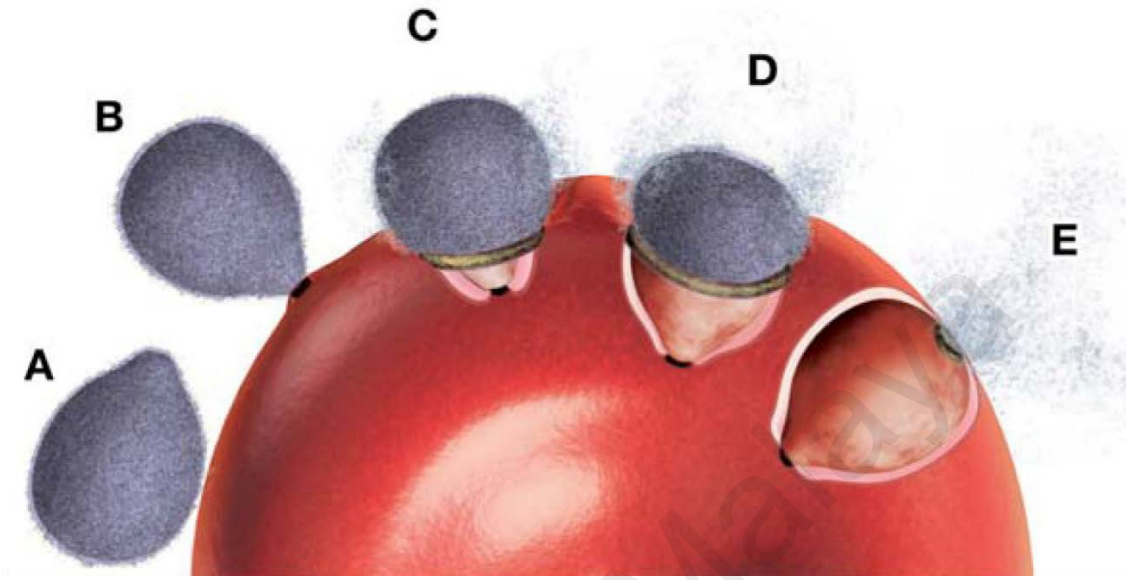

Figure 2.3: Merozoite invasion of erythrocyte. (A) Initial attachment by random collision at a low affinity level to the surface receptor; (B) Reorientation and tight-junction formation involving high affinity ligand-receptor interactions. (C and D) This tight junction then moves the whole parasite from the apical to posterior pole powered by the merozoite's actin-myosin motor. (E) Entry of the whole parasite by creating a parasitophorous vacuole. Adapted from Cowman and Crabb (2006).

(Hegner, 1938; Galinski *et al.*, 1992; Moon *et al.*, 2013). Two *Plasmodium* protein families, the erythrocyte binding-like (EBP) and the reticulocyte binding-like (RBP) protein families interact with specific surface receptors of erythrocyte in order to initiate apical attachment following reorientation (Paul *et al.*, 2015). The invasion ligands from these protein families are conserved among *Plasmodium* species. The EBP family containing Duffy binding-like (DBL) domains for receptor binding, includes the *P. falciparum* EBA-175 (where EBA stands for erythrocyte-binding protein), *P. vivax* Duffy binding protein (PvDBP), *P. knowlesi* Duffy binding protein (previously known as α protein) and *P. knowlesi* β and γ proteins (Gunalan *et al.*, 2013). Unlike the DBPs from *P. vivax* and *P. knowlesi*, the *P. falciparum* EBA-175 targets the sialic acid residues on human erythrocytes glycophorin A for invasion (Miller *et al.*, 2002). The selective recognition of the reticulocyte subpopulation for invasion by *P. vivax* is mediated by BL homologues, reticulocyte-binding protein (RBP)-1 and RBP-2 (Galinski *et al.*, 1992; Gaur *et al.*, 2004; Li & Han, 2012). Two novel *P. knowlesi* RBLs, normocyte-binding protein Xa and Xb (PkNBPXa and PkNBPXb, respectively) are highly expressed in mature schizonts and localized in the micronemes (Gunalan *et al.*, 2013). Interestingly, a recent study has shown that PkNBPXa bind to both human and macaque erythrocytes and the binding is independent of Duffy blood group system (Semenya *et al.*, 2012). Whereas PkNBPXb only exhibits specific adhesion to macaque but not to human erythrocytes (Meyer *et al.*, 2009).

2.7.2 *Plasmodium knowlesi* Duffy binding protein (PkDBP)

Plasmodium knowlesi Duffy binding protein (PkDBP) is a parasite adhesin that localized in the micronemes of late schizonts and free merozoites (Adams *et al.*, 1990). The PkDBP exist in three forms: the α, β and γ proteins. Until recently, the *P. knowlesi* α protein is designated as PkDBPα for its ability to bind Duffy-positive erythrocytes

(Adams *et al.*, 1992; Fong *et al.*, 2014; Fong *et al.*, 2015). The invasion of *P. knowlesi* to human erythrocytes is dependent on the interaction of PkDBPα to Duffy antigen/receptor for chemokines (DARC) (Figure 2.4) (Dvorak *et al.*, 1975; Miller *et al.*, 1975; Miller *et al.*, 1976; Hadley & Peiper, 1997). PkDBPα is divided into seven regions (I-VII), whereby the N-terminal cysteine rich region II (PkDBPαII) contains the Duffy-binding-like (DBL) domains for binding to the DARC on the erythrocytes (Adams *et al.*, 1992; Chitnis *et al.*, 1996; Fong *et al.*, 2015). Besides being able to bind Duffy-positive human erythrocytes, PkDBPαII can also bind to Duffy-positive macaque erythrocytes. In contrast, the region II of the *P. knowlesi* β and γ proteins have different binding specificities where they bind to alternative receptors on macaque erythrocytes and may mediate invasion by Duffy-independent pathways (Mason *et al.*, 1977; Miller *et al.*, 1977; Adams *et al.*, 1992; Chitnis & Miller, 1994; Ranjan & Chitnis, 1999; Gaur *et al.*, 2004).

The PkDBPαII is a 35 kDa (approximately 338 amino acid residues) segment with 12 conserved cysteine residues, which has been identified as the binding site to the cellular domain of human DARC (Singh *et al.*, 2003). Within this region, surface-exposed contact residues Tyr 94, Asn 95, Lys 96, Arg 103, Leu 168 and Ile 175 were identified as the vital residues for Duffy recognition on human erythrocytes. Site-directed mutagenesis on these residues has been proven to disrupt the PvDBP-DARC or PkDBPαII-DARC interaction (Singh *et al.*, 2006). Apart from that, sulfated Tyr 41 in the binding site of DARC has also been proven to be critical for interaction of PvDBP and PkDBP (Choe *et al.*, 2005).

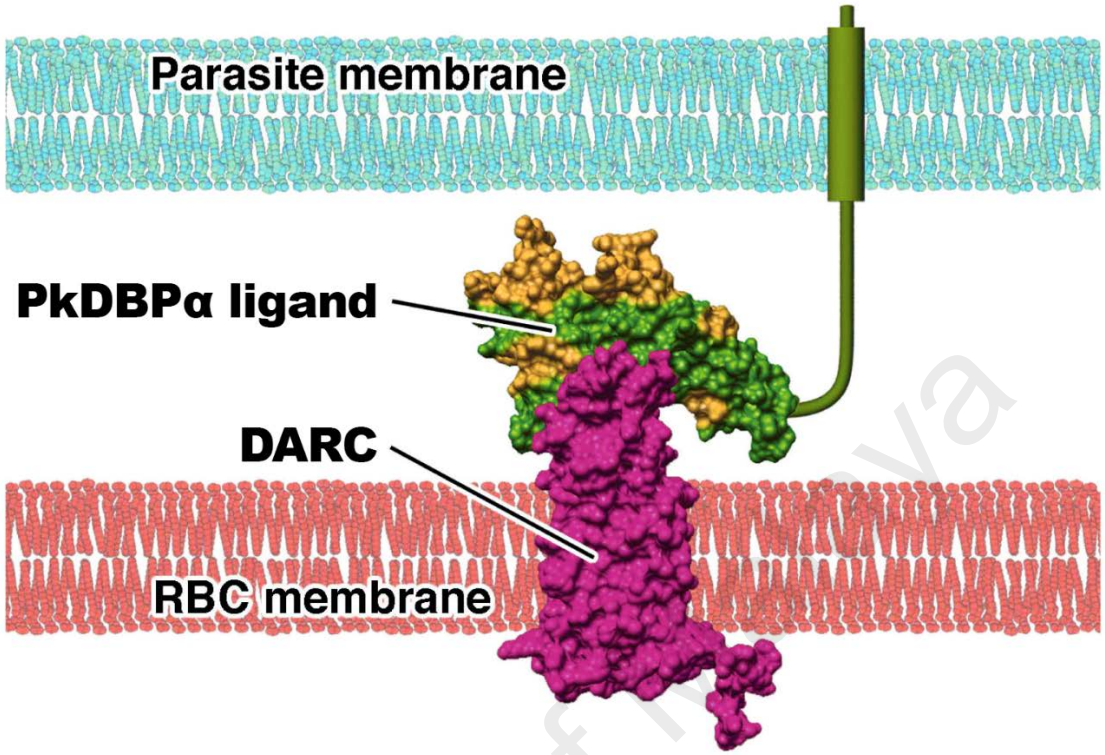

Figure 2.4: Illustration of the interaction between the parasite's ligand (PkDBPα) and the erythrocyte receptor (DARC). Modified from Beeson and Crabb (2007).

2.8 Duffy blood group system (Duffy antigen/receptor for chemokines)

The Duffy blood group system or Duffy antigen/receptor for chemokines (DARC) was named after the discovery of a new antibody, anti-Fy^a, found in the sera of multiply transfused hemophiliac patient and the anti-Fy^b antibody was discovered shortly thereafter (Cutbush *et al.*, 1950; Ikin *et al.*, 1951). The two principal Duffy antigens, Fy^a and Fy^b are encoded by the codominant alleles *FY*A* and *FY*B*. These alleles differ by a single nucleotide polymorphism (SNP) that produces a single amino acid change (Gly42Asp) (Figure 2.5 B) (Cutbush & Mollison, 1950; Blancher *et al.*, 1997; Sellami *et al.*, 2008; Meny, 2010). Four common phenotypes have been identified in the Duffy blood group system: Fy(a+b+), Fy(a+b–), Fy(a–b+) and Fy(a–b–) (Marsh & Schmidt, 1975). Other Duffy antigens such Fy3, Fy4 and Fy5 are also present. However, antisera against these antigens are considerably rare. Until 1987, a murine monoclonal antibody anti-Fy6 is available to define a new Duffy antigen, the Fy6 antigen, which is presents in all human erythrocytes except individuals with Duffy-negative Fy(a–b–) phenotype (Nichols *et al.*, 1987; Riwom *et al.*, 1994).

The DARC is a transmembrane glycoprotein with 336 amino acid residues consisting of a glycosylated N-terminal region (Donahue *et al.*, 1968; Hadley *et al.*, 1984; Chaudhuri *et al.*, 1993; Iwamoto *et al.*, 1996; Tournamille *et al.*, 2003). The seven-transmembrane protein (Figure 2.6) is encoded by the *Fy* gene consisting of four major alleles that give rise to various phenotypes (Chaudhuri *et al.*, 1989; Neote *et al.*, 1994). Aside from the two codominant alleles, *FY*Fy* is the third allele (Figure 2.5 A) which causes no expression of DARC at the erythroid cells and gives rise to the Duffy-negative phenotype Fy(a–b–) erythrocytes. The Duffy-negative phenotype is commonly found among Africans and it is rare in other populations (Race & Sanger, 1980). Initially, this silent allele was detected in a normal *FY*B* allele with a single nucleotide polymorphism (T46C) in the GATA promoter region, which in turn abolishes the full expression

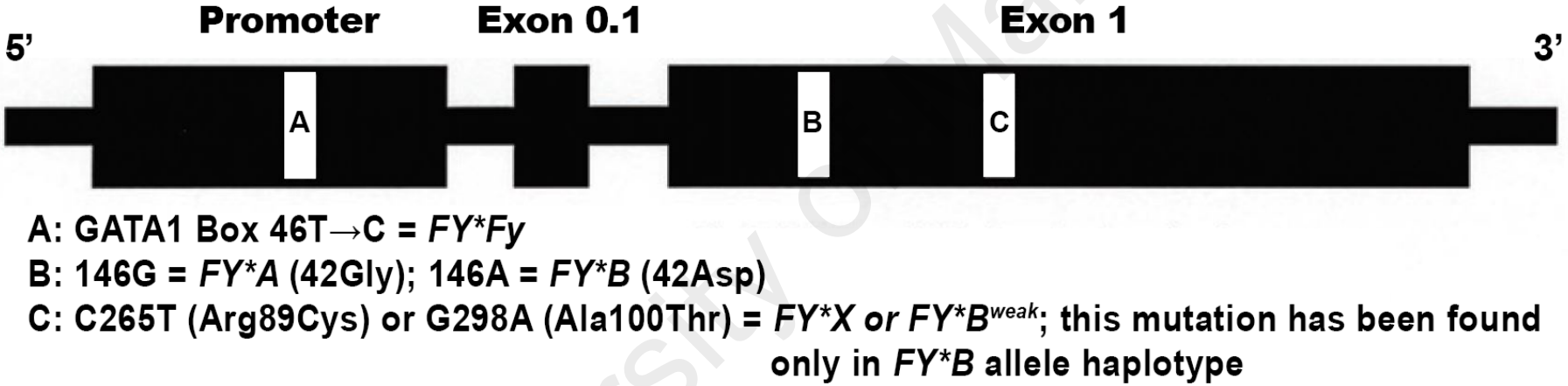

Figure 2.5: Duffy blood group gene structure. (A) Single nucleotide polymorphism (SNP) in the GATA promoter region which abolishes expression of DARC in erythroid cells. (B) Fy^a/Fy^b antigen polymorphism in DARC. (C) The two mutations in the *FY*B* allele that causes amino acid change which is responsible for the $Fy^{b\ weak}$ phenotype or weak expression of Fy^b antigen. Modified from Sellami *et al.* (2008).

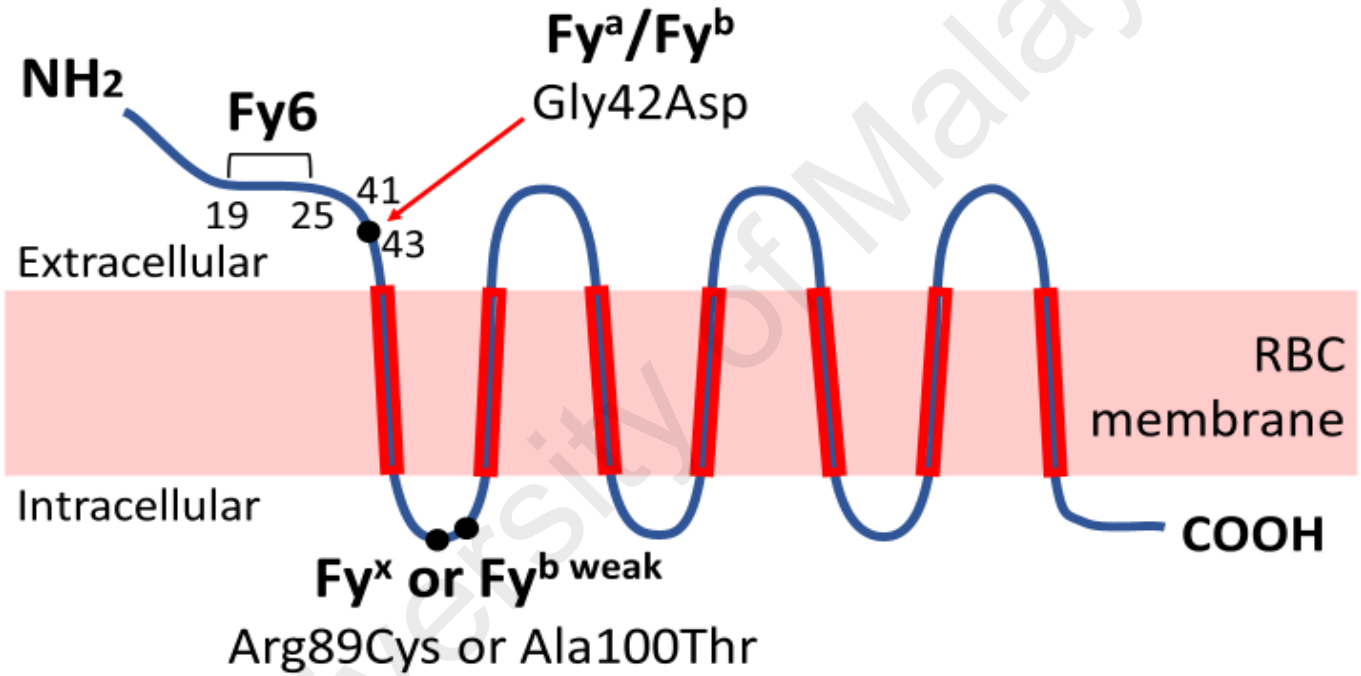

Figure 2.6: The illustration of the Duffy glycoprotein seven-transmembrane domain structure (indicated in red color) and the amino acid changes responsible for the Fy^a/Fy^b and $Fy^{b\ weak}$ polymorphism. Modified from Meny (2010).

of DARC in erythroid but not in nonerythroid cells (Chaudhuri *et al.*, 1995; Tournamille *et al.*, 1995; Iwamoto *et al.*, 1996). Later, the same point mutation was also identified in *FY*A* allele which gives rise to heterozygous (*FY*A/FY*A*^{null}) Duffy-negative erythrocytes (Zimmerman *et al.*, 1999). Interestingly, individuals with this new allele are heterozygous carriers of *FY*A*^{null} and have 50% lesser DARC expression on their erythrocytes (Zimmerman *et al.*, 1999). The fourth allele is *FY*X* (also known as *FY*B*^{weak}) which characterize for weak Fy^{b} (Fy$^{b\ weak}$ phenotype), Fy3 and Fy6 expression (Chown *et al.*, 1965; Meny, 2010). The Fy$^{b\ weak}$ phenotype is caused by the presence of mutations in either two coding regions of *FY*B*, the amino acid Arg89Cys or Ala100Thr (Figure 2.5 C) (Olsson *et al.*, 1998; Parasol *et al.*, 1998; Tournamille *et al.*, 1998; Gassner *et al.*, 2000).

In addition to erythrocytes, DARC is also expressed on other nonerythroid cells throughout the body such as the brain, kidney and endothelium (Hadley *et al.*, 1994; Peiper *et al.*, 1995; Horuk *et al.*, 1996; Chaudhuri *et al.*, 1997; Le Van Kim *et al.*, 1997) The biological function as a chemokine receptor on erythrocytes and other nonerythroid cells are yet to be clearly defined but it has been shown to serve as a chemokine "sink" or scavenger to bind selected acute and chronic inflammation chemokines such as IL-8 (interleukin-8) and RANTES (regulated on activation, normal T cell expressed and secreted) (Mohandas & Narla, 2005).

DARC has been proven to be an important receptor for *P. vivax* and *P. knowlesi* to invade human erythrocytes. Individual with Duffy-negative Fy(a–b–) erythrocytes, which lack DARC is refractory to invasion by these parasites (Miller *et al.*, 1975; Miller *et al.*, 1976; Mason *et al.*, 1977). The formation of a junction is necessary for erythrocyte invasion and *P. knowlesi* uses DARC as a receptor for junction formation (Chitnis & Miller, 1994).

Furthermore, the discovery of heterozygous (*FY*A/FY*A*^{null}) Duffy-negative individuals from Papua New Guinea, whom with reduced expression of DARC on their erythrocytes were found to have lower binding activity to *P. vivax* Duffy binding protein (PvDBPII) and reduced susceptibility to *P. vivax* infection *in vivo* (Michon *et al.*, 2001; Kasehagen *et al.*, 2007). Additionally, studies have shown that the susceptibility of a healthy individual to *P. vivax* infection is greatly associated with the Fy^a/Fy^b antigen polymorphism in human erythrocyte (King *et al.*, 2011). Duffy-positive Fy(a+b–) phenotype in human erythrocyte has been shown to diminish binding of PvDBPII at the erythrocyte surface and reduce susceptibility to vivax malaria clinically (King *et al.*, 2011; Zimmerman *et al.*, 2013). In the case of *P. knowlesi*, studies have shown that the PkDBPαII preferentially bind to Duffy-positive Fy(a–b+) human erythrocytes compared with Duffy-positive Fy(a+b–) human erythrocytes, both in vivo and in vitro (Mason *et al.*, 1977; Haynes *et al.*, 1988).

2.9 Study approach

The incidence rate of *P. knowlesi* malaria in humans is rising and it is widely distributed in Malaysia (Yusof *et al.*, 2014; Barber *et al.*, 2017; Ooi *et al.*, 2017). Knowlesi malaria can result in hyperparasitemia leading to severe infection with possible fatal consequences (Jongwutiwes *et al.*, 2004; Cox-Singh *et al.*, 2008; Cox-Singh & Singh, 2008; Ng *et al.*, 2008; Cox-Singh *et al.*, 2010; Lee *et al.*, 2013). Similar to severe falciparum malaria, hyperparasitemia has become an indication for severe knowlesi malaria (Cox-Singh *et al.*, 2008) In patients with severe infection, parasite counts (parasitemia) were significantly higher and patients often present with a history of fever and chills (William *et al.*, 2011).

Clinical isolates of *P. knowlesi* collected from human infections are genetically diverse (Singh *et al.*, 2004; Lee *et al.*, 2011). In Malaysia, the PkDBPαII has been observed to

have high level of genetic polymorphism (Fong *et al.*, 2014; Fong *et al.*, 2015). A total of 74 haplotypes were identified and these haplotypes can be further clustered into allele group I and allele group II. Through neighbor-joining method, majority of PkDBPαII haplotypes were clustered into allele group I and 6 haplotypes were clustered into allele group II. Interestingly, the PkDBPαII haplotypes of Peninsular Malaysia were genetically distinct from those identified in Malaysian Borneo. Haplotype H2 is the most frequent among haplotypes in Peninsular Malaysia and H47 for Malaysian Borneo. Since PkDBPαII is a crucial protein for the invasion of *P. knowlesi* merozoite into human erythrocytes, diversity in the functional regions of the protein may influence its ability as a competent ligand to DARC of human erythrocytes. Moreover, studies also revealed most cases of severe knowlesi infection with hyperparasitemia were more prominent in Malaysian Borneo compared to Peninsular Malaysia (William *et al.*, 2011; Rajahram *et al.*, 2012; William *et al.*, 2014).

The ability of malaria parasite ligands to bind erythrocyte receptors have been studied using the Erythrocyte-binding assays (EBAs, also refers as erythrocyte-rosetting assays) and it has been proven very effective in many studies (Figure 2.7) (Chitnis & Miller, 1994; Chitnis *et al.*, 1996; Ranjan & Chitnis, 1999; Michon *et al.*, 2000; Singh *et al.*, 2002; Singh *et al.*, 2003; King *et al.*, 2011; Semenya *et al.*, 2012; Cheng *et al.*, 2013; Batchelor *et al.*, 2014; Chootong *et al.*, 2014; Cheng *et al.*, 2016; Ntumngia *et al.*, 2016; Min *et al.*, 2017). This method was first described by Chitnis and Miller (1994), where segments of PvDBP and PkDBPα were cloned and expressed onto COS-7 cell surface, and allowed to interact with free floating erythrocytes. In addition to that, newer technology such as Surface Plasmon Resonance (SPR) and Isothermal Titration Calorimetry (ITC) were also used to evaluate specific binding interaction between PvDBPII and DARC (Hans *et al.*, 2005; Batchelor *et al.*, 2014).

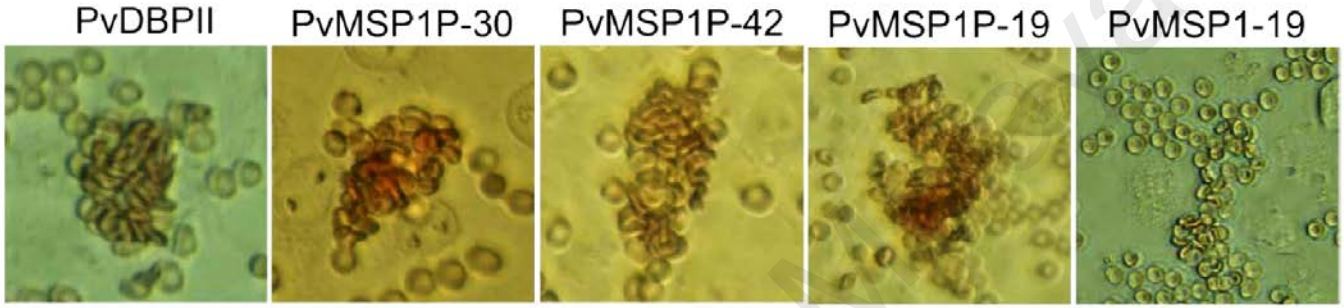

(A)

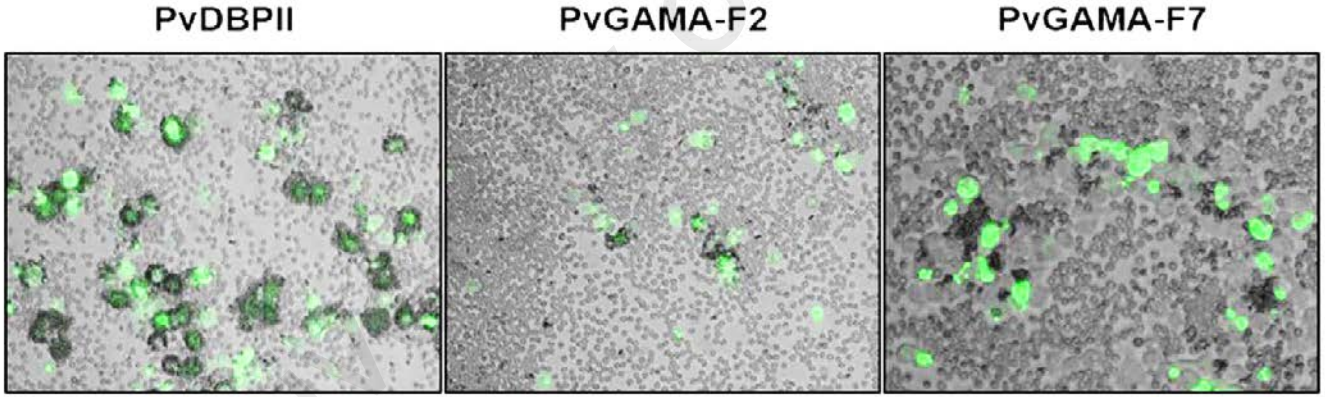

(B)

Figure 2.7: Ability of the malaria parasite ligands to bind erythrocyte receptors via Erythrocyte-binding assays. (A) Erythrocyte binding rosettes formed on the surfaces of COS-7 cells expressing PvDBPII or different fragments of PvMSP1P or PvMSP1-19 were visualized under inverted light microscopy; Images adapted from Cheng *et al.* (2013). (B) Erythrocyte-binding rosettes formed on the surface of HEK-293T cells expressing PvDBPII or different fragments of PvGAMA were visualized under inverted fluorescence microscopy. Adapted from Cheng *et al.* (2016).

CHAPTER 3: METHODOLOGY

3.1 Overview

Earlier studies on *P. knowlesi* clinical isolates reported distinct PkDBPαII haplotypes from Peninsular Malaysia and Malaysian Borneo. The predominant haplotype in Peninsular Malaysia and Malaysia Borneo were haplotype H2 (clinical isolate HAN) and H47 (clinical isolate SBH31) respectively. This work was intended to investigate the binding activity of PkDBPαII of these two haplotypes to human erythrocytes. This research project was carried out using two specific molecular interaction assays: Erythrocyte-binding assays (binding activity) and Isothermal Titration Calorimetry (binding affinity). PkDBPαII of each clinical isolate was expressed on the surface of the COS-7 cells and allowed to interact with fresh erythrocytes. The degree of bound erythrocytes was evaluated and the binding activity of PkDBPαII from Peninsular Malaysia and Malaysian Borneo were compared and analyzed. The PkDBPαII of each isolate was then expressed and purified using prokaryotic expression system. The binding affinity was confirmed with the use of highly precise and sensitive instrument, Isothermal Titration Calorimetry (ITC).

3.2 Oligonucleotide primers

Oligonucleotide primers used in the study were synthesized by First BASE Laboratories Sdn. Bhd. (Malaysia). The stock concentration of all primers used in this project was 100 µM. All primers were diluted with ddH_2O to 10 µM working concentration prior to usage. The details of each primer used in this study are presented in Table 3.1.

Table 3.1: List of oligonucleotide primers used in this study

Purpose	Primer Name	Primer Sequence (5'-3')
PCR of *PkDBPαII* gene	*PkDBPαII*-pDisplay_forward	GGCAGATCTGTTATTAATCAAACTTTTCTTC
	PkDBPαII-pDisplay_reverse	AGATCTGTTCAGTTATCGGATTAGAACTG
	PkDBPαII-pET30a(+)_forward	GGATCCGTTATTAATCAAACTTTTCTTCAA
	PkDBPαII-pET30a(+)_reverse	GGATCCCTATTCAGTTATCGGATTAGAAC
PCR of *AcGFP1* gene	*AcGFP1*-pDisplay_forward	GTCGACGCCACCATGGTGAGCAAG
	AcGFP1-pDisplay_reverse	GTCGACCTTGTACAGCTCATCCATGCC
Duffy blood group genotyping	*FY*_forward	CCCTCATTAGTCCTTGGCTCTTCT
	*FY*A*_reverse	CAGCTGCTTCCAGGTTGGCTC
	*FY*B*_reverse	CAGCTGCTTCCAGGTTGGCTT
	*FY*B^{es}*_forward	CCCTCATTAGTCCTTGGCTCTTTC

Table 3.1, continued: List of oligonucleotide primers used in this study

Purpose	Primer Name	Primer Sequence (5'-3')
Selection of positive recombinant pGEM-T-*PkDBPαII*-pDisplay, pGEM-T-*AcGFP1*-pDisplay and pGEM-T-*PkDBPαII*-pET30a(+) clones	M13F (-40)	CAGGGTTTTCCCAGTCACGAC
	M14R (-48)	AGCGGATAACAATTTCACACAGG
Selection of positive recombinant pDisplay-*PkDBPαII-AcGFP1* and pET30a(+)-*PkDBPαII* clones	T7 Promoter	TAATACGACTCACTATAGGG
	BGH Reverse	TAGAAGGCACAGTCGAGG

3.3 Reagents and chemicals

All commonly used reagents and chemicals that include methanol, hydrochloric acid, absolute ethanol, isopropanol, calcium chloride, magnesium chloride, sodium hydroxide and acetone were of AnalaR or AR (analytical reagents) grades available from Amresco, Inc., USA and Sigma-Aldrich, Inc., USA

For human and *P. knowlesi* genomic DNA extraction, DNeasy® blood & tissue kit was purchased from Qiagen, Germany. For polymerase chain reaction (PCR), GoTaq® Flexi DNA polymerase and deoxyribonucleotide triphosphates (dNTPs) were purchased from Promega Corp., USA. The QIAquick® Gel Extraction Kit from Qiagen, Germany, was used for PCR product purification. For agarose gel electrophoresis, agarose powder was purchased from Promega Corp., USA; Tris base was purchased from Bio-Rad Laboratories, USA; Acetic acid glacial and ethylenediaminetetraacetic acid (EDTA) were purchased from Sigma-Aldrich, Inc., USA.; GeneRuler™ 100 bp+ DNA ladder, 1 kb DNA ladder, 1 kb+ DNA ladder and 6× DNA loading dye were from Thermo Scientific™, USA.; SYBR® Safe DNA gel stain was from Invitrogen Corp., USA.

For PCR product cloning, pGEM®-T Vector System was purchased from Promega Corp., USA; One Shot™ TOP10 Chemically Competent *E. coli* was purchased from Invitrogen Corp., USA. For maintenance and propagation of *Escherichia coli* cultures, Luria-Bertani (LB) broth and agar were prepared by tryptone, yeast extract (purchased from Conda Pronadisa, Spain) and sodium chloride (purchased from Amresco Inc., USA); Antibiotics namely ampicillin, chloramphenicol and kanamycin were purchased from Bio Basic Inc., Canada. For cloning into expression vector, restriction enzymes (RE) *Bgl*II, *Sal*I and *Bam*HI, T4 DNA ligase and calf intestine alkaline phosphatase (CIAP) were purchased from New England Biolabs, USA; Expression vectors, pDisplay™ and Novagen® pET-30a(+) were purchased from Invitrogen Corp., USA and Merck KGaA.,

Germany, respectively. For extraction of plasmid DNA, QIAprep® spin Miniprep kit was purchased from Qiagen, Germany.

For mammalian tissue culture, Dulbecco's Modified Eagle's Medium-high glucose (DMEM-high glucose) and its supplements; sodium pyruvate, fetal bovine serum (FBS), L-glutamine, penicillin-streptomycin antibiotics (Pen-strep), TrypLE™ express enzyme (1X) with phenol red, MEM Non-Essential Amino Acids (NEAA), Recovery™ cell culture freezing medium and Opti-MEM® I reduced-serum medium were purchased from Gibco™, Invitrogen Corp., USA.

For transfection, Lipofectamine™ 3000 transfection reagent was purchased from Invitrogen Corp., USA. For fluorescence nuclei staining, Hoechst 33342, trihydrochloride, trihydrate, 100 mg was purchased from Thermo Scientific™, USA; Anti-fade solution Calbiochem® FluorSave™ reagent was obtained from Merck KGaA., Germany.

For prokaryotic protein expression, isopropyl β-D-1-thiogalactopyranoside (IPTG) of molecular biological grade was purchased from Invitrogen Corp., USA. For sodium dodecyl sulfate polyacrylamide gel electrophoresis (SDS-PAGE), acrylamide/bis-acrylamide (30%) pre-mix solution, tetramethylethylenediamine (TEMED), tris base, glycine, SDS and Coomassie Brilliant Blue (CBB) powder were purchased from Bio-Rad Laboratories, USA; Ammonium persulfate and β-mercaptoethanol from Amresco Inc., USA; Glycerol of molecular biological grade from Sigma-Aldrich, Inc., USA; PageRuler™ prestained protein ladder (10 kDa to 150 kDa) was purchased from Thermo Scientific™, USA.

For Western Blot assay, polyvinylidene difluoride (PVDF) membrane was purchased from Bio-Rad Laboratories, USA.; Tween-20 was purchased from Amresco Inc., USA; Biotin-labelled goat anti-mouse antibodies and streptavidin-alkaline phosphatase were purchased from KPL Inc., USA.; Novagen® His•Tag® monoclonal antibody was from

Merck KGaA., Germany; 5-bromo-4-chloro-3-indolyl phosphate/nitro blue tetrazolium (BCIP/NBT) tablets were from Sigma-Aldrich, Inc., USA.

For protein purification, polypropylene column and nickel-NTA agarose resin were purchased from Qiagen, Germany; Guanidine hydrochloride, sodium phosphate NaH_2PO_4 monobasic, sodium phosphate (Na_2HPO_4) dibasic and imidazole were purchased from Sigma-Aldrich, Inc., USA; Urea was from Bio Basic Inc., Canada. For protein dialysis, Slide-A-Lyzer™ G2 Dialysis Cassette (10K MWCO) was purchased from Thermo Scientific™, USA. For concentrating purified protein samples, Vivaspin® 20 centrifugal concentrator was purchased from Sartorius Lab Instruments GmbH & Co.KG., Germany. For protein concentration quantification, Quick Start™ Bradford protein assay was purchased from Bio-Rad Laboratories, USA.

3.4 Stock solutions and buffers

3.4.1 Materials for agarose gel electrophoresis

50× Tris-Acetate-EDTA (TAE) buffer

Tris base		242	g
Acetic acid		57.1	mL
0.5 M EDTA		100	mL
ddH_2O	to	1000	mL

The buffer solution was stored at room temperature and diluted 50× with ddH_2O before use.

3.4.2 Materials for cloning of PCR product

Luria-Bertani (LB) broth

Tryptone		5.0	g
Yeast Extract		2.5	g
NaCl		5.0	g
ddH_2O	to	500	mL

The LB medium was steam-sterilized by autoclaving at 121 ºC for 20 min and stored at 4 ºC.

Ampicillin (100 mg/mL)

One gram of ampicillin, sodium powder, was dissolved in 10 mL of ddH_2O. The solution was filtered-sterilized using a 0.22 µm filter. The ampicillin solution was stored in aliquots at –20 °C.

Chloramphenicol (34 mg/mL)

Chloramphenicol, 0.34 g, was dissolved in 10 mL of absolute ethanol. The solution was filter-sterilized using 0.22 µm filter. The chloramphenicol solution was stored in aliquots at –20 °C.

Kanamycin (30 mg/mL)

Kanamycin, 0.30 g, was dissolved in 10 mL of ddH_2O. The solution was filter-sterilized using 0.22 µm filter. The kanamycin solution was stored in aliquots at –20 °C.

LB agar plates containing antibiotic

Tryptone	10.0	g
Yeast extract	5.0	g

NaCl		10.0	g
Bacto-Agar		15.0	g
ddH_2O	to	1000	mL

The mixture was steam-sterilized by autoclaving at 121 ºC for 20 min. When the mixture has cooled to about 50 – 55 °C, ampicillin (100 mg/mL) or kanamycin (30 mg/mL) or chloramphenicol (34 µg/mL) stock solution were added to a final concentration of 100 µg/mL, 30 µg/mL and 34 µg/mL respectively. Finally, approximately 20 mL of mixture was poured into each sterile petri dish and allowed to solidify. Plates were carefully stored at 4 °C under aseptic condition.

3.4.3 Materials for Erythrocyte-binding assays

Incomplete RPMI 1640 medium (Blood washing medium), pH 7.25

RPMI 1640 medium powder		16.2	g
ddH_2O	to	1000	mL

The incomplete RPMI 1640 medium was prepared under aseptic condition by dissolving 16.2 g RPMI 1640 powder in 1000 mL of ddH_2O without addition of any supplement. The pH of the solution was adjusted to pH 7.25, filter-sterilized using 0.22 µm filter and stored at 4 °C.

Dulbecco's Phosphate Buffered Saline (1× PBS), pH 7.4

Dulbecco's phosphate buffered saline powder		9.6	g
ddH_2O	to	1000	mL

The solution was prepared by dissolving 9.6 g of Dulbecco's phosphate buffered saline powder in 1000 mL of ddH_2O to yield 0.01 M phosphate buffered saline, pH 7.4 at room temperature. The solution was filter-sterilized using 0.22 µm filter and stored at 4°C.

1% Paraformaldehyde fixative solution

Paraformaldehyde		0.1	g
ddH_2O	to	10	mL

The solution was prepared in a chemical fume chamber. Paraformaldehyde powder, 0.1 g was dissolved in 10 mL of ddH_2O. The solution was gently heated to 50 – 60 °C and stirred until completely dissolved. The paraformaldehyde fixative solution was stored in aliquots at –20 °C.

3.4.4 Materials for protein expression, purification and dialysis

Isopropyl β-D-1-thiogalactopyranoside (IPTG) solution (100 mM)

IPTG powder, 0.476 g was dissolved in 20 mL of ddH_2O. The solution was filter-sterilized using 0.22 µm filter and stored at –20 °C under dark condition.

50% Glycerol stock solution

Ten milliliters of glycerol were added to 10 mL ddH_2O. The solution was filter-sterilized on a 0.22 µm filter and stored at 4 °C.

10× Stock solution A

200 mM Sodium phosphate, monobasic (NaH_2PO_4)		2.76	g
5 M NaCl		29.29	g
ddH_2O	to	100	mL

The solution was stored at room temperature.

10× Stock solution B

200 mM Sodium phosphate, dibasic (Na_2HPO_4)		2.84	g
5 M NaCl		29.29	g

ddH_2O	to	100	mL

The solution was stored at room temperature.

5× Native purification buffer, pH 8.0

250 mM sodium phosphate, monobasic (NaH_2PO_4)		7.0	g
2.5 M NaCl		29.29	g
ddH_2O	to	200	mL

The pH of the buffer was adjusted to pH 8.0 and stored at room temperature.

3 M Imidazole, pH 6.0

Imidazole		20.6	g
10× Stock solution A		8.77	mL
10× Stock solution B		1.23	mL
ddH_2O	to	100	mL

The pH of the solution was adjusted to pH 6.0 and stored at room temperature.

Guanidinium lysis buffer, pH 7.8

10× Stock solution A		1.16	mL
10× Stock solution B		18.84	mL
Guanidine hydrochloride		114.6	g
ddH_2O	to	200	mL

The pH of the buffer was adjusted to pH 7.8. The solution was filter-sterilized using 0.45 µm filter and stored at room temperature.

Denaturing binding buffer, pH 7.8

10× Stock solution A		0.58	mL

10× Stock solution B		9.42	mL
Urea		48.1	g
ddH_2O	to	100	mL

The solution was stirred with gentle heating at 50 – 60 °C until completely dissolved. When cooled to room temperature, the pH was adjusted to pH 7.8. The buffer was filter-sterilized using 0.45 µm filter and stored at room temperature.

Denaturing wash buffer, pH 6.0

10× Stock solution A		7.38	mL
10× Stock solution B		2.62	mL
Urea		48.1	g
ddH_2O	to	100	mL

The solution was stirred with gentle heating at 50 – 60 °C until completely dissolved. When cooled to room temperature, the pH was adjusted to pH 6.0. The buffer was filter-sterilized using 0.45 µm filter and stored at room temperature.

1× Native purification buffer, pH 8.0

5× Native purification buffer, 50 mL was diluted with 200 mL of ddH_2O. The pH of the buffer was adjusted to pH 8.0 and stored at room temperature.

Native wash buffer, pH 8.0 (with 20 mM imidazole)

1× Native purification buffer		100	mL
3 M Imidazole, pH 6.0		670	µL

The pH of buffer was adjusted to pH 8.0 and stored at room temperature.

Native elution buffer, pH 8.0 (with 250 mM imidazole)

1× Native purification buffer	13.75	mL
3 M Imidazole, pH 6.0	1.25	mL

The pH of buffer was adjusted to pH 8.0 and stored at room temperature.

Dialysis buffer (pH 7.4)

Dulbecco's phosphate buffered saline powder		9.6	g
ddH_2O	to	1000	mL

The solution was prepared by dissolving 9.6 g of Dulbecco's phosphate buffered saline powder in 1000 mL of ddH_2O to yield 0.01 M phosphate buffered saline, pH 7.4 at room temperature.

3.4.5 Solutions for Tris-Glycine SDS-PAGE

12% Resolving gel solution

ddH_2O	1.6	mL
Acrylamide-bisacrylamide (30%)	2.0	mL
1.5 M Tris-HCl, pH 8.8	1.3	mL
10% SDS	50.0	µL
10% Ammonium persulfate (APS)	50.0	µL
TEMED	2.0	µL

All the components were mixed well and poured immediately in between the plates after the addition of TEMED.

5% Stacking gel solution

ddH_2O	1.1	mL
Acrylamide-bisacrylamide (30%)	0.33	mL

0.5 M Tris-HCl, pH 6.8		0.5	mL
10% SDS		20.0	µL
10% Ammonium persulfate (APS)		20.0	µL
TEMED		2.0	µL

All the components were mixed thoroughly and poured immediately in between the plates after the addition of TEMED.

10× Tris-Glycine electrophoresis buffer (SDS-PAGE running buffer)

Tris base		30.3	g
Glycine		144.0	g
SDS		10.0	g
ddH_2O	to	1000	mL

The buffer was diluted 10× with ddH_2O before used.

2× Sample loading buffer (SDS reducing buffer)

0.5 M Tris-HCl, pH 6.8		4.0	mL
10% SDS		8.0	mL
Bromophenol blue		0.04	g
Glycerol		4.0	mL
β-mercaptomethanol		0.5	mL
ddH_2O	to	20	mL

β-mercaptomethanol was added to destroy disulphide bridges in protein samples. The buffer was mixed well and stored at 4 °C.

Coomassie Brilliant Blue staining solution

Coomassie Brilliant Blue		1.25	g
Methanol		250	mL
Acetic acid		50	mL
ddH_2O	to	500	mL

The solution was filtered with filter paper and stored at room temperature.

Destaining solution

Acetic acid		70	mL
Methanol		50	mL
ddH_2O	to	1000	mL

The solution was mixed well and stored at room temperature.

3.4.6 Solutions for Western Blot assay

10× Transfer buffer (Blotting buffer)

Tris base		15.15	g
Glycine		72	g
ddH_2O	to	500	mL

The solution was mixed well and stored at room temperature. The transfer buffer was diluted 10× with ddH_2O before use.

5× Tris-borate-saline (TBS), pH 7.6

Tris base		12.11	g
NaCl		40.0	g
ddH_20	to	1000	mL

The pH of the buffer was adjusted to pH 7.6 with concentrated HCl and stored at room temperature.

1× Tris-borate-saline (TBS), pH 7.6

5× Tris-borate-saline (TBS), 100 mL was diluted with 900 mL of ddH_2O. The pH of the buffer was adjusted to pH 7.6 and stored at room temperature.

0.2% TBS-Tween-20 (TBS-T) (washing buffer)

1× TBS		1000	mL
Tween-20		2	mL

5% Blocking buffer

Skimmed milk powder		0.5	g
1× TBS	to	10	mL

3.5 Blood samples collection and DNA extraction.

Use of human and macaque (*M. fascicularis*) samples in this study was approved by University of Malaya Medical Centre Medical Ethics Committee (Appendix A) and University of Malaya Institutional Animal Care and Use Committee (Appendix B).

3.5.1 Extraction of DNA from *P. knowlesi* clinical isolates for cloning

The *P. knowlesi* infected blood samples, HAN and SBH31, were obtained from the earlier studies (Fong *et al.*, 2014; Fong *et al.*, 2015). For each isolate, the *P. knowlesi* genomic DNA was extracted using commercialized DNeasy® Blood & Tissue Kit (Qiagen, Germany) according to the manufacturer's protocol for nonnucleated erythrocytes. Proteinase K, 20 µL, was pipetted into a 1.5-mL microcentrifuge tube

followed by the addition of 100 µL anticoagulant-treated blood. The sample was added with 100 µL of 1×PBS solution prior to the addition of 200 µL Buffer AL. The sample was mixed thoroughly by vortexing and incubated at 56 °C for 10 min. Then, 200 µL of absolute ethanol (96 – 100%) was added and mixed by vortexing. The mixture was pipetted into the DNeasy® Mini spin column placed in a 2-mL collection tube and centrifuged at 8000 rpm for 1 min. The flow-through and collection tube were discarded and the DNeasy® Mini spin column was placed in a new 2-mL collection tube. Five hundred microliters of Buffer AW1 was added and the column was centrifuge at 8000 rpm for 1 min. The flow-through and collection tube were discarded and the DNeasy® Mini spin column was placed in a new 2-mL collection tube. Next, 500 µL of Buffer AW2 was added and centrifuged for 3 min at 14000 rpm. The flow-through and collection tube were discarded and the DNeasy® Mini spin column was transferred to a new 1.5-mL centrifuge tube. Elution of DNA was done by pipetting 100 µL of Buffer AE directly onto the center of DNeasy® Mini spin column membrane, incubated at room temperature for 3 min and subsequently centrifuged at 8000 rpm for 1 min. Extracted DNA was stored at –20 °C.

3.5.2 Extraction of human genomic DNA for Duffy genotyping

Blood from a healthy human donor was collected by venous puncture into lithium-heparin tubes. The human genomic DNA was extracted using commercialized DNeasy® Blood & Tissue Kit as mentioned in section 3.5.1. Extracted DNA was stored at –20 °C.

3.6 Binding activity of PkDBPαII using Erythrocyte-binding assay

3.6.1 Polymerase chain reaction (PCR)

3.6.1.1 PCR of *PkDBPαII* for cloning into pDisplay™ vector

The plasmid pDisplay™ (Invitrogen Corp., USA) is a mammalian expression system that was designed to target recombinant protein to the surface of mammalian cells. The *PkDBPαII* region was amplified by specific primers containing a *Bgl*II restriction enzyme cut site (Table 3.1) before cloned into the pDisplay™ vector. The PCR reaction mixtures were prepared according to the following:

Reagent	**Volume (µL)**
ddH_2O	10.3
5× PCR buffer (20 mM $MgCl_2$)	5.0
$MgCl_2$ (25 mM)	4.0
10 mM dNTPs (2.5 mM each)	0.5
PkDBPαII-pDisplay_forward primer (10 µM)	0.5
PkDBPαII-pDisplay_reverse primer (10 µM)	0.5
GoTaq® Flexi DNA polymerase (Promega Corp., USA, 5 U/µL)	0.2
DNA template/ddH_2O*	4.0
Total reaction volume	25.0

*ddH_2O, instead of *P. knowlesi* DNA template was added into the non-template control (NTC) reaction.

The PCR amplification reaction was performed using the following thermal cycling condition: 94 °C for 5 min, 35 cycles at 94 °C for 45 s, 52 °C for 45 s and 72 °C for 70 s, followed by a 10-min extension at 72 °C. PCR products were visualized under UV after analyzed by gel electrophoresis on a 1% agarose gel, while the remaining amplicons were stored at –20 °C. All amplicons were cloned into pGEM®-T vector system (Promega Corp., USA) and sequenced.

3.6.1.2 PCR of *AcGFP1* for cloning into pDisplay™ vector

In this study, the fluorescent reporter gene, *AcGFP1* (green fluorescent protein from *Aequorea coerulescens*), was added to the C-terminal of the insert site of pDisplay™ plasmid to facilitate direct visualization of the expressed protein (PkDBPαII) *in vitro*. The *AcGFP1* gene was amplified from pAcGFP1-C1 plasmid (Clontech Laboratories, Inc., USA) using specific primers containing a *Sal*I restriction enzyme cut site (Table 3.1) and carried out using the following reagents:

Reagent	**Volume (µL)**
ddH_2O	13.8
5× PCR buffer (20 mM $MgCl_2$)	5.0
$MgCl_2$ (25 mM)	4.0
10 mM dNTPs (2.5 mM each)	0.5
AcGFP1-pDisplay_forward primer (10 µM)	0.5
AcGFP1-pDisplay_reverse primer (10 µM)	0.5
GoTaq® Flexi DNA polymerase (Promega Corp., USA, 5 U/µL)	0.2
pAcGFP1-C1 plasmid/ddH_2O*	0.5
Total reaction volume	25.0

*ddH_2O, instead of pAcGFP1-C1 plasmid was added into the non-template control (NTC) reaction.

The gene amplification of *AcGFP1* was performed using the following thermal cycling condition: 94 °C for 5 min, 30 cycles at 94 °C for 45 s, 64 °C for 45 s and 72 °C for 50 s, followed by a 10-min extension at 72 °C. The PCR products were visualized under UV after analyzed by gel electrophoresis on a 1% agarose gel, while the remaining amplicons were stored at –20 °C. All amplicons were cloned into pGEM®-T vector system and sequenced.

3.6.1.3 Duffy blood group genotype of healthy human erythrocytes

The Duffy genotyping was determined using allele-specific PCR based on four sets of primers described previously (Cotorruelo *et al.*, 2009; De Silva *et al.*, 2014). The extracted human genomic DNA was subjected to three different PCR reactions containing a combination of *FY*_forward primer with *FY*A*_reverse primer, *FY*_forward primer with *FY*B*_reverse primer and *FY*B*^{ES}_forward primer with *FY*B*_reverse primer. The PCR reaction mixtures were carried out using the following reagents:

Reagent	**Volume (µL)**
ddH_2O	10.3
5× PCR buffer (20 mM $MgCl_2$)	4.0
$MgCl_2$ (10 mM)	1.6
10 mM dNTPs (2.0 mM each)	0.4
*FY*_forward/*FY*B*^{ES}_forward primer (10 µM)	0.8
*FY*A*_reverse/ *FY*B*_reverse primer (10 µM)	0.8
GoTaq® Flexi DNA polymerase (Promega Corp., USA, 5 U/µL)	0.1
DNA template/ddH_2O*	2.0
Total reaction volume	20.0

*ddH_2O, instead of human genomic DNA template was added into the non-template control (NTC) reaction.

The PCR reaction conditions were optimized to ensure specific amplification and the PCR amplification reaction was performed using the following thermal cycling condition: 94 °C for 5 min, 30 cycles at 94 °C for 30 s, 60 °C for 60 s and 72 °C for 60 s, followed by a 10-min extension at 72 °C. The PCR products were visualized under UV after analyzed by gel electrophoresis on a 2% agarose gel.

3.6.2 Agarose gel electrophoresis

Agarose gel, 1.0% or 2.0% were used for electrophoresis. For 1.0% agarose gel, 0.30 g of electrophoresis-grade agarose powder (Promega Corp., USA) was dissolved in 30 mL of 1× TAE buffer in a 100-mL conical flask. The mixture was heated in a microwave oven for nearly 70 s to melt the agarose. The melted agarose gel was cooled to approximately 50 °C prior to the addition of 1 µL SYBR® Safe DNA gel stain (Invitrogen Corp., USA). The mixture was homogenized gently and poured into a casting tray with gel comb inserted. After the gel has hardened, the gel comb was removed and the cast was placed in electrophoresis tank. Sufficient amount of 1× TAE buffer was poured into the tank to completely cover the gel. GeneRuler1 kb Plus DNA Ladder, ready-to-use (Thermo Scientific™, USA) was used for PCR product size estimation. PCR products were loaded into wells and electrophoresis was run at 100 V for 30 min. The gel was visualized under UV using Molecular Imager® Gel Doc™ XR+ Imaging System (Bio-Rad, USA).

3.6.3 Cloning of PCR products into pGEM®-T Vector

3.6.3.1 Purification of PCR products

Gel purification was performed using commercialized QIAquick® Gel Extraction Kit (Qiagen, Germany) with the protocol provided. The expected size of PCR products for *PkDBPαII* (~ 1011 bp) and *AcGFP1* (~ 723 bp) were noted during UV visualization of the gel. Each target fragment was excised carefully using a thin glass coverslip and placed into 1.5-mL microcentrifuge tubes. The gel slices were weighed and 3 volumes of Buffer QG was added to 1 volume of gel (typically, 100 mg is equivalent to 100 µL). For each sample, the mixture was tapped gently and incubated at 50 ºC for 10 min to ensure the gel slice is completely dissolved. One volume of isopropanol was added to the sample and mixed. The samples were then pipetted into the QIAquick® spin columns and

centrifuged for 1 min at 13000 rpm. The flow-through was discarded and 500 µL of Buffer QG was added, followed by a centrifugation step at 13000 rpm for 1 min. Next, the column was washed with 750 µL of Buffer PE at 13000 rpm for 1 min. The flow-through was discarded and the QIAquick® spin columns were centrifuged once more at 13000 rpm for 1 min to remove residual wash buffer. The QIAquick® spin columns were placed in clean 1.5-mL microcentrifuge tubes and 30 µL of Buffer EB was added to the center of the membrane. The column was incubated at room temperature for 4 min before being centrifuged at 13000 rpm for 1 min. The gel purified DNA fragments were stored at –20 °C.

3.6.3.2 Ligation of PCR products into pGEM®-T Vector

The gel-purified PCR amplified fragments were cloned into pGEM®-T Vector using the commercialized pGEM®-T Vector System I (Promega Corp., USA). The ligation mixtures were carried out using the following reagents:

Reagent	**Volume (µL)**
2× Rapid Ligation Buffer	5.0
pGEM®-T Vector (50 ng)	1.0
T4 DNA Ligase	1.0
Gel-purified DNA	3.0
Total reaction volume	10.0

The ligation mixtures were mixed gently and incubated overnight at 16 °C.

3.6.3.3 Transformation into competent *E. coli* TOP10F' cells

Total volume of 10 µL ligation mixture was added into 100 µL of competent cells *E. coli* TOP10F' and mixed gently. The mixture was incubated on ice for 30 min. Next, the competent cells were subjected to heat-shock at 42 °C for 30 s and immediately

transferred to ice for 5 min. Then, 900 µL of LB broth was added into the tube. The tube was shaken at 250 rpm at 37 °C for 1 h. The transformed cells were then pelleted by centrifuging at 10000 rpm for 1 min. The pellet was resuspended in 100 µL LB broth and spread on pre-warmed LB agar plates containing 100 µg/mL ampicillin. The plate was incubated overnight at 37 °C

3.6.3.4 Colony PCR for selection of positive recombinant clones

Colony PCR was performed to select positive recombinant clones. Colonies on the transformation plates were picked by using 10-µL tips and dipped into the sample reaction PCR tubes except for non-template control PCR tube. PCR reaction mixtures were prepared according to the following:

Reagent	**Volume (µL)**
ddH_2O	4.6
2× DreamTaq™ Green PCR Master Mix (Thermo Scientific™)	5.0
M13F (-40) primer (10 µM)	0.2
M13R (-48) primer (10 µM)	0.2
Total reaction volume	10.0

The thermal cycle commenced with an initial denaturing step at 95 °C for 1 min (step 1), followed by 35 cycles of denaturation at 95 °C for 30 s, annealing at 50 °C for 45 s, and elongation at 72 °C for 1 min. A final elongation step is performed at 72 °C for 10 min. PCR products were visualized under UV after analyzed by gel electrophoresis on a 1% agarose gel. Positive recombinant clones were selected for plasmid extraction.

3.6.3.5 Plasmids extraction of positive recombinant clones

Selected positive bacteria clones were grown overnight in separate 5 mL of LB broth containing 100 µg/mL ampicillin, shaken at 37 °C and 250 rpm. Bacterial cultures were

pelleted by centrifuging at 7800 rpm for 3 min at room temperature. Plasmids of the selected positive recombinant bacteria colonies were extracted using QIAprep® Spin Miniprep kit (Qiagen, Germany) according to the manufacturer instructions. Pelleted bacterial cells were resuspended in 250 µL Buffer P1 and transferred into a 1.5-mL microcentrifuge tube. Buffer P2 (250 µL) containing LyseBlue reagent was added and mixed thoroughly by inverting the tubes 4 – 6 times. Next, 350 µL of Buffer N3 was added and mixed immediately by inverting the tubes for 4 – 6 times. The mixture was centrifuged at 13000 rpm for 10 min at room temperature. The supernatant was carefully transferred to the QIAprep® spin column and centrifuged for 1 min at 13000 rpm. The flow-through was discarded and the column was washed for 1 min at 13000 rpm with 500 µL of Buffer PB. The flow-through was discarded. The column was further washed with 750 µL of Buffer PE at 13000 rpm for 1 min. An additional centrifugation step at 13000 rpm for 1 min was performed to remove any residual wash buffer. For elution of DNA, 40 µL of Buffer EB was added to the center of the membrane and incubated for 4 min at room temperature. Finally, the column was centrifuged at 13000 rpm for 1 min and plasmid DNA was eluted in 1.5-mL microcentrifuge tubes. The purified plasmid DNA was stored at –20 °C.

3.6.4 Cloning of target fragments into pDisplay™ vector

The *PkDBPαII* of each haplotype was cloned into the pDisplay™ plasmid using restriction enzyme (RE) cloning method. The cloning procedure commenced with the insertion of *AcGFP1* into the C-terminal insert site of pDisplay™ plasmid, followed by the insertion of *PkDBPαII* onto upstream of *AcGFP1* gene, resulting in the pDisplay-*PkDBPαII-AcGFP1* plasmid.

3.6.4.1 Digestion of pGEM-T-*PkDBPαII* and pGEM-T-*AcGFP1* plasmids with RE

Digestion of pGEM-T- *PkDBPαII* by RE *Bgl*II was performed with the following reagents:

Reagent	**Volume (µL)**
Plasmid DNA	25.0
Restriction enzyme *Bgl*II (New England Biolabs, Inc., USA)	2.0
10× NEBuffer 3.1	4.0
ddH_2O	9.0
Total reaction volume	40.0

Digestion of pGEM-T-*AcGFP1* by RE *Sal*I was carried out with following reagents:

Reagent	**Volume (µL)**
Plasmid DNA	25.0
Restriction enzyme *Sal*I (New England Biolabs, Inc., USA)	2.0
10× NEBuffer 3.1	4.0
ddH_2O	9.0
Total reaction volume	40.0

The digestion mixtures were incubated at 37 °C for 3 h.

3.6.4.2 Digestion and dephosphorylation of expression vector pDisplay™

For *AcGFP1*, pDisplay™ plasmid was digested with RE *Sal*I. Digestion of pDisplay™ was carried as mentioned in section 3.6.4.1. Then, the RE digested pDisplay™ was dephosphorylated by calf intestinal alkaline phosphatase (CIAP) to prevent plasmid self-ligation and the dephosphorylation was carried out with the following reagents:

Reagent	**Volume (µL)**
Digested pDisplay™ plasmid	40.0

10× NEBuffer 3.1	0.5
CIAP (New England Biolabs, Inc., USA)	2.0
ddH_2O	2.5
Total reaction volume	45.0

The mixture was incubated for 30 min at 37 °C. Then, the dephosphorylation reaction was terminated by incubation at 85 ºC for 15 min.

For *PkDBPαII*, the cloning procedure was carried out after obtaining successive pDisplay-*AcGFP1* plasmids. Digestion with RE *Bgl*II and dephosphorylation of pDisplay-*AcGFP1* plasmids were performed as mentioned above.

3.6.4.3 Purification of digested fragments and pDisplay™ plasmids

Agarose gel electrophoresis was performed on digested recombinant pGEM-T-*PkDBPαII*, pGEM-T-*AcGFP1*, pDisplay™ and pDisplay-*AcGFP1* plasmids using 1.0% agarose gel. Digested target fragments with expected size were excised from the gel and purified using QIAquick® Gel Extraction Kit as mentioned in section 3.6.3.1.

3.6.4.4 Ligation of purified target fragments into pDisplay™ vector system

Ligation of purified target fragments *AcGFP1* into pDisplay™ vector was performed with the following reagents:

Reagent	**Volume (µL)**
*Sal*I-digested pDisplay™ vector	2.0
*Sal*I-digested *AcGFP1*	6.0
T4 DNA ligase (New England Biolabs, Inc., USA)	1.0
10× ligation buffer	1.0
Total reaction volume	10.0

Ligation of *PkDBPαII* into pDisplay-*AcGFP1* vector was carried out with following reagents:

Reagent	**Volume (µL)**
*Bgl*II-digested pDisplay-*AcGFP1* vector	1.0
*Bgl*II-digested *PkDBPαII*	7.0
T4 DNA ligase (New England Biolabs, Inc., USA)	1.0
10× ligation buffer	1.0
Total reaction volume	10.0

The ligation mixtures were incubated at 16°C for overnight.

3.6.4.5 Transformation into propagation and maintenance host *E. coli* TOP10F' cells

The transformation of ligation mixture into competent *E. coli* TOP10F' cells was carried out as mentioned in section 3.6.3.3.

3.6.4.6 Directional PCR for selection of positive recombinant clones

Positive recombinant clones with sense orientation of cloned fragment were selected using directional PCR. Directional PCR was performed using the similar protocol as mentioned in section 3.6.3.4, by using *AcGFP1*-pDisplay_forward primer and BGH reverse primer for *AcGFP1* insert, and T7 promoter primer and *PkDBPαII*-pDisplay_reverse primer for *PkDBPαII* insert.

3.6.4.7 Plasmids extraction of positive recombinant clones

Plasmids of selected positive recombinant clones were extracted from *E. coli* TOP10F' cells using commercialized QIAprep® Spin Miniprep kit as mentioned in section 3.6.3.5.

3.6.4.8 Recombinant plasmid sequencing and sequence analysis

Nucleotide sequence of the recombinant plasmid pGEM-T-*AcGFP1*, pGEM-T-*PkDBPαII*, pDisplay-*AcGFP1* and pDisplay-*PkDBPαII-AcGFP1* were confirmed by sequencing services from First BASE Laboratories Sdn. Bhd. (Malaysia). The amino acid sequences of insert fragments were deduced from the nucleotide sequences using BioEdit Sequence Alignment Editor v7.2.3 (Hall, 1999). Basic Local Alignment Search Tool (BLAST) (https://blast.ncbi.nlm.nih.gov/Blast.cgi) (Altschul *et al.*, 1990) was used to compare these nucleotide and amino acid sequences to previously published *PkDBPαII* nucleotide and protein sequences (haplotype H2 and H47) available in the National Centre for Biotechnology Information (NCBI) database in order to confirm their identity. On the other hand, the nucleotide sequence of *AcGFP1* was translated and compared against the AcGFP1 sequence in the plasmid pAcGFP1-C1 (Clontech Laboratories, Inc., USA). Additionally, the isoelectric point (pI) for each PkDBPαII haplotype was determined using the isoelectric point calculator (IPC) (Kozlowski, 2016).

3.6.5 Mammalian COS-7 cell culture

3.6.5.1 Preparation of complete DMEM-high glucose media

Mammalian cell line, COS-7 (ATCC® CRL-1651™) cells were grown in complete DMEM-high glucose media supplemented with 10% heat-inactivated Fetal Bovine Serum (FBS), 1 mM Sodium pyruvate, 2 mM L-glutamine, 1× MEM non-essential amino acids and 1% Penicillin-streptomycin at 37 °C in a 5% CO_2 incubator. All reagents used were from Gibco™ (Invitrogen Corp., USA). The culture media was prepared under aseptic condition with various additions as follows:

Reagents	Volume (mL)
DMEM-high glucose	430.0
Fetal bovine serum	50.0

Sodium pyruvate (100 mM)		5.0
L-glutamine (200 mM)		5.0
MEM NEAA (100×)		5.0
Penicillin-Streptomycin (10,000 U/mL)		5.0
	Total volume	500.0

The freshly prepared complete DMEM-high glucose medium was stored at 4 °C.

3.6.5.2 Maintenance of COS-7 cells: thawing, sub-culture and cryopreservation

Cryovial containing the frozen COS-7 cells was removed from liquid nitrogen storage and immediately placed into a 37 °C water bath. The frozen COS-7 cells were quickly thawed by gently swirling in the 37 °C water bath until there is just a small bit of ice left in the vial. Then, the vial was transferred into a level-2 biosafety cabinet. Before opening the cap, the vial was immersed in 70% ethanol and handled aseptically. The COS-7 cells were carefully transferred into a T-75 tissue culture flask (75 cm^2) using a 1000-µL micropipette. Ten milliliters of pre-warmed complete DMEM-high glucose medium was added to a T-75 tissue culture flask containing revived COS-7 cells. The COS-7 cell cultures were gently rocked back and forth several times for homogenization. Finally, the cells were grown at 37 °C in a 5% CO_2 incubator.

For sub-culturing or cryopreservation, the T-75 flask containing confluence COS-7 cells were carefully removed from the CO_2 incubator and placed into a level-2 biosafety cabinet. The spent culture media was aspirated and discarded. Cell culture grade Dulbecco's Phosphate Buffered Saline (1× PBS) wash solution was added gently to the interior of the flask, opposite the attached cell layer to avoid disturbing the cell layer, and the culture flask was rocked back and forth several times. The wash solution was removed and discarded, and the washing step was repeated once more. Five milliliters of pre-warmed dissociation agent, TrypLE™ Express Enzyme (Gibco™, Invitrogen Corp.,

USA), were added to ensure complete coverage of COS-7 cell monolayer. The flask was incubated at 37 °C for about 5 – 10 min or until cells have detached. The complete detachment of cell monolayer was observed using an inverted microscope. Pre-warmed complete DMEM-high glucose medium, 20 mL was added to the flask and rinsed thoroughly. The cell suspension was transferred to a 50-mL centrifuge tube and spun at 1100 rpm for 10 min. The supernatant was aspirated and discarded carefully using a pipette. For sub-culturing, the pelleted COS-7 cells were seeded with pre-warmed complete DMEM-high glucose medium in a 1:8 ratio for optimum growth.

As for cryopreservation, the pelleted COS-7 cells were resuspended in chilled (2 – 8 °C) cryopreservation medium instead of complete culture medium. Two milliliters of Recovery™ Cell Culture Freezing Medium (Gibco™, Invitrogen Corp., USA) was used to gently resuspend the COS-7 cells pellet. The homogeneous cell suspension was dispensed in 1 mL aliquots into 2-mL cryovials. The cryovials containing the cell suspension were stored in liquid nitrogen.

3.6.6 Transfection of recombinant plasmid pDisplay-*PkDBPαII-AcGFP1* into mammalian COS-7 cells

For transfection, COS-7 cells were seeded into 6-well culture plates and transfected with the pDisplay-*PkDBPαII-AcGFP1* plasmid DNA using Lipofectamine™ 3000 transfection reagent (Invitrogen Corp., USA). The preparation of transfection reagent was performed in a level-2 biosafety cabinet and reagents were chilled to room temperature prior usage. Ten microliters of Lipofectamine 3000™ reagent were added to a 1.5-mL microcentrifuge tube containing 125 µL Opti-MEM® I Reduced-Serum Medium (Gibco™, Invitrogen Corp., USA) and mixed thoroughly by inverting the tube. Using another 1.5-mL microcentrifuge tube, 1 µg of plasmid DNA was resuspended with 125 µL Opti-MEM® I reduced-serum medium. The two mixtures were mixed gently and

incubated at room temperature for 15 min. Then, the DNA-lipid complex was added to 70 – 90% confluent COS-7 cells in a dropwise manner. The 6-well plate was rocked back and forth several times. The cells were allowed to grow at 37 °C in a 5% CO_2 incubator. After 24 h, the transfection medium was replaced with complete DMEM-high glucose culture medium and incubated for another 24 h. The confluent monolayer of transfected COS-7 cells was used in the Erythrocyte-binding assay.

3.6.7 Erythrocyte-binding assays

3.6.7.1 Pre-experiment preparation of erythrocytes

Erythrocytes from healthy human donor or macaque (*M. fascicularis*) were collected by venous puncture into lithium-heparin tubes. The lithium-heparin tubes were centrifuged at 1800 rpm for 5 min. The plasma supernatant with buffy coat fraction was discarded and the remaining erythrocytes were resuspended with twice its volume of incomplete RPMI 1640 medium. Then, it was subjected to centrifugation for 10 min at 1800 rpm and the supernatants were removed. The washing steps were repeated twice and the erythrocytes were finally resuspended to an approximate 50% hematocrit (e.g. 1 mL of packed erythrocytes resuspended with 1 mL of incomplete RPMI 1640 medium). Washed erythrocytes (50% hematocrit) were stored at 4 °C. Finally, erythrocytes were further diluted with incomplete DMEM-high glucose medium to achieve 1% hematocrit, prior to the incubation in the Erythrocyte-binding assay.

3.6.7.2 Incubation of erythrocytes on transfected COS-7 cells

Confluent monolayer of COS-7 cells were used 48 h after transfection. Six-well plate containing transfected cells was carefully taken to level-2 biosafety cabinet. For each well, spent culture medium was gently aspirated and discarded using a pipette. The COS-7 cells were carefully washed with 1× PBS and the supernatant was discarded.

The washing steps were repeated for twice. Finally, 2 mL of human erythrocytes [Duffy-positive Fy(a+b–) phenotype, blood group O+, 1% hematocrit in incomplete DMEM-high glucose] were gently added into each well and incubated for 2 h at 37 °C in a 5% CO_2 incubator. For Erythrocyte-binding assay with macaque (*M. fascicularis*) erythrocytes, 2 mL of macaque erythrocytes (1% hematocrit) were used. All Erythrocyte-binding assays were performed in triplicates.

3.6.7.3 Cells fixation and fluorescence microscopy

After 2 h of incubation, the 6-well plate was taken to level-2 biosafety cabinet and subjected to several washings to remove non-adherent erythrocytes. The erythrocytes were gently aspirated and discarded. Then, 1 mL of 1% paraformaldehyde (diluted in 1× PBS) was added for cell morphology fixation, incubated for 10 min and the solution was discarded. The nuclei of COS-7 cells were stained with 1 µg/mL Hoechst 33342 dye (Invitrogen Corp., USA). For staining, 2 µL of Hoechst 33342 nuclei dye (1 mg/mL) diluted in 2 mL of 1× PBS solution was added into each well, incubated for 1 min and the solution was discarded. Finally, 2 mL of 1× PBS was gently added into each well.

The transfected green fluorescent COS-7 cells with bound erythrocytes (rosette) were counted using fluorescence microscopy with a FITC-filter (488 nm excitation wavelength) mounted on a Nikon ECLIPSE TE300 inverted microscope (Nikon, Japan). Rosettes were evaluated at 200× magnification. Positive rosettes were defined as adherent erythrocytes covering more than 50% of COS-7 cell surface (Michon *et al.*, 2000; Cheng *et al.*, 2013; Cheng *et al.*, 2016). Binding was scored negative when no rosettes were seen in the entire well.

3.6.8 Evaluation of the recombinant PkDBPαII binding specificity

To assess the binding specificity of the recombinant PkDBPαII, human and macaque erythrocytes were incubated with the anti-Fy6 monoclonal antibody (1 mg/μL) at 1:2000 dilution in incomplete DMEM at 37 °C for 1 h prior to the incubation with the transfected COS-7 cells. Anti-Fy6, which recognizes the Fy6 epitope on the DARC N-terminal region, was kindly provided by Professor Laurent Rénia (Singapore Immunology Network, A*Star). For treatment of erythrocytes, 5 μL of anti-Fy6 monoclonal antibody was pipetted into a 15-mL centrifuge tube containing 10 mL of diluted erythrocytes (1% hematocrit) in a level-2 biosafety cabinet. The mixture was incubated for 1 h at 37 °C in a 5% CO_2 incubator. Erythrocyte-binding assays using anti-Fy6-treated erythrocytes were performed as mentioned in section 3.6.7.

3.6.9 Statistical analysis

The overall statistical analysis was conducted using the GraphPad Prism (version 7.03) statistical software (GraphPad Software., USA) and Microsoft Excel 2016 (Microsoft, USA). For Erythrocyte-binding assays, two-way ANOVA was used to compare the mean differences of each group. Differences of $p < 0.05$ were considered significant.

3.7 Binding affinity of PkDBPαII using Isothermal Titration Calorimetry (ITC)

3.7.1 PCR of *PkDBPαII* for cloning into pET30a(+) vector

Novagen® pET30a(+) vector (Merck KGaA., Germany) is a prokaryotic expression system developed for the cloning and expression of recombinant proteins in *E. coli*. The *PkDBPαII* region was amplified by specific primers containing a *Bam*HI restriction enzyme cut site (Table 3.1) according to the following:

Reagent	**Volume (µL)**
ddH_2O	10.3
5× PCR buffer (20 mM $MgCl_2$)	5.0
$MgCl_2$ (25 mM)	4.0
10 mM dNTPs (2.5 mM each)	0.5
PkDBPαII-pDisplay_forward primer (10 µM)	0.5
PkDBPαII-pDisplay_reverse primer (10 µM)	0.5
GoTaq® Flexi DNA polymerase (5 U/µL)	0.2
DNA template/ddH_2O*	4.0
Total reaction volume	25.0

*ddH_2O, instead of *P. knowlesi* DNA template was added into the non-template control (NTC) reaction.

The PCR amplification reaction was commenced with an initial denaturing step at 94°C for 5 min, followed by 35 cycles at 94 °C for 45 s, 51.5 °C for 45 s and 72 °C for 70 s. A final 10 min extension at 72 °C was added to the last cycle and the reaction was held at 4 °C. PCR products were visualized under UV after running electrophoresis on a 1% agarose gel. The remaining PCR amplicons were stored at –20 °C. All amplicons were cloned into pGEM®-T vector system sequenced.

3.7.2 Agarose gel electrophoresis

Agarose gel, 1.0% was used for gel electrophoresis. The preparation of agarose gel and gel electrophoresis was performed as mentioned in section 3.6.2. Then, the gel was visualized using Molecular Imager® Gel Doc™ XR+ Imaging System.

3.7.3 Cloning of PCR products into pGEM®-T Vector

Before cloning into pET30a(+) vector system, the *PkDBPαII* gene of clinical isolates from Peninsular Malaysia and Malaysian Borneo were cloned into pGEM®-T vector system as mentioned in section 3.6.3.

3.7.4 Cloning of target fragments into pET30a(+) vector

3.7.4.1 Digestion of pGEM-T-*PkDBPαII* plasmids with RE

RE *Bam*HI-HF (high-fidelity) was used to digest the extracted pGEM-T-*PkDBPαII* plasmid using the following reagents:

Reagent	**Volume (µL)**
Plasmid DNA	25.0
RE *Bam*HI-HF (New England Biolabs, Inc., USA)	2.0
10× CutSmart buffer	4.0
ddH_2O	9.0
Total reaction volume	40.0

The digestion mixture was incubated at 37 °C for 3 h.

3.7.4.2 Digestion and dephosphorylation of expression vector pET30a(+)

The pET30a(+) plasmid was digested RE *Bam*HI-HF. Digestion of pET30a(+) was carried out as mentioned in section 3.7.4.1. The dephosphorylation of RE digested pET30a(+) plasmid was carried out as mentioned in section 3.6.4.2.

3.7.4.3 Purification of digested fragments and pET30a(+) plasmids

Agarose gel electrophoresis was performed on digested pGEM-T-*PkDBPαII* and pET30a(+) plasmids using 1.0% agarose gel. Digested target fragments with expected size were carefully excised from the gel and purified using QIAquick® Gel Extraction Kit as mentioned in section 3.6.3.1.

3.7.4.4 Ligation of purified target fragments into pET30a(+) vector system

Ligation of purified target fragments of *PkDBPαII* into pET30a(+) was performed with the following reagents:

Reagent	**Volume (µL)**
*Bam*HI-digested pET30a(+) vector	2.0
*Bam*HI-digested *PkDBPαII*	6.0
T4 DNA ligase (New England Biolabs, Inc., USA)	1.0
10× ligation buffer	1.0
Total reaction volume	10.0

The ligation mixture was incubated at 16 °C for overnight.

3.7.4.5 Transformation into maintenance host *E. coli* TOP10F' cells

The ligation mixture was transformed into propagation host *E. coli* TOP10F' competent cells as described in section 3.6.4.5. The transformed cells were resuspended in 100 µL LB broth and spread on pre-warmed LB agar plate containing 30 µg/mL kanamycin. The plate was incubated overnight at 37 °C.

3.7.4.6 Directional PCR and plasmid extraction of positive recombinant clones

Directional PCR was carried out using similar protocol as described in section 3.6.4.6., by using T7 promoter and *PkDBPαII*-pET30a(+)_reverse primers. The plasmids of

selected positive recombinant clones were extracted using commercialized QIAprep® Spin Miniprep kit as mentioned in section 3.6.3.5.

3.7.4.7 Transformation into competent *E. coli* expression host T7 Express *lysY/I^q*

Successive pET30a(+)-*PkDBPαII* plasmids for Peninsular Malaysia and Malaysian Borneo were transformed into *E. coli* expression host T7 Express *lysY/I^q* (New England Biolabs, Inc., USA). Cryovials containing T7 Express *lysY/I^q* (high efficiency) competent cells were thawed on ice for 1 – 2 min. For the initial 30 min incubation on ice, 0.5 µL of pET30a(+)-*PkDBPαII* plasmids were added into the tube and mixed gently by tapping. The transformation procedures were performed as mentioned in section 3.6.3.3. Finally, the pelleted bacterial cells were resuspended in 100 µL LB broth and finally spread on pre-warmed LB agar plate containing 34 µg/mL chloramphenicol and 30 µg/mL kanamycin. The plate was incubated overnight at 37 °C.

3.7.4.8 Directional PCR for selection of positive recombinant clones

Directional PCR was performed to ensure pET30a(+)-*PkDBPαII* plasmids were successfully transformed into T7 Express *lysY/I^q* expression host. The PCR reaction was carried out as mentioned in section 3.7.4.6.

3.7.4.9 Confirmation of inserted *PkDBPαII* nucleotide and deduced amino acid sequences by sequence analysis

Nucleotide sequence of the recombinant plasmids pET30a(+)-*PkDBPαII* from Peninsular Malaysia and Malaysian Borneo were confirmed by sequencing services from First BASE Laboratories Sdn. Bhd. (Malaysia). The sequence analysis of pET30a(+)-*PkDBPαII* was performed as mentioned in section 3.6.4.8.

3.7.5 Expression of recombinant PkDBPαII in *E. coli* expression system

3.7.5.1 Small-scale protein expression

Single recombinant T7 Express *lysY/I*^{q} colony carrying PkDBPαII from Peninsular Malaysia and Malaysia Borneo were inoculated and propagated overnight in LB medium containing 34 µg/mL chloramphenicol and 30 µg/mL kanamycin, shaken at 37 °C and 250 rpm. Next day, the overnight bacterial cultures were diluted with LB broth to achieve optical density (OD_{600}) of 0.1 with a final volume of 10 mL, and the cultures were allowed to grow exponentially to OD_{600} value of 0.4 to 0.6. IPTG stock solution (100 mM), 100 µL, were added aseptically into the cultures for induction of protein expression. The bacterial cultures were incubated at 37 °C and 250 rpm. Cell culture fractions, 1 mL, was collected before IPTG induction and at every 2 h interval up to 6 h after induction. Finally, the bacterial cultures were harvested by centrifugation at 6500 rpm for 10 min. For negative control, non-recombinant clone [carrying pET30a(+) only] was used.

3.7.5.2 Large-scale protein expression

Scale-up protein expression was performed to produce larger amounts of recombinant PkDBPαII from Peninsular Malaysia and Malaysian Borneo. Recombinant PkDBPαII was expressed in volume of 1000 mL with expression conditions as mentioned in section 3.7.5.1.

3.7.6 Analysis of expressed PkDBPαII

3.7.6.1 SDS-PAGE analysis

Collected cell culture fractions at different time intervals were analyzed under denaturing conditions. Bacterial culture pellets were resuspended in 25 µL PBS solution and 25 µL of 2× sample buffer was added. The crude protein samples were boiled for 15 min. Samples of each time point were analyzed using SDS-PAGE by loading 5 µL of

the boiled samples into different wells on a 12% SDS-PAGE gel. The electrophoresis was carried out at 100 V for 90 min. The SDS-PAGE gel was stained with Coomassie Brilliant Blue staining solution for 3 min and destained overnight with destaining solution. The recombinant protein bands with expected size on the SDS-PAGE gel were identified.

3.7.6.2 Western Blot assay

The crude proteins were separated by SDS-PAGE. Before electroblotting, the SDS-PAGE gel with protein samples and western blot papers were soaked in transfer buffer for 10 min whereas PVDF membrane (Bio-Rad, USA) was soaked in absolute methanol for 5 min prior to incubation in transfer buffer. Electroblotting was performed at 15 V for 40 min using Trans-Blot® SD Semi-Dry Electrophoretic Transfer Cell Unit (Bio-Rad, USA). Next, the PVDF membrane was blocked overnight in TBS solution containing 5% skimmed milk at 4 °C. Next day, the membrane was washed 3 times with 0.2% TBS-T solution before probing with Novagen® His•Tag® monoclonal antibody (Merck KGaA., Germany) at 1:2000 dilution in TBS containing 2.5% skimmed milk, where it was incubated for 1 h with constant shaking at room temperature. The membrane was washed 3 times, followed by incubation of biotin-labeled goat anti-mouse IgG (KPL, USA) at 1:2500 dilution in TBS containing 2.5% skimmed milk for 1 h with constant shaking at room temperature. Again, the membrane was washed 3 times and incubated with streptavidin-alkaline phosphatase (Invitrogen Corp., USA) at 1:2500 dilution in TBS containing 2.5% skimmed milk for 1 h at room temperature. Finally, the membrane was washed three times and the protein bands were revealed by adding the chromogenic substrate NBP/BCIP (Sigma-Aldrich, Inc., USA). The purple intensity of the membrane was developed at room temperature in the dark. The membrane was washed with ddH_2O, dried and photographed.

3.7.7 Purification of PkDBPαII

The recombinant PkDBPαII proteins from clinical isolates of Peninsular Malaysia and Malaysian Borneo were affinity-purified by using ProBond™ purification system (Invitrogen Corp., USA) under hybrid condition. The pH of all purification reagents or buffers were re-adjusted to their respective optimum pH before used.

3.7.7.1 Bacterial cell lysates preparation

Bacteria cells expressing recombinant PkDBPαII proteins were harvested from 1000 mL cultures. Bacteria cultures were divided into four 50-mL centrifuge tubes and pelleted at 6500 rpm for 10 min. All supernatants were discarded and the final cell pellets in each tube were resuspended in 8 mL of pre-warmed (37 °C) guanidinium lysis buffer. The cell lysate was rocked at room temperature for 10 min to promote cell lysis. Next, the turbid cell lysates were sonicated on ice at high intensity until the lysates turned into translucent solutions. Cell lysates were centrifuged at 5000 rpm for 15 min to pellet the cellular debris. The supernatants were harvested and transferred to new tubes.

3.7.7.2 Preparation of affinity purification column

For purification using hybrid condition method, the purification polypropylene columns (Qiagen, Germany) were prepared under denaturing condition. Nickel-NTA agarose resin (Qiagen, Germany) was brought to room temperature and resuspended in its bottle by inverting and gently tapping the bottle repeatedly, and 2 mL of nickel-NTA agarose resin was pipetted into each purification column. The resin was pelleted gently by low-speed centrifugation at 800 rpm for 1 min. The supernatant was aspirated carefully using a pipette. Then, the resin was washed with 6 mL of sterile ddH_2O and pelleted gently by centrifugation at 800 rpm for 1 min. Next, the resin was resuspended in 6 mL denaturing binding buffer (pH 7.8). The resin was pelleted by centrifugation at 800 rpm

for 1 min and the supernatant was aspirated gently using a pipette. Again, the resin was resuspended with another 6 mL of denaturing binding buffer and pelleted by centrifugation at 800 rpm for 1 min. The supernatant was aspirated gently.

3.7.7.3 Purification procedure

Ten milliliters of PkDBPαII cell lysates were added to the prepared purification polypropylene columns. The lysates were allowed to bind on resin for 2 h on ice with gentle rocking to keep the resin suspended in the lysate solution. The resin was pelleted under low-speed centrifugation at 800 rpm for 1 min and the supernatant was aspirated gently. Next, the resin was resuspended in 4 mL of denaturing binding buffer (pH 7.8) for 2 min and washed by centrifuging at 800 rpm for 1 min. The supernatant was aspirated gently. The resin was washed twice with denaturing binding buffer (pH 7.8). Then, the resin was resuspended in 4 mL of denaturing wash buffer (pH 6.0) and washed gently by rocking for 2 min. The resin was pelleted at 800 rpm for 1 min and the supernatant was aspirated carefully. The resin was washed twice with denaturing wash buffer (pH 6.0). Next, the resin was resuspended in 8 mL of native wash buffer (pH 8.0) and washed gently by rocking for 2 min. The resin was pelleted at 800 rpm for 1 min and the supernatant was aspirated carefully. The resin was washed with native wash buffer for a total of four washes. Finally, the columns were clamped in a vertical position and the caps on the lower end of the columns were snapped off. The purified proteins were eluted with native elution buffer (pH 8.0) in 1-mL aliquots and stored at –80 °C.

3.7.7.4 Dialysis of purified PkDBPαII

For protein refolding, dialysis was performed on purified PkDBPαII using Slide-A-Lyzer™ G2 dialysis cassettes, 10K MWCO (Thermo Scientific™, USA). Dialysis buffer (1× PBS), 1800 mL was poured into a 2000 mL beaker and pre-cooled on ice. Slide-A-

Lyzer™ G2 dialysis cassettes were immersed in dialysis buffer for 2 min. The cassettes were removed from the dialysis buffer and placed on a paper towel. Then, the cassettes were opened by gently twisting the cap counter-clockwise until it stops and pulled out. Three milliliters of purified PkDBPαII were pipetted slowly into dialysis cassettes. The excess air in the cassettes was removed by simultaneously pressing the membrane gently on both sides and inserting the cap. The cap was inserted and locked by gently twisting it clockwise. The filled dialysis cassettes were floated vertically in the dialysis buffer and stirred gently. The proteins were dialyzed for 6 h. The dialysis buffer was replaced with new dialysis buffer and the proteins were allowed to dialyze overnight in cold room. Next day, dialysis buffer was replaced again with new dialysis buffer and the proteins were dialyzed for another 6 h. Finally, the dialyzed cassettes were removed from the buffer. The dialyzed protein samples were retrieved carefully by slowly aspirating while inserting the pipette towards the bottom of the cassette. Dialysis buffer was stirred on ice and in cold room using stirrer throughout the whole dialysis process. The dialyzed protein samples were concentrated at 5000 rpm for 15 min using Vivaspin® centrifugal concentrator (Sartorius, Germany).

3.7.8 Analysis of purified PkDBPαII

3.7.8.1 SDS-PAGE analysis

Purified PkDBPαII, 25 µL were added to 25 µL of 2× sample buffer. Samples were boiled for 5 min and analyzed using SDS-PAGE by loading 10 µL of the boiled samples into different wells on a 12% SDS-PAGE gel. Electrophoresis was performed as mentioned in section 3.7.6.1.

3.7.8.2 Western Blot assay

Purified PkDBPαII was separated using electrophoresis by loading 10 µL of the boiled samples into different wells on a 12% SDS-PAGE gel. Western Blot assay for purified PkDBPαII was performed using the same protocol as mentioned in section 3.7.6.2.

3.7.8.3 Confirmation of the recombinant protein identity by MALDI-TOF Mass Spectrometry analysis

The fragments of each purified PkDBPαII were carefully excised from the SDS-PAGE gel and sent to University Malaya Center for Proteomics Research (UMCPR) for MALDI-TOF MS analysis.

3.7.9 Protein quantification of purified PkDBPαII

The concentration of purified PkDBPαII was determined using commercialized Quick Start™ Bradford protein assay (Bio-Rad, USA). Bovine serum albumin (BSA) with concentrations of 2.0 mg/mL, 1.5 mg/mL, 1.0 mg/mL, 0.75 mg/mL, 0.5 mg/mL, 0.25 mg/mL, and 0.125 mg/mL were used as standards, while water was used as blank. The 1× dye reagent was brought to room temperature and inverted a few times before use. BSA standards and purified PkDBPαII samples, 5 µL were pipetted into separate microplate wells containing 250 µL of 1× dye reagent. The mixtures were homogenized by rocking back and forth, then, incubated at room temperature for 5 min under dark condition. Finally, the absorbance of the standards and purified PkDBPαII samples were measured at a wavelength of 595 nm using microplate reader Infinite® M200 Pro NanoQuant (Tecan Group Ltd., Switzerland). Standards and purified PkDBPαII samples were run in duplicates. The average reading of blank values was subtracted from the average values of standards and purified PkDBPαII samples. A standard curve was generated by plotting the absorbance of standard BSA at 595 nm (Y-axis) against

concentration in mg/mL (X-axis). The concentrations of purified PkDBPαII from Peninsular Malaysia and Malaysian Borneo were determined using the standard curve.

3.7.10 Evaluation of binding affinity using Isothermal Titration Calorimetry (ITC)

Isothermal Titration Calorimetry (ITC) is designed to measure the heat of binding when the ligand is injected into the sample cell containing the receptor molecules and vice versa.

3.7.10.1 Sample preparation

Freshly drawn erythrocytes acquired from the healthy human donor was prepared as mentioned in section 3.6.7.1. The human erythrocytes (50% hematocrit) were serially diluted with 1× PBS to obtain human erythrocytes with 0.001% hematocrit. Firstly, 20 µL of washed human erythrocytes (50% hematocrit) were pipetted into 1 mL microcentrifuge tube containing 980 µL of 1× PBS. The mixture was mixed thoroughly by inverting and the resulting hematocrit is 1%. Then, the mixture was further diluted 10-folds for three times with 1× PBS until the final hematocrit of 0.001% was obtained. Finally, dialysis was performed on the diluted human erythrocytes (0.001% hematocrit) using procedures as mentioned in 3.7.7.4.

Purified PkDBPαII from Peninsular Malaysia and Malaysian Borneo were resuspended in 1× PBS to obtain the desired concentration for ITC experiments. Purified PkDBPαII with concentration 10 µM was used.

3.7.10.2 Binding affinity assessment

ITC experiments of PkDBPαII binding to human erythrocytes were performed on MicroCal™ Auto-iTC200 (Malvern Instruments Ltd, UK) at a temperature of 37 °C. In a 96-deep well microtiter plate, 1.5 mL of human erythrocytes (0.001% hematocrit) were

loaded into the well position (cell source) that is to be transferred to the sample cell compartment. Next, 120 µL of purified PkDBPαII (10 µM) was pipetted into well position (syringe source) that is to be transferred to the syringe compartment. The ITC method parameters were performed with default settings as shown in the following:

Parameter	**Value**
Total number of injections	20
Cell temperature (°C)	37
Reference power (µCal/s)	10
Stirring speed (rpm)	1000
Initial injection volume (µL)	0.4
Initial spacing duration (s)	150
Subsequent injection volume (µL)	2.0
Subsequent spacing duration (s)	150

3.7.10.3 Data analysis using MicroCal Auto-iTC$_{200}$ software

The ITC data analysis was performed with the MicroCal Auto-iTC$_{200}$, Origin software (Malvern Instruments Ltd, UK). The binding affinity (K_D) of PkDBPαII from Peninsular Malaysia and Malaysian Borneo with human erythrocytes were calculated based on the formula, $K_D = 1 / K_A$, where K_A value was obtained by using the One-Site analysis method provided in the user manual.

CHAPTER 4: RESULTS

4.1 Binding activity of PkDBPαII using Erythrocyte-binding assays (EBAs)

4.1.1 Duffy genotyping of healthy human erythrocyte

Duffy genotyping was successfully performed on the extracted human genomic DNA from the healthy donor using allele specific PCR strategies for the presence of *FY*A*, *FY*B* and *FY*B^{es}* alleles. Each amplified allele is ~ 700 base pairs (bp). The Duffy genotype of the healthy human donor used in Erythrocyte-binding assays and Isothermal Titration Calorimetry was confirmed to be homozygous *FY*A*, resulting in Fy(a+b−) phenotype (Figure 4.1).

4.1.2 Construction of recombinant plasmids for COS-7 cell surface expression

4.1.2.1 PCR amplification of *PkDBPαII* and *AcGFP1* genes

Genomic DNA of *P. knowlesi* clinical isolates, HAN (Peninsular Malaysia) and SBH31 (Malaysian Borneo), were successfully extracted. The *PkDBPαII* gene was amplified by gene-specific primers containing *Bgl*II (AGATCT) restriction enzyme (RE) cut site with expected size of ~ 1011 bp (Figure 4.2 A).

The *AcGFP1* gene was amplified from pAcGFP1-C1 plasmid using gene-specific primers containing *Sal*I (GTCGAC) RE cut site with expected size of ~ 723 bp (Figure 4.2 B).

4.1.2.2 Cloning of *PkDBPαII* and *AcGFP1* fragments into pGEM®-T vector system

PCR products of *PkDBPαII* (~ 1011 bp) and *AcGFP1* (~ 723 bp) were purified and ligated into pGEM®-T vector using the commercialized pGEM®-T Vector System I (Promega., USA). The linearized pGEM®-T vector has a single overhang 3'- deoxythymidine (T) residue to facilitate the ligation of PCR product to the vector

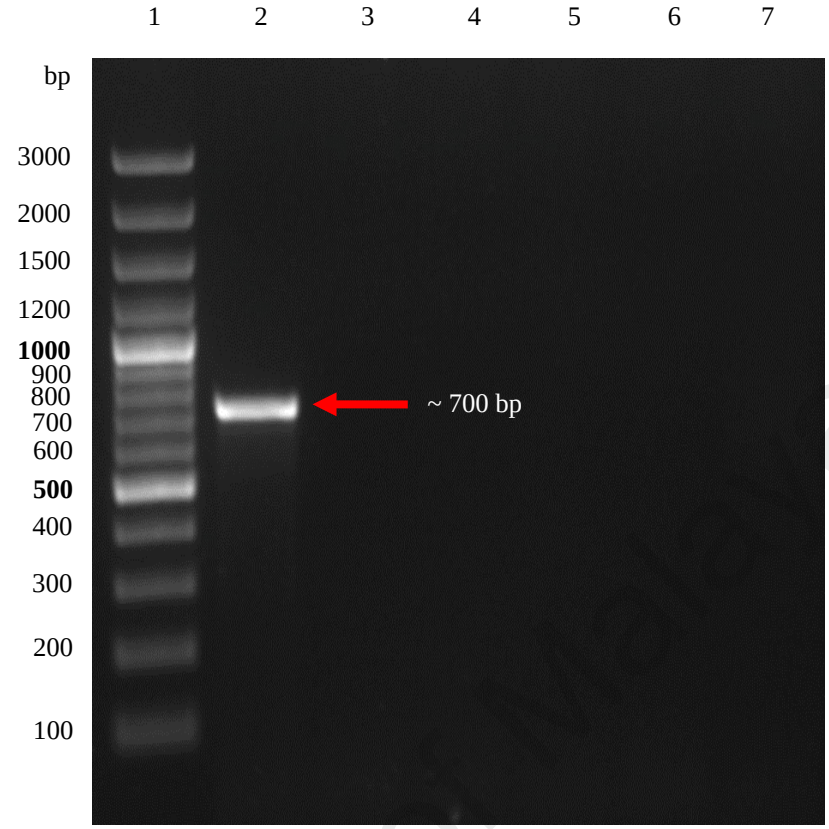

Figure 4.1: Agarose gel electrophoresis of Duffy genotyping of the healthy human donor. PCR amplification of *FY*A* allele with expected size of ~ 700 bp (lane 2). No amplifications were observed for *FY*B* and *FY*B*^{es} alleles (lanes 3 and 4, respectively). Lanes 5 – 7 denote NTC (ddH_2O) for PCR amplification of *FY*A*, *FY*B* and *FY*B*^{es} alleles, respectively. Lane 1 denotes DNA ladder.

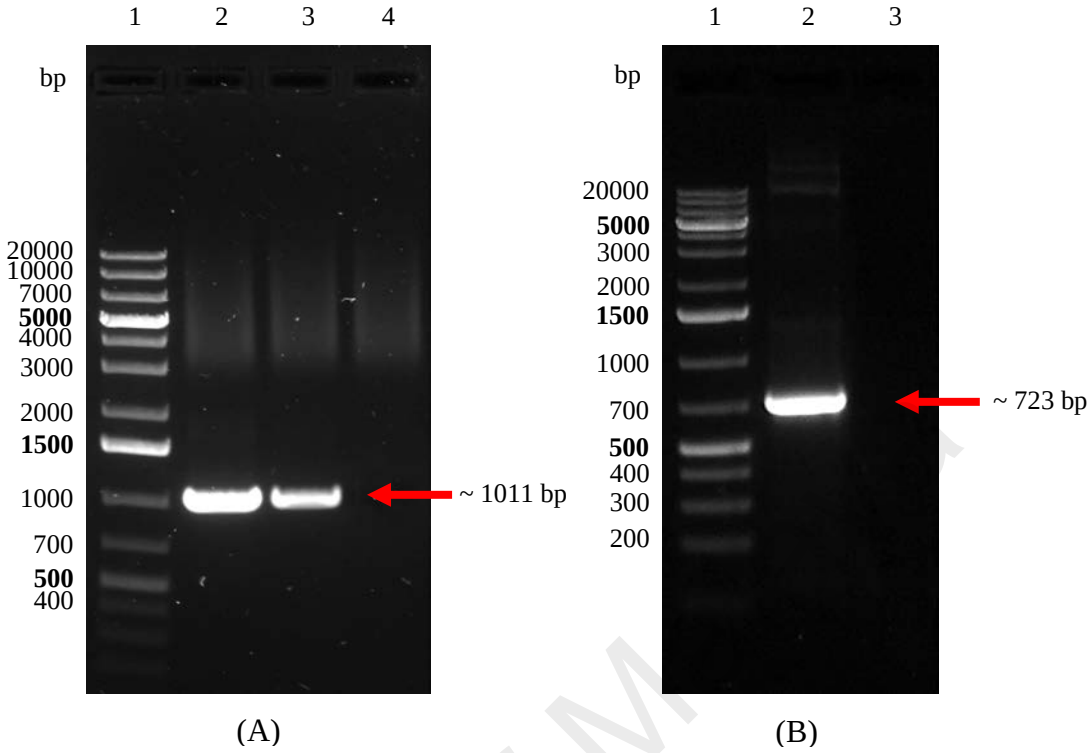

Figure 4.2: Agarose gel electrophoresis of PCR products for (A) *PkDBPαII* and (B) *AcGFP1* gene amplification. (A) PCR amplification of Peninsular Malaysia *PkDBPαII* (lane 2) and Malaysian Borneo *PkDBPαII* (lane 3) generated PCR bands with expected size of ~ 1 kb; Lane 4 denotes NTC (ddH_2O). (B) PCR amplification of *AcGFP1* generated PCR product with expected size of ~ 723 bp (lane 2); Lane 3 denotes NTC (ddH_2O). Lane 1 in both panels denotes DNA ladder.

efficiently through T-A complementary pairing (Appendix C). Overnight ligation mixtures were transformed into propagation and maintenance host *E. coli* TOPF10' cells and incubated overnight at 37 °C.

Six colonies from each transformation plate were chosen and colony PCR was carried out using M13F (-40) and M13R (-48) primers. PCR of the positive recombinant clones of pGEM-T-*PkDBPαII* generated PCR products of ~ 1.2 kb (1011 bp of *PkDBPαII* plus ~ 260 bp of the flanking regions between the M13 forward and reverse primers of the vector) (Figure 4.3 A), while the positive recombinant clones pGEM-T-*AcGFP1* generated PCR products of ~ 983 bp (723 bp of *AcGFP1* plus ~ 260 bp of the flanking regions) (Figure 4.3 B). Non-recombinant clones (no insert) showed expected size of ~ 260 bp. Plasmids of positive recombinant clones of pGEM-T-*PkDBPαII* and pGEM-T-*AcGFP1* were extracted and sent to a commercial laboratory for sequencing (First BASE Laboratories Sdn. Bhd).

4.1.2.3 Cloning of target fragments into pDisplay™ vector

The pDisplay™ vector (Invitrogen Corp., USA) is a mammalian expression system that is designed to target protein expression on the cell surface. In this study, the *AcGFP1* fluorescent reporter gene was added to the C-terminal insert site of pDisplay™ plasmid to facilitate direct visualization of transfected COS-7 cells with recombinant PkDBPαII. For construction of recombinant pDisplay-*PkDBPαII-AcGFP1* plasmid, the *AcGFP1* gene was first inserted into *Sal*I RE cut site of pDisplay™ plasmid, followed by the insertion of *PkDBPαII* gene into *Bgl*II RE cut site (in-frame insertion).

Positive recombinant pGEM-T-*AcGFP1* and pDisplay™ plasmids were digested with RE *Sal*I. The digested recombinant pGEM-T-*AcGFP1* plasmids showed

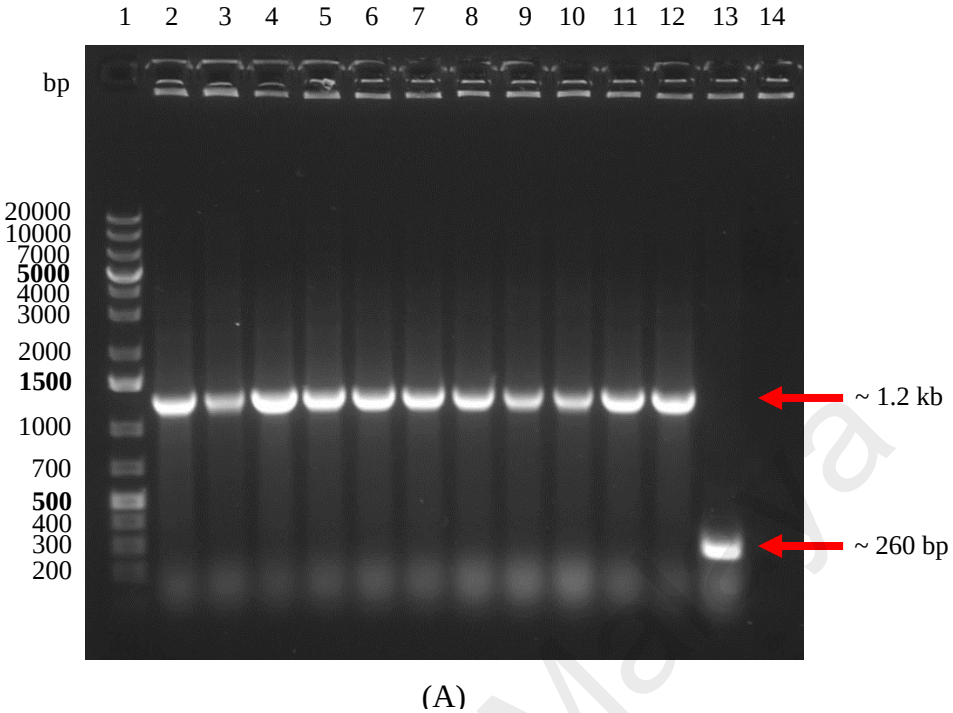

(A)

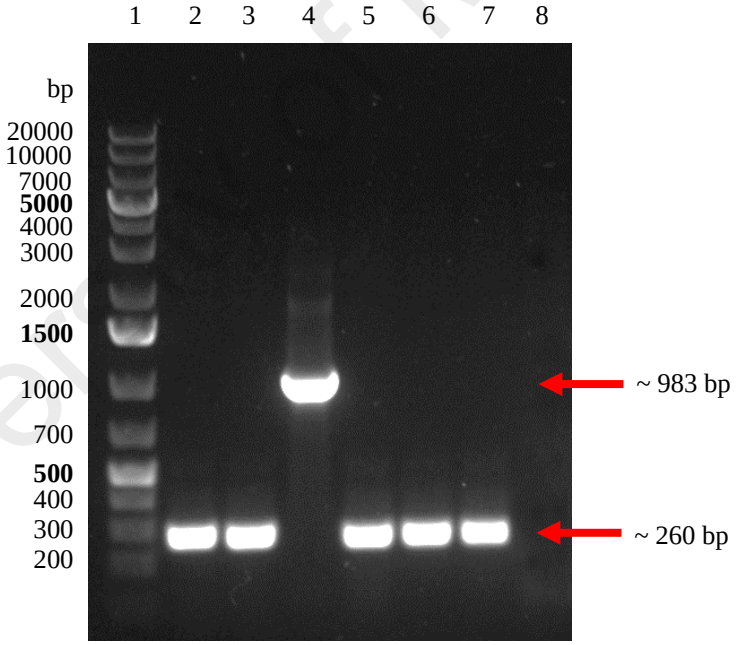

(B)

Figure 4.3: Agarose gel electrophoresis of colony PCR for selection of positive recombinant pGEM-T-*PkDBPαII* and pGEM-T-*AcGFP1* in TOP10F' cells. (A) Positive clones of recombinant pGEM-T-*PkDBPαII* of Peninsular Malaysia (lanes 2 – 7) and Malaysian Borneo (lanes 8 – 12); Lane 13 denotes non-recombinant clone; Lane 14 denotes NTC (ddH_2O). (B) Positive clone of recombinant pGEM-T-*AcGFP1* (lane 4); Lanes 2, 3, 5, 6, and 7 denote non-recombinant clones; Lane 8 denotes NTC (ddH_2O). Lane 1 in both panels denotes DNA ladder.

pGEM-T plasmids with expected size of ~ 3 kb and *AcGFP1* fragment with expected size of ~ 723 bp (Figure 4.4 A), while the digestion of pDisplay™ plasmids generated linearized plasmids with of 5.3 kb (Figure 4.4 B).

Target fragments of *AcGFP1* and linearized pDisplay™ plasmids were excised from agarose gel and purified using QIAquick® Gel Extraction Kit (Qiagen, Germany). Purified *AcGFP1* fragments were ligated to linearized pDisplay™ vector and transformed into TOP10F' cells. Five colonies were selected and directional PCR was performed to ensure sense orientation of the cloned fragments. For selection of positive recombinant pDisplay-*AcGFP1* clones with the insert in the sense orientation, *AcGFP1*-pDisplay_forward primer and BGH reverse primer were used. Figure 4.5 shows the agarose gel electrophoresis of PCR products, with the positive recombinant pDisplay-*AcGFP1* clone showing a size of ~ 983 bp (723 bp of *AcGFP1* plus ~ 260 bp of vector). No amplification was detected for non-recombinant clones or clones with the insert in the antisense orientation.

Positive recombinant plasmids of pDisplay-*AcGFP1* were excised from agarose gel and purified using QIAquick® Gel Extraction Kit (Qiagen, Germany). The purified recombinant pGEM-T-*PkDBPαII* and pDisplay-*AcGFP1* plasmids were then digested with RE *Bgl*II. Digestion of pGEM-T-*PkDBPαII* plasmids generated pGEM-T plasmid with expected size of ~ 3 kb and *PkDBPαII* fragments with expected size of ~ 1 kb (Figure 4.6 A), while the digested pDisplay-*AcGFP1* plasmid generated linearized plasmid with a size of ~ 6 kb (Figure 4.6 B).

Target fragments of Peninsular Malaysia *PkDBPαII*, Malaysian Borneo *PkDBPαII* and the linearized pDisplay-*AcGFP1* plasmids were excised from agarose gel and purified using QIAquick® Gel Extraction Kit (Qiagen, Germany). Purified target fragment of *PkDBPαII* for each haplotype were ligated to respective linearized pDisplay-*AcGFP1* plasmids. The ligation mixtures were then transformed into TOP10F' cells.

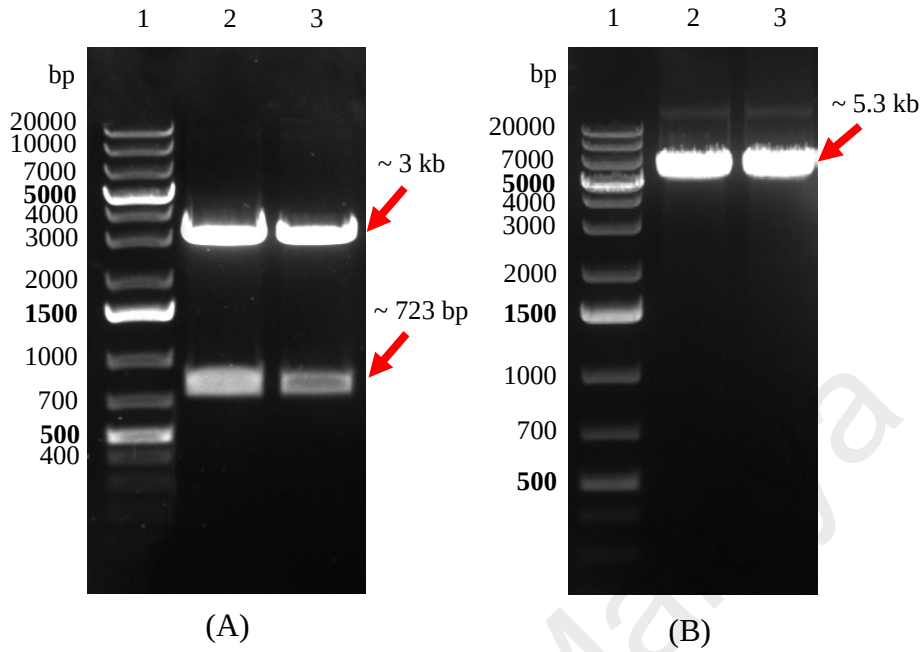

Figure 4.4: Agarose gel electrophoresis of restriction digestion of recombinant pGEM-T-*AcGFP1* and pDisplay™ plasmids. (A) Digested pGEM-T-*AcGFP1* (~ 3 kb) and *AcGFP1* fragments (~ 723 bp) (lanes 2 and 3). (B) Linearized plasmids of pDisplay™ (~ 5.3 kb) (lanes 2 and 3). Lane 1 in both panels denotes DNA ladder.

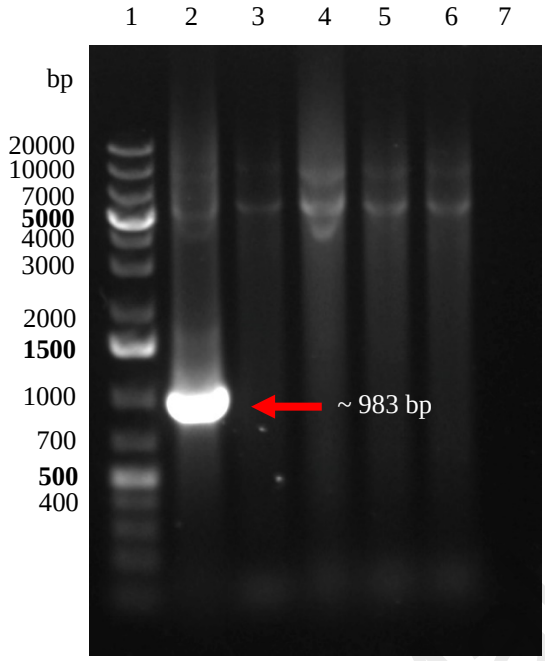

Figure 4.5: Agarose gel electrophoresis of directional PCR for selection of positive recombinant pDisplay-*AcGFP1* in TOP10F' cells. Positive recombinant pDisplay-*AcGFP1* clone with insert in the sense orientation generated PCR band of ~ 983 bp (lane 2); No amplification was detected for non-recombinant clones or clones with antisense orientation (lanes 3 – 6); Lane 7 denotes NTC (ddH_2O); Lane 1 denotes DNA ladder.

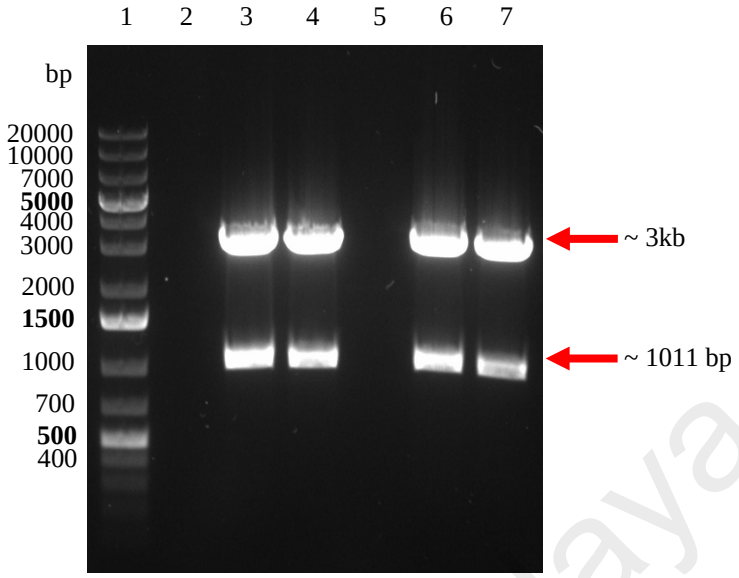

(A)

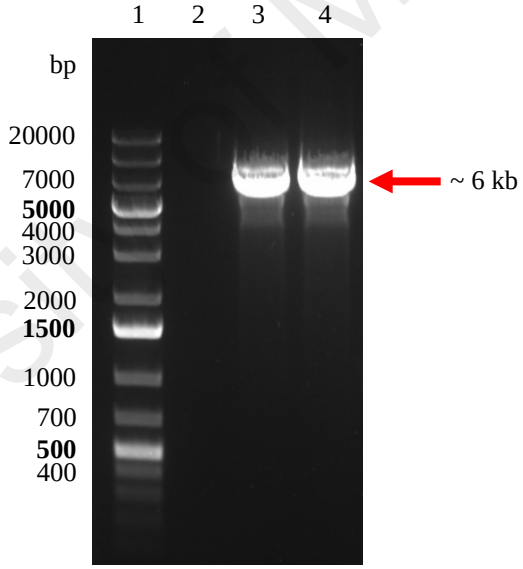

(B)

Figure 4.6: Agarose gel electrophoresis of restriction digestion of recombinant pGEM-T-*PkDBPαII* and pDisplay-*AcGFP1* plasmids. (A) Digested pGEM-T-*PkDBPαII* plasmids of Peninsular Malaysia (lanes 3 and 4) and Malaysian Borneo (lanes 6 and 7); Lanes 2 and 5 denote empty lanes. (B) Linearized plasmids of pDisplay-*AcGFP1* (~ 6 kb) (lanes 3 and 4); Lane 2 denotes empty lane. Lane 1 in both panels denotes DNA ladder.

Twelve colonies on each transformation plate were chosen for the selection of positive recombinant pDisplay-*PkDBPαII-AcGFP1* clones with the insert in the sense orientation. Directional PCR was carried out using T7 promoter primer and *PkDBPαII*-pDisplay_reverse primer. Figure 4.7 shows the agarose gel electrophoresis of PCR products, with the positive recombinant pDisplay-*PkDBPαII-AcGFP1* clones showing expected size of ~ 1.2 kb (~ 1011 bp of *PkDBPαII* plus ~ 217 bp of vector). No amplification was detected for non-recombinant clones or clones with the insert in the antisense orientation.

Nucleotide sequences of the recombinant plasmid pDisplay-*PkDBPαII-AcGFP1* from Peninsular Malaysia and Malaysian Borneo were confirmed by sequencing services from the commercial laboratory (First BASE Laboratories Sdn. Bhd). The nucleotide sequences of inserted fragments were analyzed, translated and aligned with previously published *PkDBPαII* haplotype H2 (GenBank Accession No. AGL76467.1) and H47 (GenBank Accession No. AJH76914.1) using software BioEdit Sequence Alignment Editor v7.2.3.

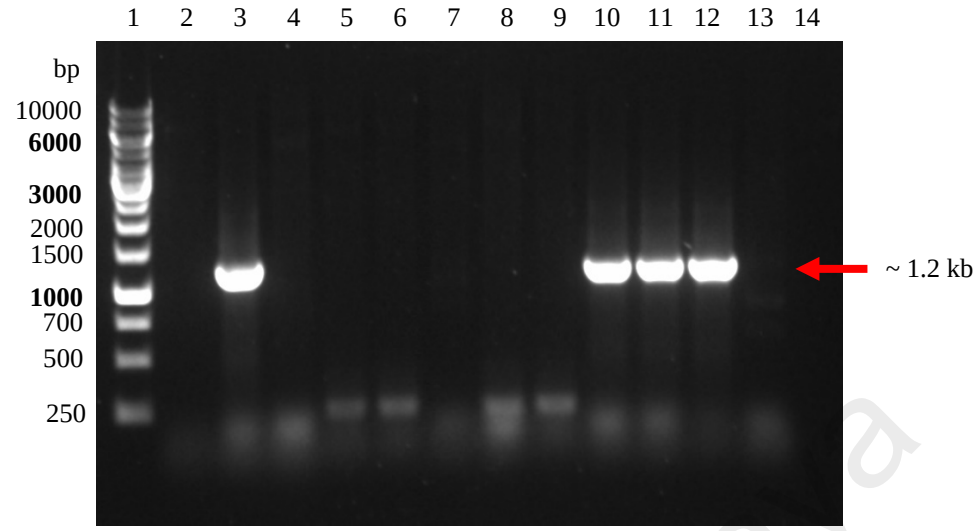

(A)

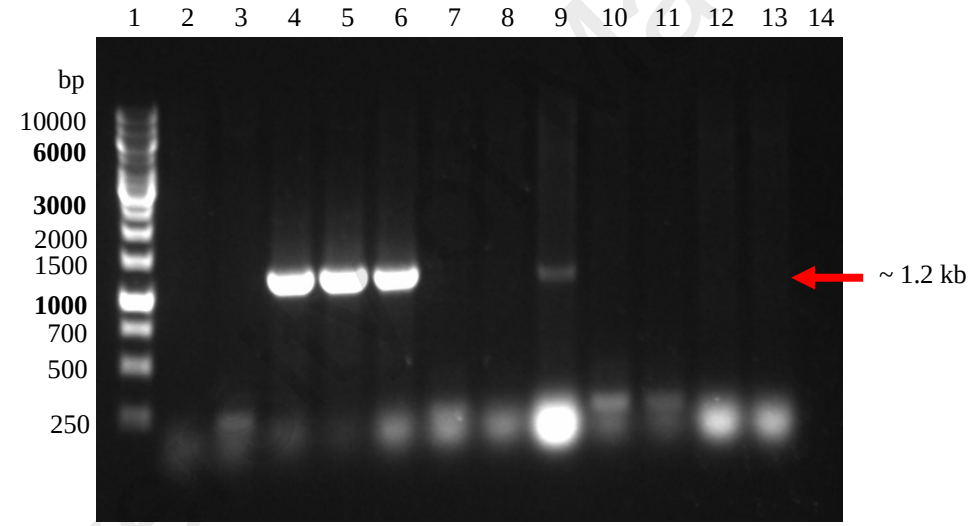

(B)

Figure 4.7: Agarose gel electrophoresis of directional PCR for selection of positive recombinant pDisplay-*PkDBPαII-AcGFP1* in TOP10F' cells. (A) PCR of clones with Peninsular Malaysia *PkDBPαII* insert in the sense orientation (lanes 3, 10, 11, and 12); No amplification was detected for non-recombinant clones or clones with the insert in the antisense orientation (lanes 2, 4, 5, 6, 7, 8, 9 and 13). (B) PCR of clones with Malaysian Borneo *PkDBPαII* insert in the sense orientation (lanes 4, 5, 6 and 9); No amplification was detected for non-recombinant clones or clones with the insert in the antisense orientation (lanes 2, 3, 7, 8, 10, 11, 12 and 13). Lanes 1 and 14 in both panels denote DNA ladder and NTC (ddH_2O), respectively.

4.1.3 Transfection into COS-7 mammalian cells & Erythrocyte-binding assays

Plasmids of recombinant pDisplay-*PkDBPαII-AcGFP1* were successfully transfected into COS-7 cells using Lipofectamine™ 3000 transfection reagent (Invitrogen Corp., USA). After 2 h of incubation in EBAs, non-adherent erythrocytes were carefully aspirated and the COS-7 cells were fixed with 1% paraformaldehyde. The nuclei of COS-7 cells were stained with Hoechst 33342 dye (Invitrogen Corp., USA). Transfected COS-7 cells (green fluorescent cells) with bound erythrocytes (rosettes) were evaluated and counted by using inverted fluorescence microscopy. Figure 4.8 shows the erythrocyte-binding assays of transfected COS-7 cells with *PkDBPαII* of *P. knowlesi* clinical isolates from Peninsular Malaysia and Malaysian Borneo. Non-transfected COS-7 cells and COS-7 cells transfected with recombinant pDisplay-*AcGFP1* plasmid (without *PkDBPαII* insert) used as negative controls, did not produce any fluorescence.

In the present study, recombinant PkDBPαII expressed on the COS-7 cell surface was able to bind to both human and macaque erythrocytes, but at different levels (Figure 4.9). In EBAs using human erythrocytes, the binding activity or number of rosettes formed with PkDBPαII of Peninsular Malaysia was three times higher than that of Malaysian Borneo PkDBPαII (156.89 ± 6.62 rosettes and 46.00 ± 3.57 rosettes, respectively; $p < 0.0001$) (Table 4.1). When assayed with macaque erythrocytes, the PkDBPαII of Peninsular Malaysia (356.56 ± 6.75 rosettes) and Malaysian Borneo (355.22 ± 11.69 rosettes) showed no significant difference in binding activity ($p = 0.77$).

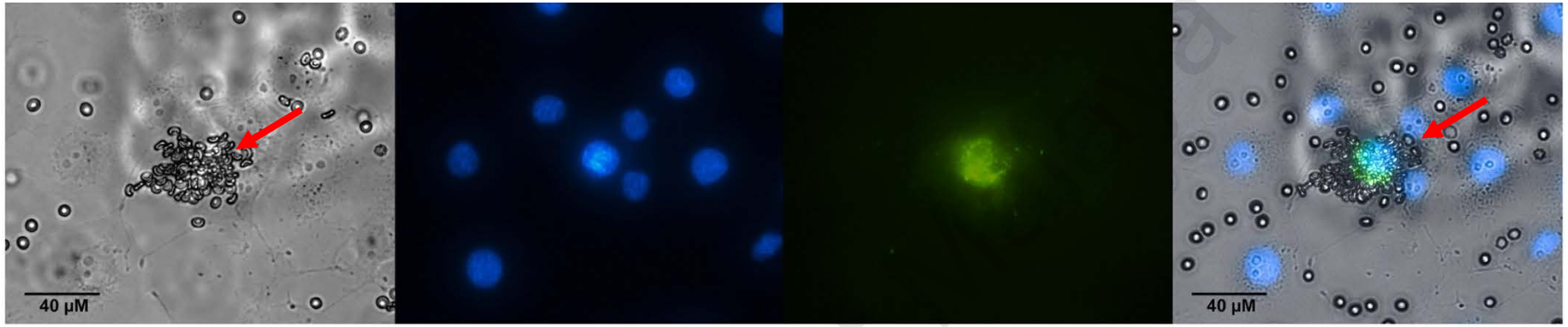

(A)

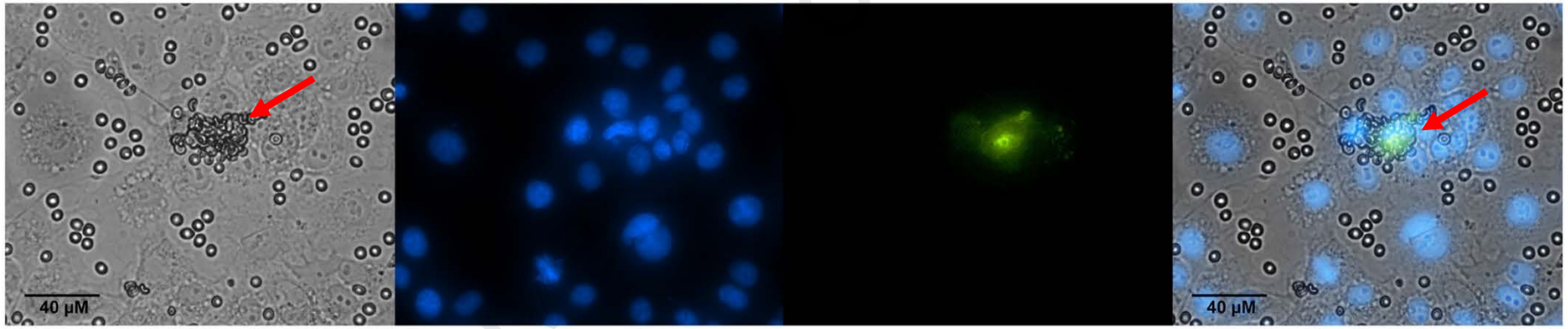

(B)

Figure 4.8: Binding of PkDBPαII expressed on transfected COS-7 cells with human erythrocytes [Duffy-positive Fy(a+b−) phenotype] to form rosettes (indicated by red arrows). (A) Transfected COS-7 cells expressing PkDBPαII of Peninsular Malaysia. (B) Transfected COS-7 cells expressing PkDBPαII from Malaysian Borneo. The transfected COS-7 cells (green) and the nuclei of COS-7 cells were visualized with Hoechst 33342 dye (blue). Images were captured using a Nikon ECLIPSE TE 300 inverted fluorescence microscope using the Plan Fluor ELWD 40×/0.45 aperture and 10× magnification eyepiece.

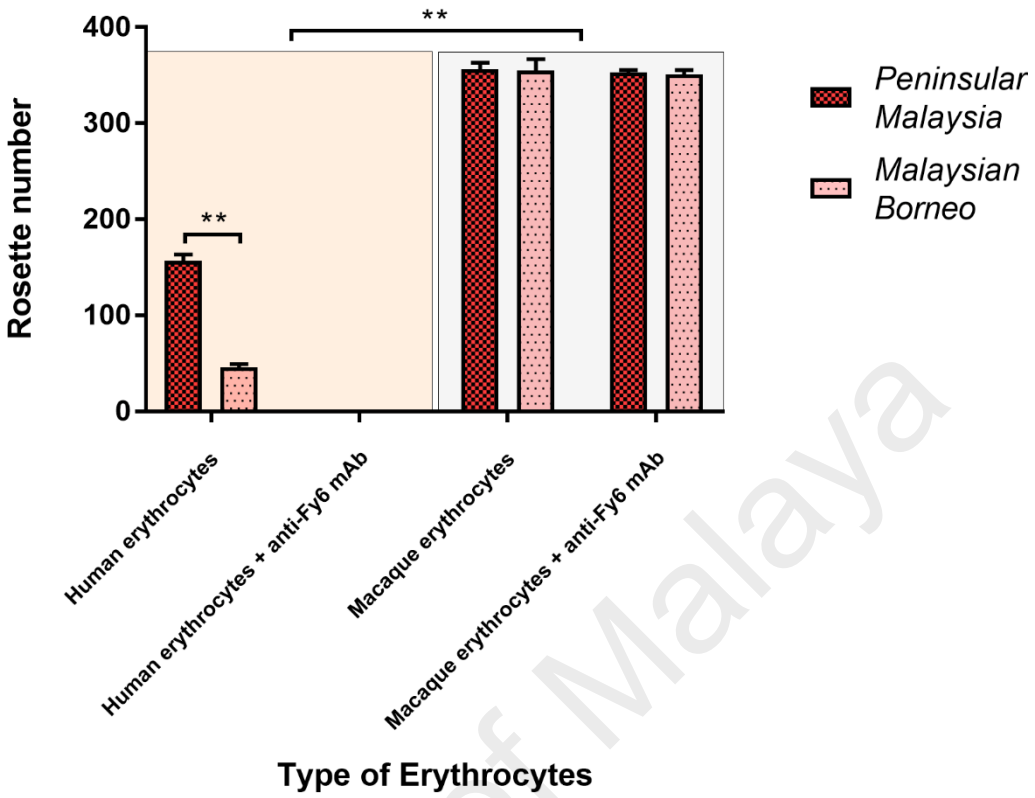

Figure 4.9: Binding activity level of PkDBPαII to human and macaque erythrocytes. Number of rosettes formed by COS-7 cells transfected with PkDBPαII of Peninsular Malaysia and Malaysian Borneo. A positive rosette is defined as more than 50% of the surface of transfected COS-7 cells covered with attached erythrocytes, and the total number of transfected COS-7 cells counted for each independent experiment was 1500 per experiment. Data are shown as the mean rosettes number of three independent experiments. The error bar represents the range of standard deviation. Statistical difference between PkDBPαII of Peninsular Malaysia and Malaysian Borneo, and between human and macaque erythrocytes are indicated with double asterisk ($p < 0.0001$).

Table 4.1: Erythrocyte-binding assays of PkDBPαII of Peninsular Malaysia and Malaysian Borneo using various erythrocytes.

Erythrocytes	Treatment	Haplotype	Binding[a]	Number of rosettes[b]
Human Fy(a+b−)	None	Peninsular	+	156.89 ± 6.62
	None	Borneo	+	46.00 ± 3.57
Macaque	None	Peninsular	+	356.56 ± 6.75
	None	Borneo	+	355.22 ± 11.67
Human Fy(a+b−)	Anti-Fy6	Peninsular	−	nil
	Anti-Fy6	Borneo	−	nil
Macaque	Anti-Fy6	Peninsular	+	352.67 ± 2.89
	Anti-Fy6	Borneo	+	351.83 ± 4.36

a Binding of erythrocytes to COS-7 cells expressing PkDBPαII of Peninsular Malaysia and Malaysian Borneo; (+) Binding; (−) No binding.

b Number of COS7 cells with rosettes (mean ± SD) seen in 35 – 40 fields at 200× magnification by fluorescence microscopy. (+) A positive rosette is defined as more than 50% the surface of the transfected cells covered with attached erythrocytes, (−) No rosettes were seen in the entire well.

4.1.4 Evaluation of the recombinant PkDBPαII binding specificity

The binding specificity of recombinant PkDBPαII expressed on COS-7 cells was evaluated with anti-Fy6 mAb. A change in binding activity was observed when the human erythrocytes were treated with anti-Fy6 mAb. The binding activity of human erythrocytes with PkDBPαII of Peninsular Malaysia and Malaysian Borneo was completely eliminated (Figure 4.10 A – D). No rosettes were seen in the entire well. However, anti-Fy6 treatment of macaque erythrocytes had no effect on the binding activity of PkDBPαII (Figure 4.10 E – H). The PkDBPαII expressed on COS-7 cell surface bound to both non-treated and anti-Fy6-treated macaque erythrocytes regardless of the expressed PkDBPαII haplotype. In fact, the binding activity using macaque erythrocytes were significantly higher than those incubated with human erythrocytes (Figure 4.9). Furthermore, the intensity of rosettes formation in the PkDBPαII of Peninsular Malaysia and Malaysian Borneo was different when incubated with human and macaque erythrocytes (Figure 4.10). The rosettes formed on COS-7 cells with macaque erythrocytes were generally larger when compared to the rosettes formed with human erythrocytes regardless of the expressed PkDBPαII haplotype.

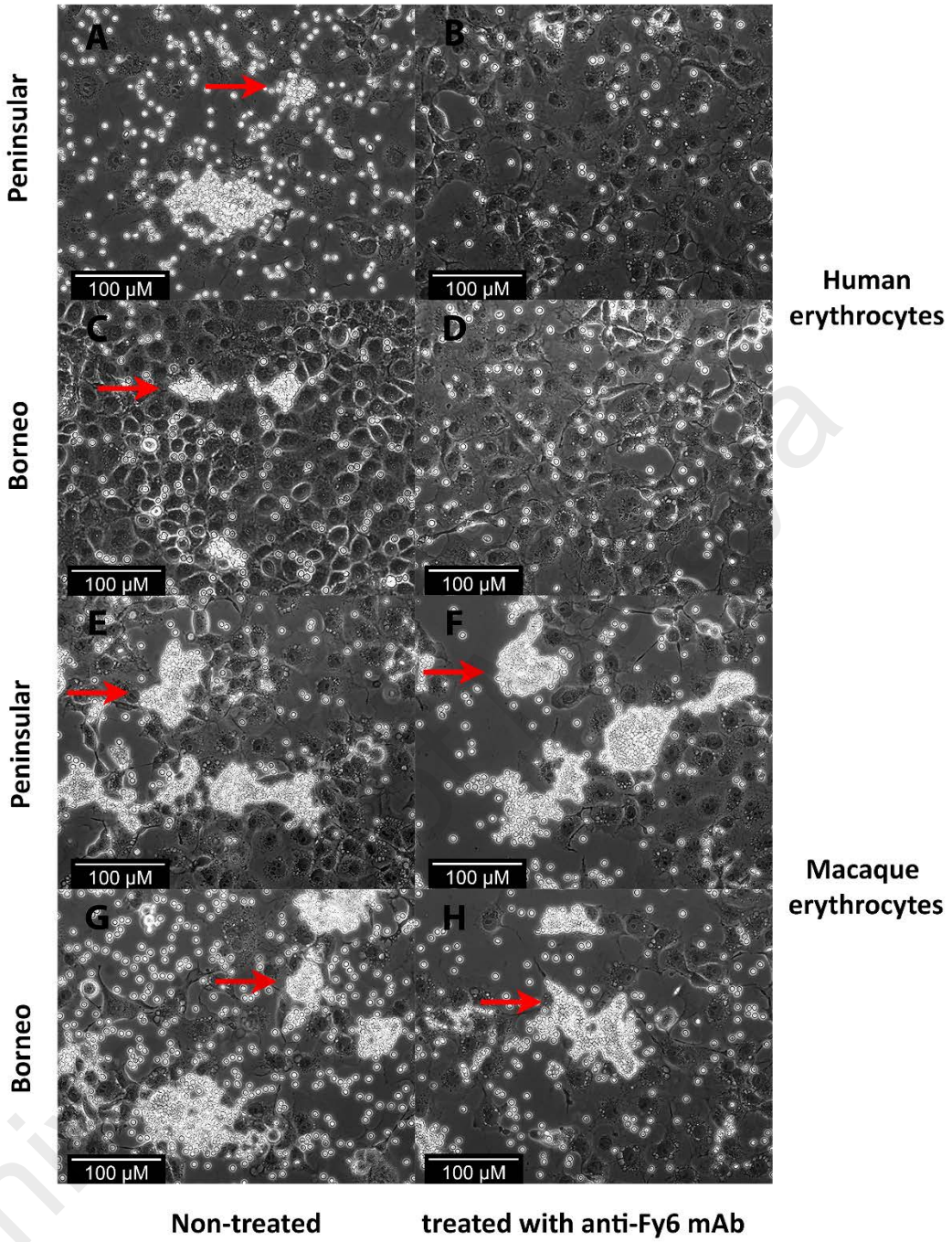

Figure 4.10: Binding inhibition of PkDBPαII to erythrocytes by anti-Fy6 treatment. **(**A – D) PkDBPαII incubated with 1% human erythrocytes; (E – H) PkDBPαII incubated with 1% macaque erythrocytes; (A, B, E and F) COS-7 cells transfected with PkDBPαII of Peninsular Malaysia; (C, D, G and H) COS-7 cells transfected with PkDBPαII of Malaysian Borneo; (A, C, E and G) Erythrocytes not treated with anti-Fy6; (B, D, F and H) Erythrocytes treated with anti-Fy6. Bound erythrocytes or rosettes (indicated in red arrows) observed under inverted light microscope at 200× magnification. No rosettes were seen in panels B and D. Rosettes were more saturated on macaque erythrocytes**.**

4.2 Binding affinity of PkDBPαII using Isothermal Titration Calorimetry (ITC)

4.2.1 Construction of pET30a(+)-*PkDBPαII* plasmids

4.2.1.1 PCR amplification of *PkDBPαII*

The *PkDBPαII* of *P. knowlesi* clinical isolates from Peninsular Malaysia and Malaysian Borneo were successfully amplified using gene-specific primers containing RE *Bam*HI cut site. Figure 4.11 shows PCR products of *PkDBPαII* with expected size of ~ 1011 bp.

4.2.1.2 Cloning of PCR products into pGEM®-T vector system

The *PkDBPαII* fragment of each haplotype was purified and ligated to pGEM®-T vector system. Overnight ligation mixtures were transformed into TOP10F' cells. By using M13F (-40) and M13R (-48) primers, colony PCR was carried out for selection of positive recombinant pGEM-T-*PkDBPαII* clones. Figure 4.12 shows the positive recombinant pGEM-T-*PkDBPαII* clones with expected size of ~ 1.2 kb (~ 1 kb of *PkDBPαII* plus ~ 260 bp of vector). PCR amplification of non-recombinant clones showed a PCR band of ~ 260 bp. Plasmids of positive recombinant pGEM-T-*PkDBPαII* were excised from agarose gel and purified.

4.2.1.3 Cloning of *PkDBPαII* fragments into Novagen® pET30a(+) vector system

Positive recombinant pGEM-T-*PkDBPαII* and pET30a(+) plasmids were digested with RE *Bam*HI. The digested recombinant pGEM-T-*PkDBPαII* plasmid generated pGEM-T plasmids with expected size of ~ 3 kb and *PkDBPαII* fragments with expected size of ~ 1 kb, while the digested pET30a(+) plasmids generated linearized plasmids of ~ 5.4 kb (Figure 4.13). Target fragments of *PkDBPαII* for each haplotype and linearized pET30a(+) plasmids were excised from agarose gel and extracted. Purified *PkDBPαII* target fragments were ligated to pET30a(+) vector and transformed into TOP10F' cells.

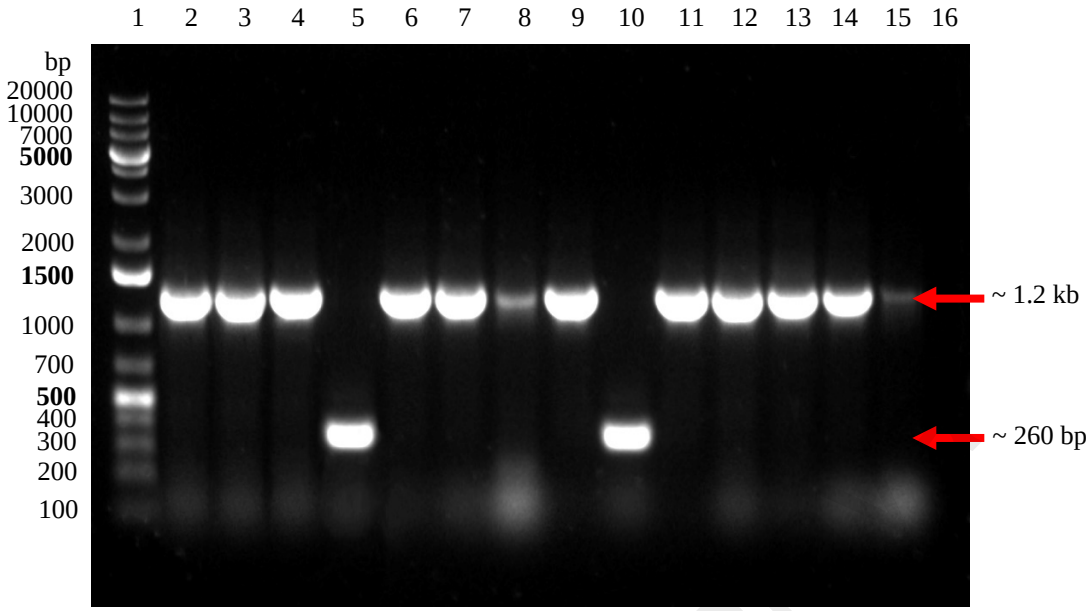

Figure 4.11: Agarose gel electrophoresis of colony PCR for selection of positive recombinant pGEM-T-*PkDBPαII* in TOP10F' cells. Positive recombinant pGEM-T-*PkDBPαII* clones of Peninsular Malaysia (lanes 2, 3, 4, 6, 7 and 8) and Malaysian Borneo (lanes 9, 11, 12, 13, 14 and 15). PCR amplification of non-recombinant clones generated a PCR band of ~ 260 bp (lanes 5 and 9). Lanes 1 and 16 denote DNA ladder and NTC (ddH_2O), respectively.

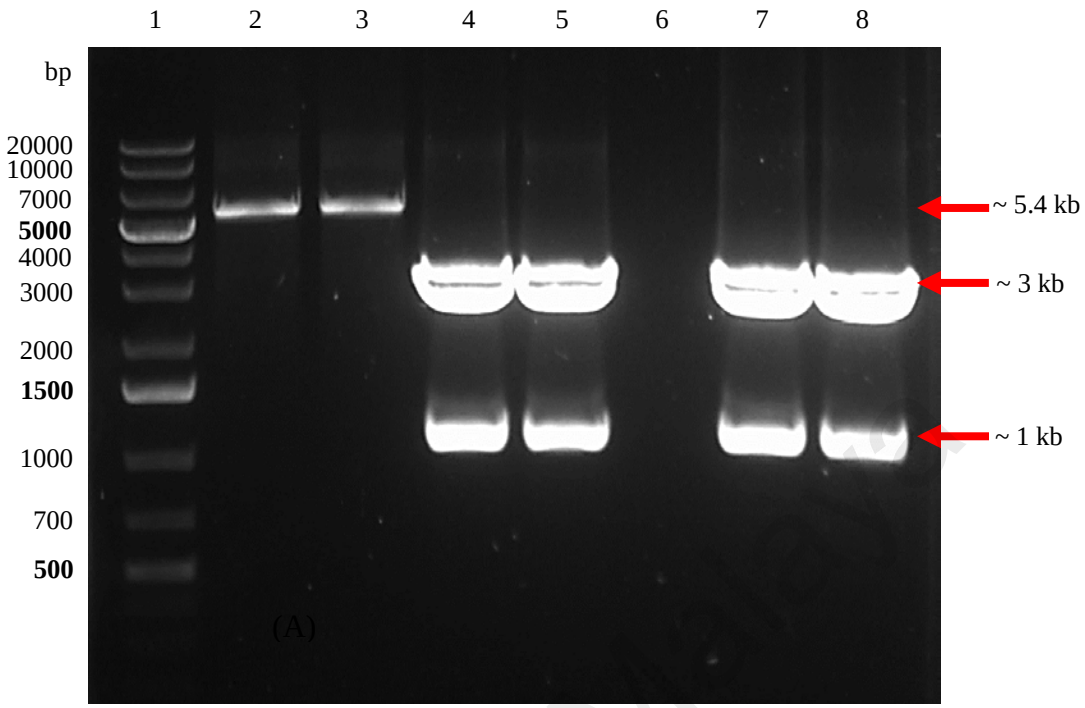

Figure 4.12: Agarose gel electrophoresis of restriction digestion of recombinant pGEM-T-*PkDBPαII* and pET30a(+) plasmids. Digested pGEM-T-*PkDBPαII* plasmids of Peninsular Malaysia (lanes 4 and 5) and Malaysian Borneo (lanes 7 and 8) generated pGEM-T plasmids with expected size of ~ 3 kb and *PkDBPαII* fragments with expected size of ~ 1kb. Linearized pET30a(+) vector with expected size of 5.4 kb (lanes 2 and 3). Lanes 1 and 6 denote DNA ladder and empty lane, respectively.

Directional PCR was performed on selected recombinant clones of pET30a(+)-*PkDBPαII* using T7 promoter primer and *PkDBPαII*-pET30a(+)_reverse primer. The PCR amplification of positive recombinant pET30a(+)-*PkDBPαII* clones with the insert in the sense orientation generated a PCR band of ~ 1.2 kb (~ 1 kb of *PkDBPαII* plus ~ 232 bp of vector) (Figure 4.14). No amplification was detected for non-recombinant clones or clones with the insert in the antisense orientation. Plasmids of positive recombinant pET30a(+)-*PkDBPαII* clones were extracted and sent for sequencing. Nucleotide sequences of *PkDBPαII* inserts for Peninsular Malaysia and Malaysian Borneo were analyzed, translated and aligned with previously published PkDBPαII haplotype H2 (GenBank Accession No. AGL76467.1) and H47 (GenBank Accession No. AJH76914.1), respectively.

4.2.1.4 Transformation into *E. coli* expression host T7 Express *lysY/I^q*

Successive plasmids of pET30a(+)-*PkDBPαII* from Peninsular Malaysia and Malaysian Borneo were transformed into expression host *E. coli* T7 express *LysY/I^q*. Three colonies from each transformation plate were selected and directional PCR was performed as mentioned above. The PCR amplification of positive pET30a(+)-*PkDBPαII* clones with the insert in the sense orientation generated PCR band of ~ 1.2 kb (Figure 4.15).

4.2.2 Protein expression of recombinant PkDBPαII in *E. coli* expression system

Recombinant PkDBPαII of Peninsular Malaysia and Malaysia Borneo have successfully expressed in *E. coli* T7 Express *LysY/I^q* cells with the use of IPTG. Bacterial cultures were cultivated at 37 °C and shaken at 250 rpm for up to 6 h. Upon reaching optimum optical density (OD_{600} = 0.5 – 0.6), 1 mM IPTG was added into the bacteria cultures to induce expression of recombinant PkDBPαII proteins. Protein samples

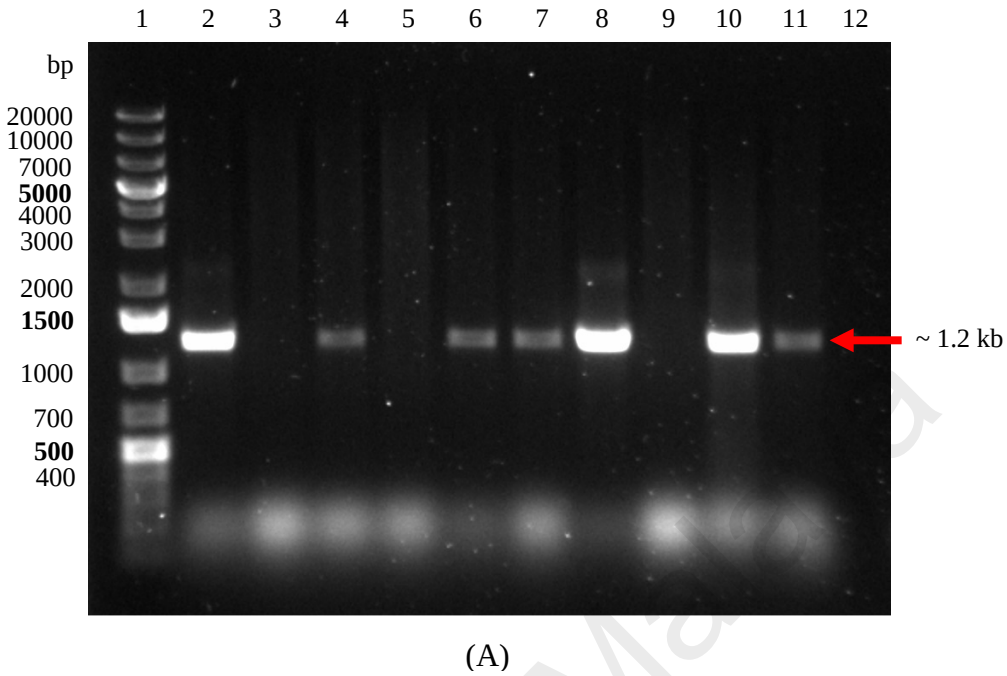

(A)

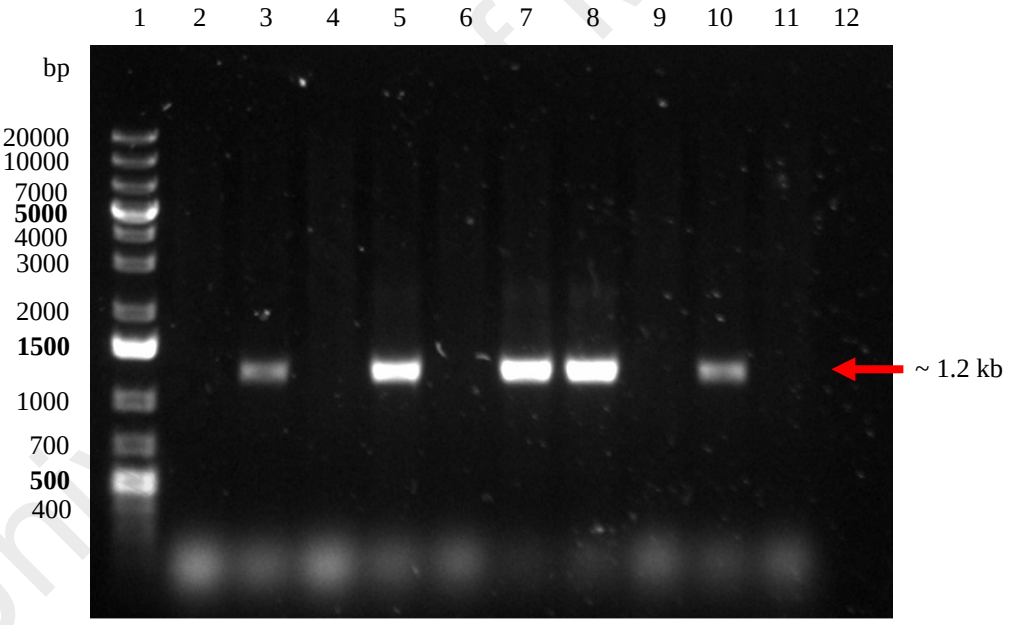

(B)

Figure 4.13: Agarose gel electrophoresis of directional PCR for selection of positive recombinant pET30a(+)-*PkDBPαII* in TOP10F' cells. (A) PCR of recombinant clones with Peninsular Malaysia *PkDBPαII* insert in the sense orientation (lanes 2, 4, 6, 7, 8, 10 and 11); No amplification was detected for non-recombinant clones or clones with the insert in the antisense orientation (lanes 3, 5 and 9). (B) PCR of recombinant clones with Malaysian Borneo *PkDBPαII* insert in the sense orientation (lanes 3, 5, 7, 8 and 10); No amplification was detected for non-recombinant clones or clones with the insert in the antisense orientation (lanes 2, 4, 6, 9 and 11). Lanes 1 and 12 in both panels denote DNA ladder and NTC (ddH_2O), respectively.

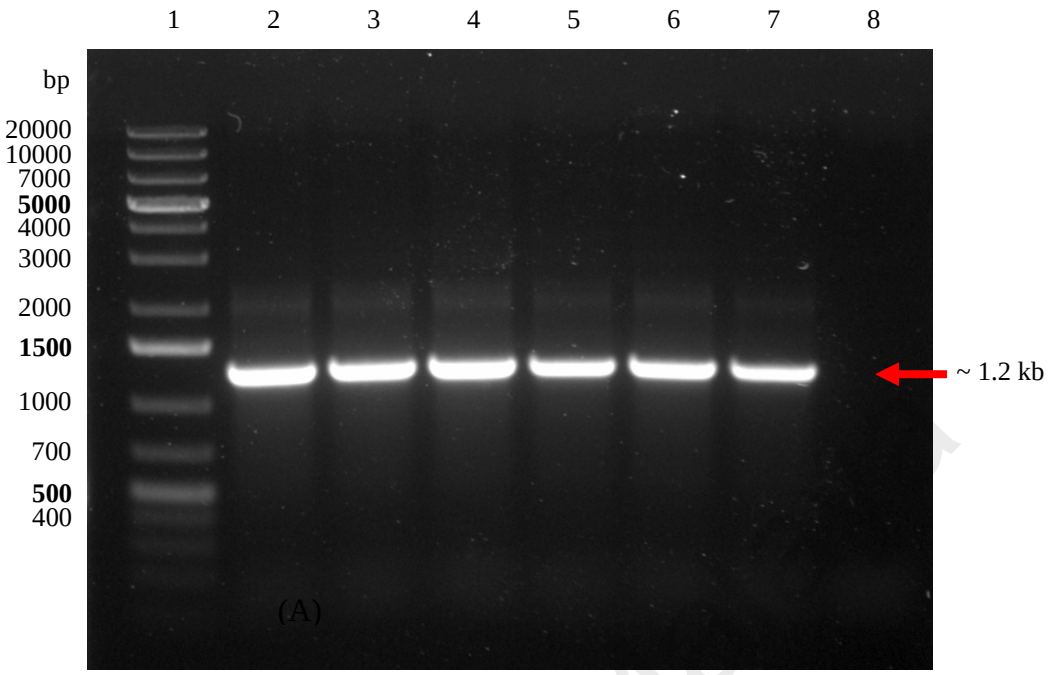

Figure 4.14: Agarose gel electrophoresis of directional PCR for selection of positive recombinant pET30a(+)-*PkDBPαII* in T7 Express *lysY/I^q* cells. Positive recombinant pET30a(+)-*PkDBPαII* clones of Peninsular Malaysia (lanes 2, 3 and 4) and Malaysian Borneo (lanes 5, 6, and 7). Lanes 1 and 8 denote DNA ladder and NTC (ddH_2O), respectively.

of 1 mL were collected at each time point (0, 2, 4 and 6 h) and electrophoresed on 12% SDS-PAGE gel. The separated proteins were transblotted onto PVDF membrane and analyzed in Western Blot assays using Novagen® His•Tag® monoclonal antibody which specifically detects the 6× histidine residues (His•Tag®) in pET30a(+) vector. Negative control sample of T7 Express *LysY/I*^{q} cells carrying pET30a(+) plasmid was included in order to differentiate recombinant PkDBPαII proteins from the native proteins of the expression host.

Figure 4.16 and 4.17 indicate the protein expression of PkDBPαII with a molecular mass of ~ 45 kDa. The optimal expression level of recombinant PkDBPαII haplotypes were achieved after 6 h of induction with 1 mM IPTG at 37 °C. This band was not observed in the negative control pET30a(+) clone.

4.2.3 Purification and dialysis of recombinant PkDBPαII

Protein purification was performed to eliminate non-specific bands from expressed proteins. The recombinant PkDBPαII proteins from Peninsular Malaysia and Malaysian Borneo were affinity-purified using ProBond^{TM} purification system (Invitrogen Corp., USA) under hybrid condition. The purified and dialyzed proteins were electrophoresed on 12% SDS-PAGE gel. Purified PkDBPαII of Peninsular Malaysia and Malaysian Borneo showed a distinct band of ~ 45 kDa, which were absent in the purified pET30a(+) clone (Figure 4.18). In addition to that, purified PkDBPαII proteins were further analyzed in Western blot assay by using Novagen® His•Tag® monoclonal antibody (Merck KGaA., Germany) in which similar result to SDS-PAGE analysis was obtained (Figure 4.19). Analysis by MALDI-TOF MS of the peptides from the 45 kDa band via Mascot search results revealed significant protein scores ($P < 0.05$) that matches the amino acid sequences of PkDBPα, therefore confirming the identity of the purified recombinant PkDBPαII (Appendix D).

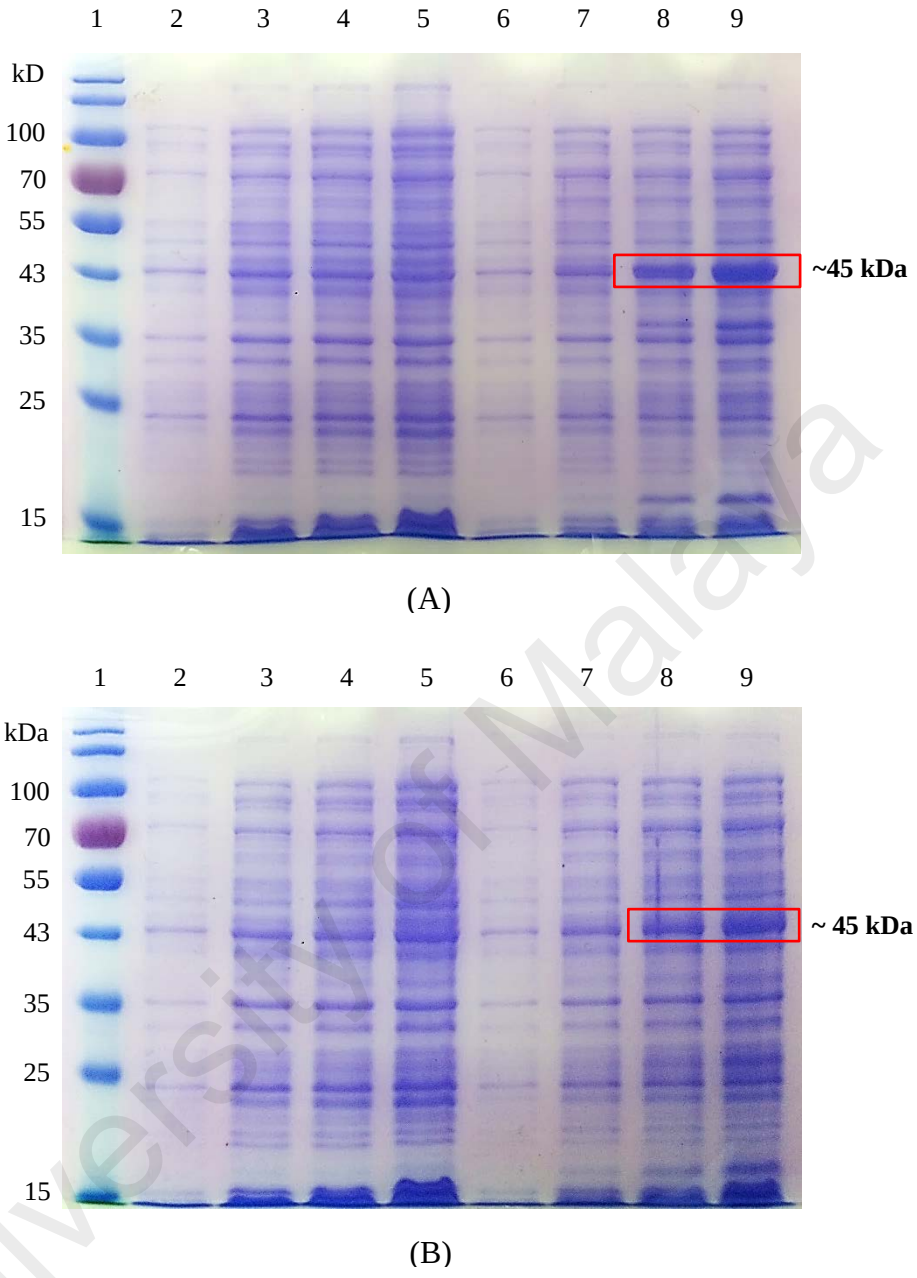

Figure 4.15: Coomassie brilliant blue-stained SDS-PAGE gel of recombinant protein expression. (A) Protein expression of recombinant PkDBPαII of Peninsular Malaysia; Lanes 2, 3, 4 and 5 represent pET30a(+) at 0, 2, 4, and 6 h after IPTG induction respectively; Lanes 6, 7, 8 and 9 represent recombinant PkDBPαII at 0, 2, 4 and 6 h after IPTG induction respectively. (B) Protein expression of recombinant PkDBPαII of Malaysian Borneo; Lanes 2, 3, 4 and 5 represent pET30a(+) at 0, 2, 4, and 6 h after IPTG induction respectively; Lanes 6, 7, 8 and 9 represent recombinant PkDBPαII at 0, 2, 4 and 6 h after IPTG induction respectively. The recombinant PkDBPαII with a size of ~ 45 kDa was detected after 4 h in both panels (indicated by red boxes). Lane 1 in both panels denotes PageRuler^{TM} prestained protein ladder.

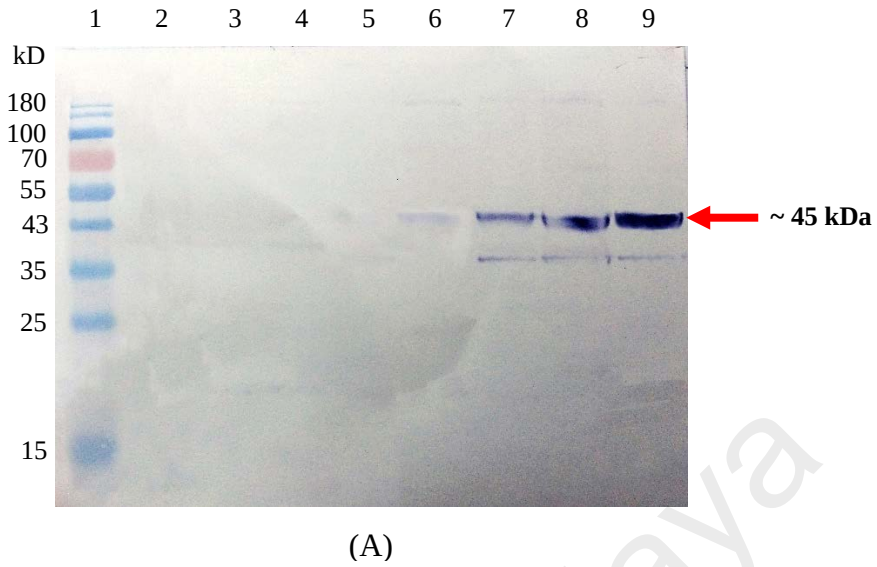

(A)

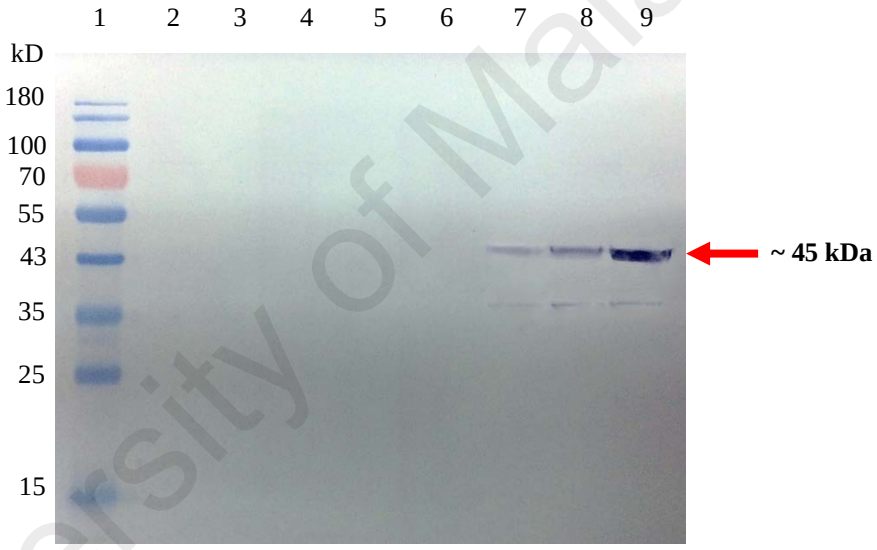

(B)

Figure 4.16: Western blot assay of recombinant protein expression. (A) Recombinant PkDBPαII of Peninsular Malaysia was probed with Novagen® His•Tag® monoclonal antibody. Lanes 2, 3, 4 and 5 represent pET30a(+) at 0, 2, 4, and 6 h after IPTG induction respectively; Lanes 6, 7, 8 and 9 represent recombinant Peninsular Malaysia PkDBPαII at 0, 2, 4 and 6 h after IPTG induction respectively. (B) Recombinant PkDBPαII of Malaysian Borneo was probed with Novagen® His•Tag® monoclonal antibody. Lanes 2, 3, 4 and 5 represent pET30a(+) at 0, 2, 4, and 6 h after IPTG induction respectively; Lanes 6, 7, 8 and 9 represent recombinant Malaysian Borneo PkDBPαII at 0, 2, 4 and 6 h after IPTG induction respectively. The recombinant PkDBPαII with a size of ~ 45 kDa was detected after 4 h in both panels (indicated by red arrows). Lane 1 in both panels denotes PageRuler^{TM} prestained protein ladder.

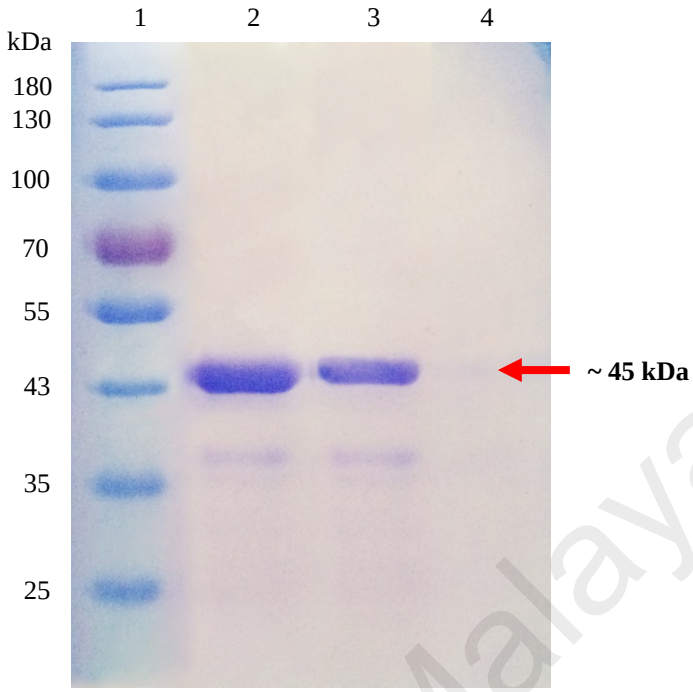

Figure 4.17: Coomassie brilliant blue-stained SDS-PAGE gel of purified PkDBPαII. Distinct band of ~ 45 kDa (indicated by red arrow) was detected in purified PkDBPαII proteins of Peninsular Malaysia (lane 2) and Malaysian Borneo (lane 3), but absent in purified pET30a(+) clone (lane 4). Lane 1 denotes PageRuler^{TM} prestained protein ladder.

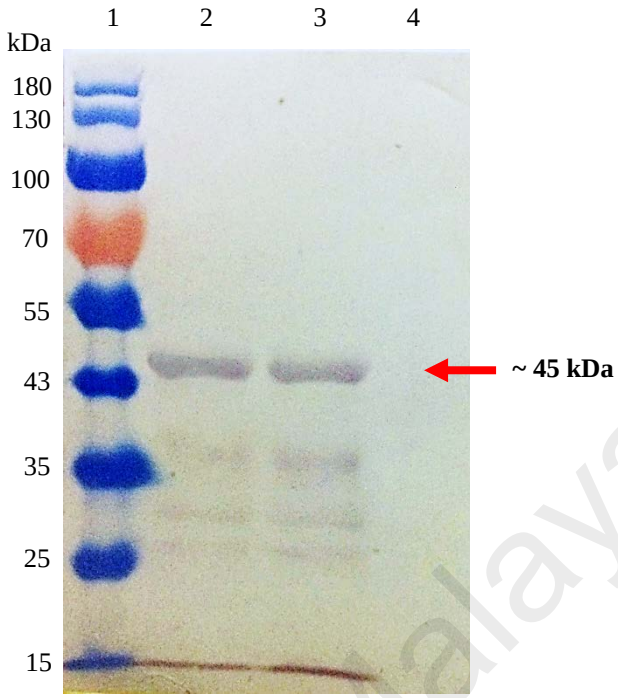

Figure 4.18: Western blot assay of purified PkDBPαII probed with Novagen® His•Tag® monoclonal antibody. Distinct band of ~ 45 kDa (indicated by red arrow) was detected in purified PkDBPαII proteins of Peninsular Malaysia (lane 2) and Malaysian Borneo (lane 3), but absent in purified pET30a(+) clone (lane 4). Lane 1 denotes PageRuler^{TM} prestained protein ladder.

4.2.4 Analysis of binding affinity using Isothermal Titration Calorimetry (ITC)

The concentration of each purified PkDBPαII was calculated based on the standard curve of Bradford protein assay. A standard curve was generated by plotting the absorbance of standard BSA at 595 nm (Y-axis) versus the protein concentration in mg/mL (X-axis) (Appendix E).

The purified PkDBPαII (10 μM) of Peninsular Malaysia and Malaysian Borneo were loaded to their respective syringe compartment and injected accordingly into sample cell compartment containing 1.5 mL of human erythrocytes with 0.001% hematocrit. Figure 4.20 shows the thermodynamic curve of binding affinity between purified PkDBPαII with human erythrocytes. From the thermodynamic curve, the interaction of purified PkDBPαII with human erythrocytes was exothermic, where heat was released during the molecular interaction of PkDBPαII-human erythrocytes.

Binding affinity was calculated based on the formula, $K_D = 1/K_A$, where the K_A value was obtained from the analysis of Wiseman plot generated during the ITC assays. Data analysis was carried out using MicroCal Auto-iTC_{200}, Origin software (Malvern Instruments Ltd, UK). The binding affinity of Peninsular Malaysia PkDBPαII-human erythrocytes and Malaysian Borneo PkDBPαII-human erythrocytes was 7.75 μM and 74.1 μM, respectively. Negative control included in the experiment was PBS-human erythrocytes with K_D of 5.4×10^9 μM (Figure 4.19 C).

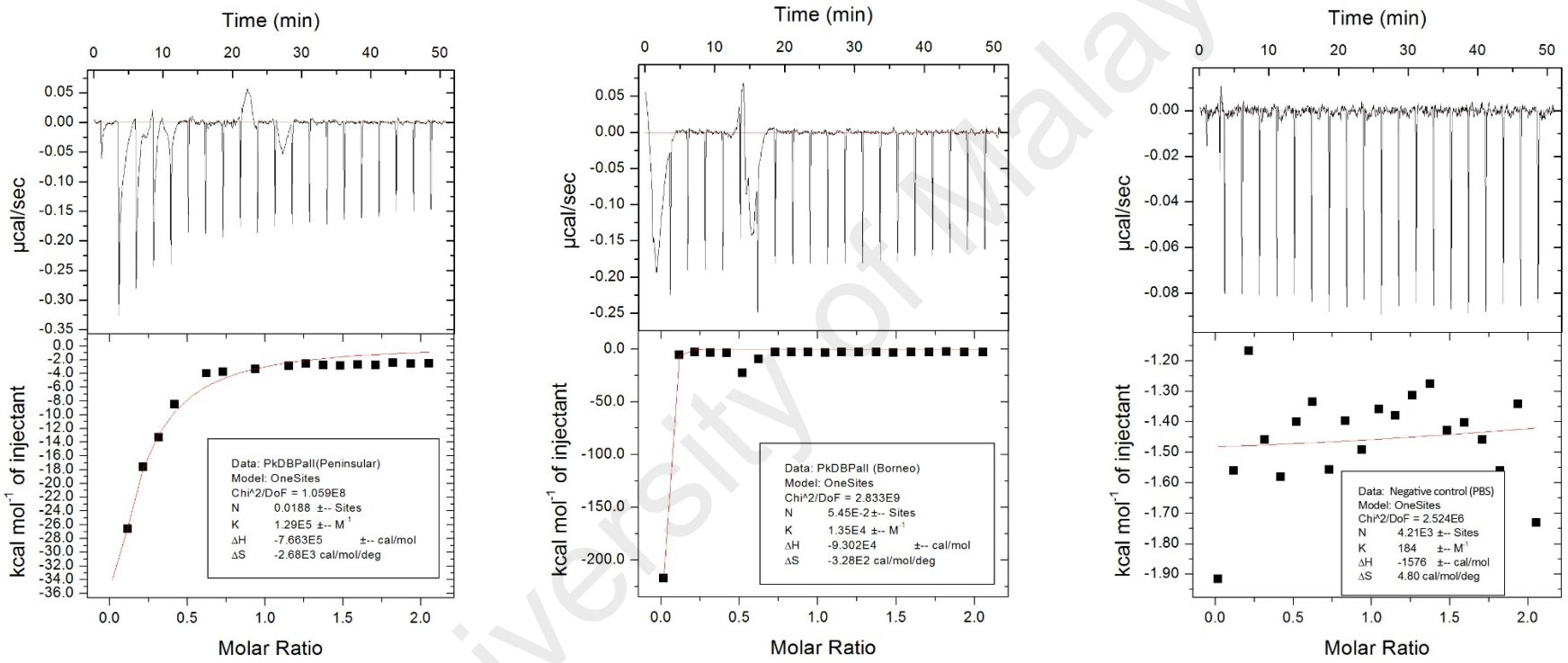

(A) (B) (C)

Figure 4.19: ITC analysis of the purified PkDBPαII-human erythrocytes interaction. Isothermal calorimetric titration of (A) 10 µM of Peninsular Malaysia PkDBPαII to human erythrocytes with 0.001% hematocrit, (B) 10 µM of Malaysian Borneo PkDBPαII to human erythrocytes with 0.001% hematocrit and (C) Negative control (1×PBS) to human erythrocytes with 0.001% hematocrit. Where N = number of binding sites; K = binding constant (K_A); ΔH = enthalpy changes; ΔS = entropy change.

CHAPTER 5: DISCUSSION

The emergence of *P. knowlesi* as the new causative agent of human malaria has alarmed public health authorities in many Southeast Asia countries. In Malaysia, despite tremendous progress towards malaria control and elimination in the past few years, *P. knowlesi* remains as the main cause of human malaria, sometimes resulting in severe infection and increased fatality. Interestingly, severe cases of knowlesi malaria with hyperparasitemia have been observed to be prominent in Malaysian Borneo than seen in Peninsular Malaysia. At the same time, the *PkDBPαII*, an important erythrocyte invasion gene in *P. knowlesi*, also showed distinct genetic differences in Peninsular Malaysia and Malaysia Borneo (Fong *et al.*, 2015). PkDBPαII haplotypes H2 and H47 are predominant in Peninsular Malaysia and Malaysian Borneo, respectively. These haplotypes were chosen for this study, with the aim of determining whether these haplotypic differences affect binding activity and affinity of the PkDBPαII with erythrocytes. The binding activity of PkDBPαII haplotypes of Peninsular Malaysia and Malaysian Borneo with human erythrocytes Fy(a+b–) and macaque (*M. fascicularis*) erythrocytes was studied by using erythrocyte-binding assays (EBAs). Human Duffy-positive Fy(a+b–) erythrocytes were chosen in the present study because this phenotype is the most common in the Malaysian population. In addition to EBA, the binding affinity of PkDBPαII with human erythrocytes was determined using the MicroCal^{TM} Isothermal Titration Calorimetry (ITC) system. Binding affinity is the strength of the binding interaction between a single ligand to its binding partners. Results from both analyses showed that the binding strength of PkDBPαII from Peninsular Malaysia to Duffy-positive Fy(a+b–) human erythrocytes was greater than that of Malaysian Borneo PkDBPαII. In the experiment using macaque erythrocytes, the binding activity level of PkDBPαII of Peninsular Malaysia and Malaysia Borneo was similar.

5.1 Binding activity of PkDBPαII

5.1.1 Selection of pDisplay™ vector

pDisplay™ is a mammalian expression vector (Appendix E) that expresses recombinant proteins on the cell surface. It consists of a murine Ig κ-chain leader sequence and platelet-derived growth factor receptor transmembrane domain (PDGFR-TM). Both work together to direct expression to the cell surface and anchors recombinant proteins to the plasma membrane for display. In this present study, the *PkDBPαII* fragment was cloned into the multiple cloning site (MCS) of pDisplay™ plasmid carrying SV40-origin, human cytomegalovirus (CMV) promoter/enhancer, T7 promoter, ATG initiation codon, bovine growth hormone (BGH) polyadenylation signal and ampicillin resistance gene (β-lactamase). The SV40-origin is suited to replicate in COS-7 cells. In addition to that, the fluorescent reporter gene *AcGFP1* (green fluorescent protein from *Aequorea coerulescens)* is added to the C-terminal of the insert site of pDisplay™ to facilitate direct visualization of the expressed recombinant proteins. This reporter gene was cloned downstream of the *PkDBPαII* fragment.

5.1.2 COS-7 mammalian cells in EBAs study

COS-7 cells were selected in this study mainly due to its efficiency as a transfection host in EBAs as demonstrated in previous studies (Chitnis & Miller, 1994; Singh *et al.*, 2002; Semenya *et al.*, 2012). COS-7 cells are derived from the African green monkey kidney cells comprising an origin-defective SV40 virus sequence. SV40 origin-containing plasmids are able to replicate efficiently in the presence of SV40 large T antigen. An estimated 100000 copies/cell can be obtained within 48 h post-transfection (Aruffo, 2001). Thus, COS-7 cells are capable of expressing high-level of recombinant proteins over a short period of time. However, the excessive burdens on the COS-7 cells, such as high copy number replication of plasmids and high level of protein expression,

may cause COS-7 cell death or lost of ability to maintain the plasmid after transfection (transient expression) (Aruffo, 2001). The ability of COS-7 as a competent mammalian host to produce biologically active cell-surface and secreted proteins have been reported in previous studies (Laub & Rutter, 1983; Warren & Shields, 1984). Furthermore, recombinant proteins are correctly processed and folded in the COS-7 cells (Mishina *et al.*, 1984). Another advantage of COS-7 expression is that the signal sequences from the plasmid vector for recombinant protein synthesis, processing, and secretion are properly recognized and executed by the cells (Verma *et al.*, 1998; Khan, 2013). Translation is initiated through eukaryotic ribosomes by recognizing the ribosome-binding site translation initiation site (Kozak sequence, GCCACC) (Kozak, 1987). In this study, Kozak sequence and the initiation codon ATG were included in the recombinant plasmids of pDisplay-*PkDBPαII-AcGFP1*. Recombinant plasmids of pDisplay-*PkDBPαII-AcGFP1* were transfected into confluent COS-7 cells with Lipofectamine™ 3000 transfection reagent.

5.1.3 Erythrocyte-binding assays (EBAs)

Erythrocyte-binding assays (EBAs) are often applied in many studies to investigate the ability of malaria parasite ligands to bind erythrocyte receptors. Although EBAs have been used as a qualitative approach for the specificity of interactions, the number of rosette formations can be quantitated by counting under an inverted fluorescent microscope (Cheng *et al.*, 2013; Cheng *et al.*, 2016). In this study, adherent erythrocytes covering more than half of the cell surface were recorded as positive binding or rosettes. In contrast, the binding was scored negative when no rosettes were seen in the entire well. Furthermore, incorporation of the *AcGFP1* reporter gene allowed transfected COS-7 cells with rosettes to be visualized directly using inverted fluorescent microscopy. Through this, immunofluorescence staining was not required. Whereas in conventional EBA,

immunofluorescence staining is required to distinguish the transfected COS-7 cells from the non-transfected and this process is often laborious and time consuming.

Results from the EBAs using Duffy-positive human erythrocytes have revealed higher binding activity with the PkDBPαII of Peninsular Malaysia compared to Malaysian Borneo PkDBPαII. The PkDBPαII targeted region was designed based on the proposed DARC recognition site by Singh *et al.* (2006). The region encompasses 12 cysteine residues (at position 16, 29, 36, 45, 99, 176, 214, 226, 231, 235, 304, 306) that form six disulfide bridges which contribute to the three-dimensional (3D) conformational structure of PkDBPαII for interaction with human DARC (Singh *et al.*, 2006). These cysteine residues have been shown to be conserved in the PkDBPαII of Peninsular Malaysia and Malaysian Borneo (Fong *et al.*, 2015). The key residues for DARC recognition, Y94, N95, K96, R103, L168 and I175 (Figure 5.1), were identified on the subdomain 2 of PkDBPαII (Singh *et al.*, 2006). Sequence alignment analysis showed that these residues were conserved except at position 95, where the PkDBPαII of Malaysian Borneo featured a substituted aspartic acid (D) residue. This finding is in agreement with previous studies, where modifications in these critical residues have been proven to disrupt the interaction between PkDBPαII and DARC (VanBuskirk *et al.*, 2004; Hans *et al.*, 2005).

Apart from this N95D substitution, 11 other amino acid differences were identified between the PkDBPαII of Peninsular Malaysia and Malaysian Borneo (Figure 5.1). The changes in these amino acid residues may have caused an aberration in the 3D conformational structure of PkDBPαII in Malaysian Borneo, thus affecting its functional ability to bind to human erythrocytes efficiently. Using the isoelectric point calculator (IPC), the predicted pI (isoelectric point) for PkDBPαII of Peninsular Malaysia and Malaysian Borneo were 7.91 and 7.73, respectively, while the glycosylated human DARC (GenBank Accession No. Q16570.3) is acidic with a predicted pI of 5.78 (Kozlowski, 2016).

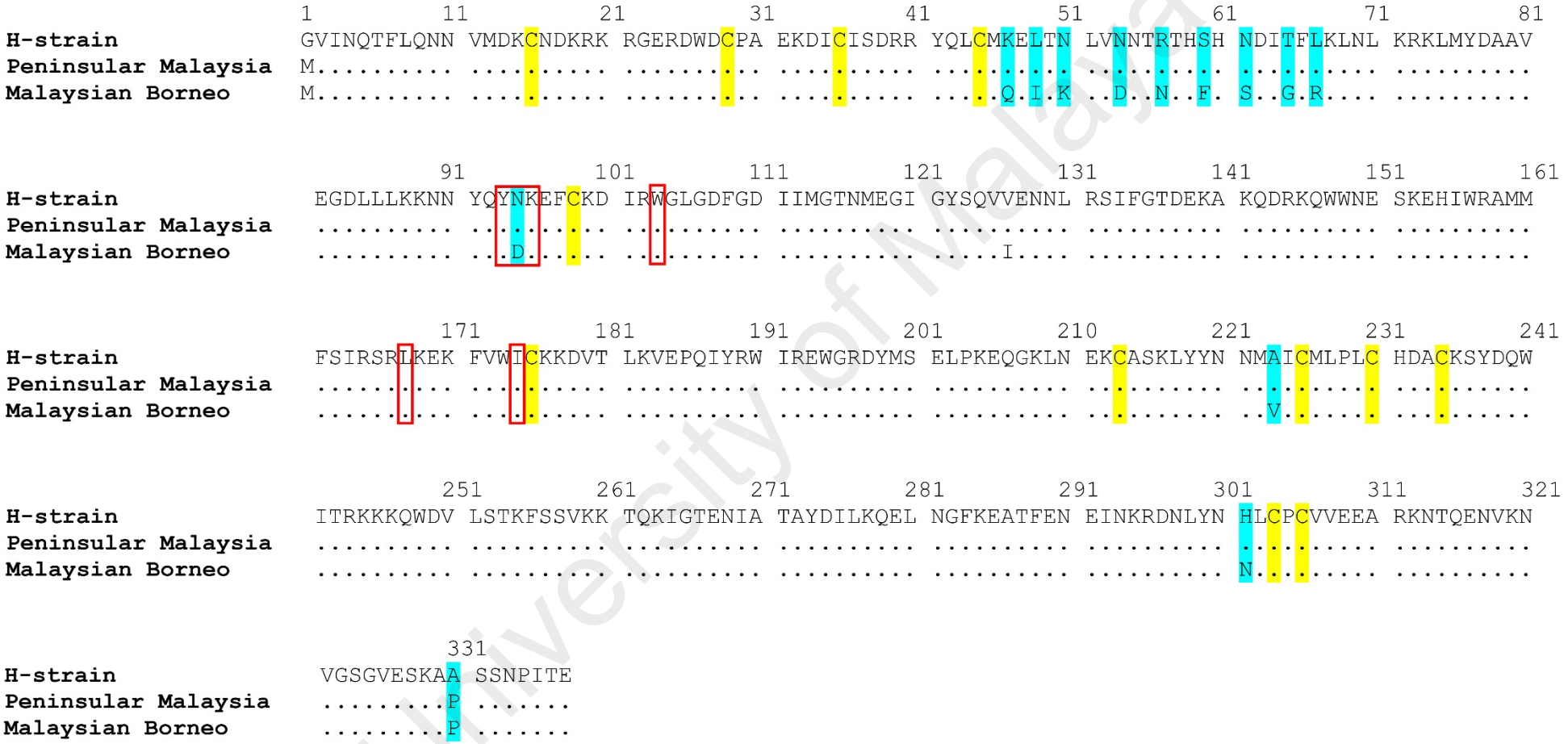

Figure 5.1: Sequence alignment of PkDBPαII from Peninsular Malaysia and Malaysian Borneo and the reference *P. knowlesi* strain H. Amino acid residues identical to those of the reference strain H (GenBank Accession No. M90466) are marked by dots. The amino acid changes and 12 highly conserved cysteine residues are highlighted in cyan and yellow, respectively. Amino acid residues, Y94, N95, K96, R103, L168 and I175, which have been identified previously as essential for binding with DARC [33, 34], are in red boxes.

Previous study has demonstrated that high affinity and specificity binding of PvDBP with DARC were mostly due to hydrophobic interactions (Hans *et al.*, 2005). The role of electrostatic interactions between opposite charges of PkDBPαII and DARC may play a role in the PkDBPαII-DARC interaction.

Unexpectedly, the EBAs with macaque erythrocytes showed no difference in the binding activity. The binding activity level of PkDBPαII with macaque erythrocytes was similar for Peninsular Malaysia and Malaysian Borneo haplotypes. The reason for this is unclear, but it may be plausible that the essential amino acid residues for interaction with macaque erythrocyte receptor are different from those of human erythrocytes. Thus, the non-synonymous mutations in PkDBPαII of either Peninsular Malaysia or Malaysian Borneo haplotypes have no effect on the binding activity level of the protein to macaque erythrocytes. Furthermore, the invasion of *P. knowlesi* into macaque erythrocytes not only relies on PkDBPαII but also on PkβII and PkγII via alternative Duffy-independent pathways (Chitnis & Miller, 1994).

The PkDBPαII plays a vital role in the invasion of parasites by mediating interaction with its corresponding receptor, the Duffy determinant (Fy^a or Fy^b) on the surface of human erythrocytes. *In vitro* and *in vivo* studies have shown that erythrocytes negative for these determinants were refractory to invasion by *P. knowlesi* and *P. vivax* (Miller *et al.*, 1975; Miller *et al.*, 1976; Barnwell *et al.*, 1989). *Plasmodium knowlesi* merozoites require the interaction between PkDBPαII with Duffy determinant Fy^a or Fy^b for binding to human erythrocytes. Thus, by blocking these determinants, it would inhibit the binding. This inhibition was observed in the present EBA experiment using anti-Fy6 treatment. The anti-Fy6 monoclonal antibody (mAb) was used to hinder the Fy^a determinant on Duffy-positive Fy(a+b–) human erythrocytes. The Fy6 epitope is located at the N-terminal extracellular domain of DARC in close proximity to the Fy^a/Fy^b determinant (Meny, 2010; Smolarek *et al.*, 2015). A previous study has shown that incubation with anti-Fy6 resulted in full inhibition of binding activity and invasion by *P. knowlesi* into

human erythrocytes (Amir *et al.*, 2016). The inability of PkDBPαII of Peninsular Malaysia and Malaysian Borneo to bind to anti-Fy6 treated human erythrocytes confirmed that the expressed PkDBPαII bound to the DARC of human erythrocytes and not to other available receptors such as sialic acids (Haynes *et al.*, 1988; Dankwa *et al.*, 2016).

In the present study, treatment of macaque erythrocyte with anti-Fy6 did not affect its binding with PkDBPαII. The Fy6 epitope is present on all human erythrocytes except those with Duffy-negative Fy(a–b–) phenotype. In contrast, the Fy6 epitope is present only in erythrocytes of some non-human primate species such as the Great Apes and New World monkeys. *Macaca fascicularis* erythrocytes are Fy^b but devoid of the Fy6 epitope (Nichols *et al.*, 1987). Hence, the inability of anti-Fy6 to hinder interaction of PkDBPαII with *M. fascicularis* erythrocytes was due to the absence of the Fy6 epitope. With the Fy^b determinant on erythrocytes remain exposed, the binding of PkDBPαII with treated *M. fascicularis* erythrocytes occurred successfully. This finding is in agreement with a previous study that postulated alternative determinants on macaque erythrocytes for binding (Nichols *et al.*, 1987). It appears that the PkDBPαII binds differently to human and macaque erythrocytes corresponding to the distribution of Duffy determinants. Furthermore, the presence of different Fy^a/Fy^b antigens in the human and macaque erythrocytes may also be the reason for this. *In vitro* invasion studies using human erythrocytes have shown increased efficiency of *P. knowlesi* to invade erythrocytes expressing Fy^b compared with those expressing Fy^a (Mason *et al.*, 1977). In addition, erythrocytes expressing Fy^b were shown to have higher binding to PvDBPII and associated with increased susceptibility to *P. vivax* infection (King *et al.*, 2011).

5.2 Binding affinity of PkDBPαII

5.2.1 Selection of pET30a(+) vector as expression vector

The pBR322 derived expression vector pET30a(+) vector was chosen for the present study. The *PkDBPαII* gene was cloned into the multiple cloning sites (MCS) of pET30a(+) plasmid carrying T7 promoter, N-terminal His•Tag® and kanamycin (*kan*) resistance coding sequence (Appendix F). The pET30a(+) expression vector is designed for regulated expression of recombinant proteins in *E. coli* with T7 promoter. IPTG is used to induce the expression of T7 RNA polymerase which specifically recognizes T7 promoter, and in turn activates the transcription. The basal expression of recombinant proteins can be influenced by the IPTG concentration. N-terminal His•Tag® in this vector is designed for affinity protein purification by immobilized metal affinity chromatography with resin, and for detection in Western blot by Novagen® His•Tag® monoclonal antibody. In addition to that, this vector also contains kanamycin (*kan*) resistance gene for selection of recombinant clones.

In the present study, *PkDBPαII* gene (~ 1011 bp) of *P. knowlesi* clinical isolates from Peninsular Malaysia and Malaysian Borneo was amplified and cloned into pGEM®-T vector. The resulting recombinant plasmids of pGEM-T-*PkDBPαII* were extracted and sequenced. These plasmids were digested with *Bam*HI-HF and cloned into the pET30a(+) vector. Recombinant plasmids pET30a(+)-*PkDBPαII* were then transformed into the expression host *E. coli* T7 Express *lysY/I*^{q} cells. The expressed recombinant PkDBPαII proteins were purified, dialyzed and concentrated prior to analysis in the ITC system.

5.2.2 Selection of *E. coli* T7 Express *lysY/I*^{q} as expression host

Generally, *E. coli* strains encoding the T7 RNA polymerase gene are useful for robust over-expression of recombinant proteins. However, the *E. coli* T7 Express *lysY/I*^{q} strain is a unique BL21 derivative carrying T7 lysozyme (*lysY)* and *lacI*^{q} genes that enables the expression of potentially toxic or difficult proteins. In the absence of IPTG, the T7 RNA

polymerase activity is inhibited by T7 lysozyme which in turn eliminated basal level expression of the gene of interest. In addition to that, leaky expression of recombinant protein is also controlled with *lacI*^{q} which enables the potentially toxic gene to be cloned (Studier, 1991).

In this study, recombinant gene expression at different incubation temperature, incubation duration and amount of IPTG were investigated. Optimum expression of recombinant PkDBPαII was achieved at 37 °C with 1 mM IPTG for 6 h. The recombinant PkDBPαII of ~ 45 kDa was detected on SDS-PAGE and Western Blot analyses.

5.2.3 Purification of recombinant PkDBPαII

The purification of His-tagged (6× histidine residues) recombinant PkDBPαII was performed using immobilized metal affinity chromatography. Ni-NTA agarose resin used in the purification column has a strong affinity towards the His-tagged proteins. Recombinant PkDBPαII proteins with the 6× histidine residues were bound to the Ni-NTA agarose resin and eluted by competitive imidazole present in the elution buffer. Purification was carried out under hybrid condition, where the recombinant protein was extracted in denaturing condition and renatured using native elution buffers to preserve the protein structure and activity (Berg *et al*., 2002). The purified recombinant PkDBPαII was detected in both SDS-PAGE and Western Blot assays, however, traces of impurities were also observed. This phenomenon is very common in single-step Ni-NTA purification system, as it is possible that the other unwanted proteins with a certain number of histidine residues capable of binding to the Ni resin non-specifically and hence are eluted together with the desired protein (Bornhorst & Falke, 2011; Kimple *et al*., 2013). Thus, an additional purification step after using Ni-NTA is usually required to obtain higher purity. In addition to that, another possible reason for that may be due to the degradation of the recombinant PkDBPαII by the endogenous proteases of the *E. coli* host resulted in truncated recombinant PkDBPαII (Ryan & Henehan, 2013). Nonetheless,

through dialysis with appropriate buffers, these unwanted low molecular weight impurities can be reduced while allowing the protein to refold optimally. Dialysis was performed using Slide-A-Lyzer™ G2 Dialysis Cassette (10K MWCO). The semi-permeable membrane of the dialysis cassette was made of low-binding regenerated cellulose that allowed diffusion of small molecules from an area of high concentration to low concentration until an equilibrium was reached. Finally, the dialyzed protein was concentrated using Vivaspin® 20 centrifugal concentrator prior to ITC experiment.

5.2.4 Binding affinity measurement by Isothermal Titration Calorimetry (ITC)

ITC is a technique used in quantitative studies and well known for its sensitivity and accuracy in measuring binding affinity between interacting molecules (Velazquez-Campoy *et al.*, 2015; Fan *et al.*, 2017). ITC measures the heat released or absorbed during molecular binding events as a result of the concomitant formation of non-covalent bonds of the interacting molecules. The ITC microcalorimeter system (MicroCal^{TM}) captures the heat changes by detecting the differential power applied to the cell heaters which are required to maintain zero temperature difference between the reference and sample cells as the binding partners are mixed. Pure samples are required because contaminants may interact and release or absorb heat. Hence, purified PkDBPαII is used in the ITC assays. In addition to that, dilution and dialysis buffers used for the ligand protein and its binding partner must be the same, so that the pH and solute content are constant. Buffer mismatch may significantly cause unwanted heat signals, thus resulting in inaccurate measurement (Rajarathnam & Rosgen, 2014). In this study, PBS was chosen as dilution buffer for human erythrocytes and dialysis buffer for purified recombinant PkDBPαII.

Binding affinity is usually indicated by the equilibrium dissociation constant (K_D). The lower the K_D value, the greater the binding affinity of the ligand for its target. From the ITC experiment, the PkDBPαII haplotype of Peninsular Malaysia (K_D = 7.75 μM) have

higher affinity towards human erythrocytes as compared to Malaysian Borneo PkDBPαII (K_D = 74.1 µM), which is in agreement with the EBA findings.

Studies on the binding affinity of PvDBPII-DARC interaction using Surface Plasmon Resonance (SPR) and ITC reported K_D of 8.7 nM and 2.2 µM, respectively (Hans *et al.*, 2005; Batchelor *et al.*, 2014). This discrepancy is mainly due to different approaches or technologies were used to investigate the binding constant of PvDBPII-DARC interaction. In the present study, the binding constant of the PkDBPαII-erythrocyte interaction measured by ITC approach is consistent with previous finding, where the negative control sample (PBS-erythrocytes) showed insignificant K_D of 5.4×10^9 µM. Thus, ITC is an appropriate instrument to determine which PkDBPαII haplotype have a higher binding affinity towards human erythrocytes.

ITC is commonly used to study interaction of biological macromolecules involving protein-protein, protein-DNA, and antibody-antigen, hormone-receptor (Pierce *et al.*, 1999). The ITC in this study is the first report of successful measuring of binding affinity of protein ligand (PkDBPαII) with the whole cell (erythrocytes). Further improvements are necessary to enhance its reliability and feasibility for measuring binding strength of other important invasive ligands. When ITC experiments are optimized, useful binding parameters such as stoichiometry (n), enthalpy (ΔH), entropy (ΔS) and binding constant (K_D) are obtained (Duff *et al.*, 2011). These could be achieved by running additional experiments using different concentration of ligands and receptors, buffer concentrations or temperature conditions (Freyer & Lewis, 2008).

An advantage of ITC is that it does not require immobilization of interacting molecules on a sensor chip nor the use of fluorescence labels as required in other interaction-measuring technology such as SPR and spectroscopic assays. ITC is a relatively straightforward, reliable, sensitive and label-free assay that allows the binding affinity of binding partners to be measured in their native states.

CHAPTER 6: CONCLUSION

The present study is the first report of phenotypic difference between PkDBPαII haplotypes in Malaysia. The PkDBPαII haplotypes were successfully cloned and expressed on COS-7 cell surface. The direct visualization of chimeric PkDBPαII-AcGFP1 was achieved using inverted fluorescence microscope. In the EBAs, the PkDBPαII of Peninsular Malaysia showed higher binding activity level with Duffy-positive Fy(a+b–) human erythrocytes compared to that of Malaysian Borneo PkDBPαII. Evaluation with anti-Fy6 mAb showed that the PkDBPαII bound specifically to human DARC. In addition, PkDBPαII of Peninsular Malaysia and Malaysian Borneo showed higher binding activity to macaque erythrocytes compared to human erythrocytes. Similarly, in the ITC assay, higher affinity towards human erythrocytes was observed using PkDBPαII of Peninsular Malaysia compared to Malaysian Borneo PkDBPαII.

Clinical and epidemiological findings revealed high number of severe knowlesi malaria in Malaysian Borneo. Results from this study found lower binding activity level of the Malaysian Borneo PkDBPαII haplotype compared to that of Peninsular Malaysia. The biological implication of this finding is yet to be determined. Therefore, further studies need to be carried out to determine whether this differential binding level is associated with severity of knowlesi malaria in human. It has been postulated that enhanced virulence and multiplication rates of *Plasmodium* parasites may related to genetic polymorphisms that improve binding ability of the parasites to human erythrocytes. A study has reported that *P. knowlesi* normocyte binding protein (PkNBPXa) polymorphisms are important determinants of high parasitemia and disease severity in *P. knowlesi* infection (Ahmed *et al.*, 2014). Furthermore, it has been demonstrated that PkNBPXa is required for invasion of human erythrocytes, and its role is believed to occur after initial merozoite attachment (Moon *et al.*, 2016). Aside from the

parasite's invasive mechanism, the role of Fy^a/Fy^b polymorphisms in human DARC should be taken into consideration, as it has been shown to be associated with susceptibility to *P. vivax* malaria. The binding preference of the parasite's ligand to a particular human Duffy phenotype may also be one of the important factors for increased susceptibility to *P. knowlesi* infection. Nevertheless, further research needs to be conducted to determine whether there is an interaction between PkDBPαII and PkNBPXa in the invasion process, the binding preference of PkDBPαII to particular Duffy phenotype, and polymorphism of PkDBPαII in part contributes to disease severity.

REFERENCES

Abeyasinghe, R. (2017, Mar). *Outcomes from the Evidence Review Group on Plasmodium knowlesi*. Paper presented at the Malaria Policy Advisory Committee, Geneva, Switzerland.

Adams, J. H., Hudson, D. E., Torii, M., Ward, G. E., Wellems, T. E., Aikawa, M., & Miller, L. H. (1990). The Duffy receptor family of *Plasmodium knowlesi* is located within the micronemes of invasive malaria merozoites. *Cell, 63*(1), 141-153.

Adams, J. H., Sim, B. K., Dolan, S. A., Fang, X., Kaslow, D. C., & Miller, L. H. (1992). A family of erythrocyte binding proteins of malaria parasites. *Proceedings of the National Academy of Sciences of the United States of America, 89*(15), 7085-7089.

Ahmed, A. M., Pinheiro, M. M., Divis, P. C., Siner, A., Zainudin, R., Wong, I. T., . . . Cox-Singh, J. (2014). Disease progression in *Plasmodium knowlesi* malaria is linked to variation in invasion gene family members. *PLOS Neglected Tropical Diseases, 8*(8), e3086.

Aikawa, M., Miller, L. H., Johnson, J., & Rabbege, J. (1978). Erythrocyte entry by malarial parasites. A moving junction between erythrocyte and parasite. *Journal of Cell Biology, 77*(1), 72-82.

Amir, A., Russell, B., Liew, J. W., Moon, R. W., Fong, M. Y., Vythilingam, I., . . . Lau, Y. L. (2016). Invasion characteristics of a *Plasmodium knowlesi* line newly isolated from a human. *Scientific Reports, 6*, 24623.

Aruffo, A. (2001). Transient expression of proteins using COS cells. *Current Protocols in Neuroscience, 2*, 1-4.

Barber, B. E., Rajahram, G. S., Grigg, M. J., William, T., & Anstey, N. M. (2017). World Malaria Report: time to acknowledge *Plasmodium knowlesi* malaria. *Malaria Journal, 16*, 135.

Barber, B. E., William, T., Dhararaj, P., Anderios, F., Grigg, M. J., Yeo, T. W., & Anstey, N. M. (2012). Epidemiology of *Plasmodium knowlesi* malaria in north-east Sabah, Malaysia: family clusters and wide age distribution. *Malaria Journal, 11*, 401.

Barber, B. E., William, T., Grigg, M. J., Menon, J., Auburn, S., Marfurt, J., . . . Yeo, T. W. (2013a). A prospective comparative study of knowlesi, falciparum, and vivax malaria in Sabah, Malaysia: high proportion with severe disease from *Plasmodium knowlesi* and *Plasmodium vivax* but no mortality with early referral and artesunate therapy. *Clinical Infectious Diseases, 56*(3), 383-397.

Barber, B. E., William, T., Grigg, M. J., Yeo, T. W., & Anstey, N. M. (2013b). Limitations of microscopy to differentiate *Plasmodium species* in a region co-endemic for *Plasmodium falciparum*, *Plasmodium vivax* and *Plasmodium knowlesi*. *Malaria Journal, 12*, 8.

Barber, B. E., William, T., Jikal, M., Jilip, J., Dhararaj, P., Menon, J., . . . Anstey, N. M. (2011). *Plasmodium knowlesi* malaria in children. *Emerging Infectious Diseases, 17*(5), 814-820.

Barnwell, J. W., Nichols, M. E., & Rubinstein, P. (1989). In vitro evaluation of the role of the Duffy blood group in erythrocyte invasion by *Plasmodium vivax*. *Journal of Experimental Medicine, 169*(5), 1795-1802.

Batchelor, J. D., Malpede, B. M., Omattage, N. S., DeKoster, G. T., Henzler-Wildman, K. A., & Tolia, N. H. (2014). Red blood cell invasion by *Plasmodium vivax*: structural basis for DBP engagement of DARC. *PLOS Pathogens, 10*(1), 1003869.

Beeson, J. G., & Crabb, B. S. (2007). Towards a vaccine against *Plasmodium vivax* malaria. *PLOS Medicine, 4*(12), 350.

Berg J. M., Tymoczko J. L., Stryer, L. (2002). *Biochemistry: the purification of proteins is an essential first step in understanding their function.* New York, U.S.A.: W. H. Freeman.

Blancher, A., Klein, J., & Socha, W. (1997). *Molecular biology and evolution of blood group and MHC antigens in primates*. Berlin, Germany: Springer Science & Business Media.

Bornhorst, J. A., & Falke, J. B. (2000). Purification of proteins using polyhistidine affinity tags. *Methods in Enzymology, 326*, 245-254.

Boström, S., Giusti, P., Arama, C., Persson, J. O., Dara, V., Traore, B., . . . Troye-Blomberg, M. (2012). Changes in the levels of cytokines, chemokines and malaria-specific antibodies in response to *Plasmodium falciparum* infection in children living in sympatry in Mali. *Malaria Journal, 11*, 109.

Bronner, U., Divis, P. C. S., Farnert, A., & Singh, B. (2009). Swedish traveller with *Plasmodium knowlesi* malaria after visiting Malaysian Borneo. *Malaria Journal, 8*, 15.

Chaudhuri, A., Nielsen, S., Elkjaer, M. L., Zbrzezna, V., Fang, F., & Pogo, A. O. (1997). Detection of Duffy antigen in the plasma membranes and caveolae of vascular endothelial and epithelial cells of nonerythroid organs. *Blood, 89*(2), 701-712.

Chaudhuri, A., Polyakova, J., Zbrzezna, V., & Pogo, A. (1995). The coding sequence of Duffy blood group gene in humans and simians: restriction fragment length polymorphism, antibody and malarial parasite specificities, and expression in nonerythroid tissues in Duffy-negative individuals. *Blood, 85*(3), 615-621.

Chaudhuri, A., Polyakova, J., Zbrzezna, V., Williams, K., Gulati, S., & Pogo, A. O. (1993). Cloning of glycoprotein D cDNA, which encodes the major subunit of the Duffy blood group system and the receptor for the *Plasmodium vivax* malaria parasite. *Proceedings of the National Academy of Sciences, 90*(22), 10793-10797.

Chaudhuri, A., Zbrzezna, V., Johnson, C., Nichols, M., Rubinstein, P., Marsh, W. L., & Pogo, A. O. (1989). Purification and characterization of an erythrocyte membrane protein complex carrying Duffy blood group antigenicity. Possible receptor for *Plasmodium vivax* and *Plasmodium knowlesi* malaria parasite. *Journal of Biological Chemistry, 264*(23), 13770-13774.

Cheng, Y., Lu, F., Wang, B., Li, J., Han, J. H., Ito, D., . . . Han, E. T. (2016). *Plasmodium vivax* GPI-anchored micronemal antigen (PvGAMA) binds human erythrocytes independent of Duffy antigen status. *Scientific Reports, 6*, 35581.

Cheng, Y., Wang, Y., Ito, D., Kong, D. H., Ha, K. S., Chen, J. H., . . . Han, E. T. (2013). The *Plasmodium vivax* merozoite surface protein 1 paralog is a novel erythrocyte-binding ligand of *Plasmodium vivax*. *Infection and Immunity, 81*(5), 1585-1595.

Chin, W., Contacos, P. G., Coatney, G. R., & Kimball, H. R. (1965). A naturally acquired quotidian-type malaria in man transferable to monkeys. *Science, 149*(3686), 865-865.

Chitnis, C. E., Chaudhuri, A., Horuk, R., Pogo, A. O., & Miller, L. H. (1996). The domain on the Duffy blood group antigen for binding *Plasmodium vivax* and *Plasmodium knowlesi* malarial parasites to erythrocytes. *Journal of Experimental Medicine, 184*(4), 1531-1536.

Chitnis, C. E., & Miller, L. H. (1994). Identification of the erythrocyte binding domains of *Plasmodium vivax* and *Plasmodium knowlesi* proteins involved in erythrocyte invasion. *Journal of Experimental Medicine, 180*(2), 497-506.

Choe, H., Moore, M. J., Owens, C. M., Wright, P. L., Vasilieva, N., Li, W., . . . Farzan, M. (2005). Sulphated tyrosines mediate association of chemokines and *Plasmodium vivax* Duffy binding protein with the Duffy antigen/receptor for chemokines (DARC). *Molecular Microbiology, 55*(5), 1413-1422.

Chootong, P., McHenry, A. M., Ntumngia, F. B., Sattabongkot, J., & Adams, J. H. (2014). The association of Duffy binding protein region II polymorphisms and its antigenicity in *Plasmodium vivax* isolates from Thailand. *International Journal for Parasitology, 63*(6), 858-864.

Chown, B., Lewis, M., & Kaita, H. (1965). The Duffy Blood Group System in Caucasians: Evidence for a new allele. *American Journal of Human Genetics, 17*, 384-389.

Coatney, G. R., Collins, W. E., Warren, M., & Contacos, P. G. (1971). *The primate malarias*. Bethesda, U.S.A.: U.S. Department of Health, Education and Welfare, National Institutes of Health.

Coatney, G. R., Collins, W. E., Warren, M., & Contacos, P. G. (2003). The primate malarias *Division of Parasitic Disease, producers*. Atlanta, GA, U.S.A.: CDC.

Cowman, A. F., Berry, D., & Baum, J. (2012). The cellular and molecular basis for malaria parasite invasion of the human red blood cell. *Journal of Cell Biology, 198*(6), 961-971.

Cowman, A. F., & Crabb, B. S. (2006). Invasion of red blood cells by malaria parasites. *Cell, 124*(4), 755-766.

Cox-Singh, J., Davis, T. M., Lee, K. S., Shamsul, S. S., Matusop, A., Ratnam, S., . . . Singh, B. (2008). *Plasmodium knowlesi* malaria in humans is widely distributed and potentially life threatening. *Clinical Infectious Diseases, 46*(2), 165-171.

Cox-Singh, J., Hiu, J., Lucas, S. B., Divis, P. C., Zulkarnaen, M., Chandran, P., . . . Krishna, S. (2010). Severe malaria - a case of fatal *Plasmodium knowlesi* infection with post-mortem findings: a case report. *Malaria Journal, 9*, 10.

Cox-Singh, J., & Singh, B. (2008). Knowlesi malaria: newly emergent and of public health importance? *Trends in Parasitology, 24*(9), 406-410.

Cutbush, M., & Mollison, P. L. (1950). The Duffy blood group system. *Heredity, 4*(3), 383-389.

Cutbush, M., Mollison, P. L., & Parkin, D. M. (1950). A new human blood group. *Nature, 165*(4188), 188-189.

Daneshvar, C., Davis, T. M., Cox-Singh, J., Rafa'ee, M. Z., Zakaria, S. K., Divis, P. C., & Singh, B. (2009). Clinical and laboratory features of human *Plasmodium knowlesi* infection. *Clinical Infectious Diseases, 49*(6), 852-860.

Daniels, R. F., Deme, A. B., Gomis, J. F., Dieye, B., Durfee, K., Thwing, J. I., . . . Ndiaye, D. (2017). Evidence of non-*Plasmodium falciparum* malaria infection in Kédougou, Sénégal. *Malaria Journal, 16*, 9.

Dankwa, S., Lim, C., Bei, A. K., Jiang, R. H. Y., Abshire, J. R., Patel, S. D., . . . Duraisingh, M. T. (2016). Ancient human sialic acid variant restricts an emerging zoonotic malaria parasite. *Nature Communications, 7*, 11187.

Donahue, R. P., Bias, W. B., Renwick, J. H., & McKusick, V. A. (1968). Probable assignment of the Duffy blood group locus to chromosome 1 in man. *Proceedings of the National Academy of Sciences of the United States of America, 61*(3), 949-955.

Duff, M. R., Grubbs, J., & Howell, E. E. (2011). Isothermal Titration Calorimetry for measuring macromolecule-ligand affinity. *Journal of Visualized Experiments* (55), 2976.

Dvorak, J. A., Miller, L. H., Whitehouse, W. C., & Shiroishi, T. (1975). Invasion of erythrocytes by malaria merozoites. *Science, 187*(4178), 748-750.

Eede, P. V. D., Van, H. N., Van Overmeir, C., Vythilingam, I., Duc, T. N., Hung, L. X., . . . Erhart, A. (2009). Human *Plasmodium knowlesi* infections in young children in central Vietnam. *Malaria Journal, 8*, 249.

Fan, L., Xie, P. J., Wang, Y., Huang, Z., & Zhou, J. (2017). Biosurfactant-Protein interaction: Influences of mannosylerythritol lipids-A on beta-glucosidase. *Journal of Agricultural and Food Chemistry, 66*(1), 238-246.

Fatih, F. A., Siner, A., Ahmed, A., Woon, L. C., Craig, A. G., Singh, B., . . . Cox-Singh, J. (2012). Cytoadherence and virulence - the case of *Plasmodium knowlesi* malaria. *Malaria Journal, 11*, 33.

Figtree, M., Lee, R., Bain, L., Kennedy, T., Mackertich, S., Urban, M., . . . Hudson, B. J. (2010). *Plasmodium knowlesi* in human, Indonesian Borneo. *Emerging Infectious Diseases, 16*(4), 672-674.

Fong, M. Y., Lau, Y. L., Chang, P. Y., & Anthony, C. N. (2014). Genetic diversity, haplotypes and allele groups of Duffy binding protein (PkDBPαII) of *Plasmodium knowlesi* clinical isolates from Peninsular Malaysia. *Parasites & Vectors, 7*, 161.

Fong, M. Y., Rashdi, S. A., Yusof, R., & Lau, Y. L. (2015). Distinct genetic difference between the Duffy binding protein (PkDBPαII) of *Plasmodium knowlesi* clinical isolates from North Borneo and Peninsular Malaysia. *Malaria journal, 14*, 91.

Fong, Y. L., Cadigan, F. C., & Coatney, G. R. (1971). A presumptive case of naturally occurring *Plasmodium knowlesi* malaria in man in Malaysia. *Transactions of the Royal Society of Tropical Medicine and Hygiene, 65*(6), 839-840.

Freyer, M. W., & Lewis, E. A. (2008). Isothermal Titration Calorimetry: experimental design, data analysis, and probing macromolecule/ligand binding and kinetic interactions. *Methods in Cell Biology, 84*, 79-113.

Galinski, M. R., & Barnwell, J. W. (2009). Monkey malaria kills four humans. *Trends in Parasitology, 25*(5), 200-204.

Galinski, M. R., Medina, C. C., Ingravallo, P., & Barnwell, J. W. (1992). A reticulocyte-binding protein complex of *Plasmodium vivax* merozoites. *Cell, 69*(7), 1213-1226.

Garnham, P. C. C. (1966). Malaria parasites and other Haemosporidia. *Science, 157*(3792), 1029.

Gassner, C., Kraus, R. L., Dovc, T., Kilga-Nogler, S., Utz, I., Mueller, T. H., . . . Schoenitzer, D. (2000). *Fyx* is associated with two missense point mutations in its gene and can be detected by PCR-SSP. *Immunohematology, 16*(2), 61-67.

Gaur, D., Mayer, D. C., & Miller, L. H. (2004). Parasite ligand-host receptor interactions during invasion of erythrocytes by *Plasmodium* merozoites. *International Journal for Parasitology, 34*(13-14), 1413-1429.

Gunalan, K., Gao, X., Yap, S. S., Huang, X., & Preiser, P. R. (2013). The role of the reticulocyte-binding-like protein homologues of *Plasmodium* in erythrocyte sensing and invasion. *Cell Microbiology, 15*(1), 35-44.

Hadley, T. J., David, P. H., McGinniss, M. H., & Miller, L. H. (1984). Identification of an erythrocyte component carrying the Duffy blood group Fy^a antigen. *Science, 223*(4636), 597-599.

Hadley, T. J., Lu, Z. H., Wasniowska, K., Martin, A. W., Peiper, S. C., Hesselgesser, J., & Horuk, R. (1994). Postcapillary venule endothelial cells in kidney express a multispecific chemokine receptor that is structurally and functionally identical to the erythroid isoform, which is the Duffy blood group antigen. *Journal of Clinical Investigation, 94*(3), 985-991.

Hadley, T. J., & Peiper, S. C. (1997). From malaria to chemokine receptor: the emerging physiologic role of the Duffy blood group antigen. *Blood, 89*(9), 3077-3091.

Hans, D., Pattnaik, P., Bhattacharyya, A., Shakri, A. R., Yazdani, S. S., Sharma, M., . . . Chitnis, C. E. (2005). Mapping binding residues in the *Plasmodium vivax* domain that binds Duffy antigen during red cell invasion. *Molecular Microbiology, 55*(5), 1423-1434.

Hay, S. I., Guerra, C. A., Tatem, A. J., Noor, A. M., & Snow, R. W. (2004). The global distribution and population at risk of malaria: past, present, and future. *The Lancet Infectious Diseases, 4*(6), 327-336.

Haynes, J. D., Dalton, J. P., Klotz, F. W., McGinniss, M. H., Hadley, T. J., Hudson, D. E., & Miller, L. H. (1988). Receptor-like specificity of a *Plasmodium knowlesi* malarial protein that binds to Duffy antigen ligands on erythrocytes. *Journal of Experimental Medicine, 167*(6), 1873-1881.

Hegner, R. (1938). Relative frequency of ring-stage *Plasmodia* in reticulocytes and mature erythrocytes in man and monkey. *American Journal of Epidemiology, 27*(3), 690-718.

Horuk, R., Martin, A., Hesselgesser, J., Hadley, T., Lu, Z. H., Wang, Z. X., & Peiper, S. C. (1996). The Duffy antigen receptor for chemokines: structural analysis and expression in the brain. *Journal of Leukocyte Biology, 59*(1), 29-38.

Ikin, E. W., Mourant, A. E., Pettenkofer, H. J., & Blumenthal, G. (1951). Discovery of the expected haemagglutinin, anti-Fyb. *Nature, 168*(4288), 1077-1078.

Iwamoto, S., Li, J., Sugimoto, N., Okuda, H., & Kajii, E. (1996). Characterization of the Duffy gene promoter: evidence for tissue-specific abolishment of expression in Fy(a–b–) of black individuals. *Biochemical and Biophysical Research Communications, 222*(3), 852-859.

Jeremiah, S., Janagond, A. B., & Parija, S. C. (2014). Challenges in diagnosis of *Plasmodium knowlesi* infections. *Tropical Parasitology, 4*(1), 25-30.

Jeslyn, W. P., Huat, T. C., Vernon, L., Irene, L. M., Sung, L. K., Jarrod, L. P., . . . Ching, N. L. (2011). Molecular epidemiological investigation of *Plasmodium knowlesi* in humans and macaques in Singapore. *Vector-Borne and Zoonotic Diseases, 11*(2), 131-135.

Jiang, N., Chang, Q., Sun, X., Lu, H., Yin, J., Zhang, Z., . . . Chen, Q. (2010). Co-infections with *Plasmodium knowlesi* and other malaria parasites, Myanmar. *Emerging Infectious Diseases, 16*(9), 1476-1478.

Jongwutiwes, S., Buppan, P., Kosuvin, R., Seethamchai, S., Pattanawong, U., Sirichaisinthop, J., & Putaporntip, C. (2011). *Plasmodium knowlesi* Malaria in humans and macaques, Thailand. *Emerging Infectious Diseases, 17*(10), 1799-1806.

Jongwutiwes, S., Putaporntip, C., Iwasaki, T., Sata, T., & Kanbara, H. (2004). Naturally acquired *Plasmodium knowlesi* malaria in human, Thailand. *Emerging Infectious Diseases, 10*(12), 2211-2213.

Kain, K. C., Harrington, M. A., Tennyson, S., & Keystone, J. S. (1998). Imported malaria: prospective analysis of problems in diagnosis and management. *Clinical Infectious Diseases, 27*(1), 142-149.

Kasehagen, L. J., Mueller, I., Kiniboro, B., Bockarie, M. J., Reeder, J. C., Kazura, J. W., . . . Zimmerman, P. A. (2007). Reduced *Plasmodium vivax* erythrocyte infection in Papua New Guinea Duffy-negative heterozygotes. *PLOS One, 2*(3), 336.

Kawai, S., Hirai, M., Haruki, K., Tanabe, K., & Chigusa, Y. (2009). Cross-reactivity in rapid diagnostic tests between human malaria and zoonotic simian malaria parasite *Plasmodium knowlesi* infections. *International Journal for Parasitology, 58*(3), 300-302.

Keeley, A., & Soldati, D. (2004). The glideosome: a molecular machine powering motility and host-cell invasion by Apicomplexa. *Trends in Cell Biology, 14*(10), 528-532.

Khan, K. H. (2013). Gene expression in mammalian cells and its applications. *Advanced Pharmaceutical Bulletin, 3*(2), 257-263.

Khim, N., Siv, S., Kim, S., Mueller, T., Fleischmann, E., Singh, B., . . . Ménard, D. (2011). *Plasmodium knowlesi* infection in humans, Cambodia, 2007-2010. *Emerging Infectious Diseases, 17*(10), 1900-1902.

Kimple, M., Brill, A., & Pasker, R. (2013). Overview of affinity tags for protein purification. *Current Protocols in Protein Science, 73*(9.9), 1-23.

Kimura, M., Kaneko, O., Liu, Q., Zhou, M., Kawamoto, F., Wataya, Y., . . . Tanabe, K. (1997). Identification of the four species of human malaria parasites by nested PCR that targets variant sequences in the small subunit rRNA gene. *International Journal for Parasitology, 46*(2), 91-95.

King, C. L., Adams, J. H., Xianli, J., Grimberg, B. T., McHenry, A. M., Greenberg, L. J., . . . Zimmerman, P. A. (2011). Fya/Fyb antigen polymorphism in human erythrocyte Duffy antigen affects susceptibility to *Plasmodium vivax* malaria. *Proceedings of the National Academy of Sciences of the United States of America, 108*(50), 20113-20118.

Knowles, R., & Gupta, B. (1932). A study of monkey malaria, and its experimental transmission to man.(A preliminary report.). *Indian Medical Gazette, 67*(6), 301-320.

Kozak, M. (1987). An analysis of 5'-noncoding sequences from 699 vertebrate messenger RNAs. *Nucleic Acids Research, 15*(20), 8125-8148.

Kozlowski, L. P. (2016). IPC – Isoelectric Point Calculator. *Biology Direct, 11*(1), 55.

Lau, Y. L., Lai, M. Y., Fong, M.-Y., Jelip, J., & Mahmud, R. (2016). Loop-mediated isothermal amplification assay for identification of five human *Plasmodium* Species in Malaysia. *American Journal of Tropical Medicine and Hygiene, 94*(2), 336-339.

Laub, O., & Rutter, W. J. (1983). Expression of the human insulin gene and cDNA in a heterologous mammalian system. *Journal of Biological Chemistry, 258*(10), 6043-6050.

Le Van Kim, C., Tournamille, C., Kroviarski, Y., Cartron, J. P., & Colin, Y. (1997). The 1.35-kb and 7.5-kb Duffy mRNA isoforms are differently regulated in various regions of brain, differ by the length of their 5' untranslated sequence, but encode the same polypeptide. *Blood, 90*(7), 2851-2853.

Lee, K. S., Cox-Singh, J., Brooke, G., Matusop, A., & Singh, B. (2009a). *Plasmodium knowlesi* from archival blood films: further evidence that human infections are widely distributed and not newly emergent in Malaysian Borneo. *International Journal for Parasitology, 39*(10), 1125-1128.

Lee, K. S., Cox-Singh, J., & Singh, B. (2009b). Morphological features and differential counts of *Plasmodium knowlesi* parasites in naturally acquired human infections. *Malaria Journal, 8*, 73.

Lee, K. S., Divis, P. C., Zakaria, S. K., Matusop, A., Julin, R. A., Conway, D. J., . . . Singh, B. (2011). *Plasmodium knowlesi*: reservoir hosts and tracking the emergence in humans and macaques. *PLOS Pathogens*, 7(4), 1002015.

Lee, W. C., Chin, P. W., Lau, Y. L., Chin, L. C., Fong, M. Y., Yap, C. J., . . . Mahmud, R. (2013). Hyperparasitaemic human *Plasmodium knowlesi* infection with atypical morphology in peninsular Malaysia. *Malaria Journal, 12*, 88.

Li, J., & Han, E. T. (2012). Dissection of the *Plasmodium vivax* reticulocyte binding-like proteins (PvRBPs). *Biochemical and Biophysical Research Communications, 426*(1), 1-6.

Luchavez, J., Espino, F., Curameng, P., Espina, R., Bell, D., Chiodini, P., . . . Singh, B. (2008). Human Infections with *Plasmodium knowlesi*, the Philippines. *Emerging Infectious Diseases, 14*(5), 811-813.

Marsh, W. L., & Schmidt, P. J. (1975). Present status of the Duffy Blood Group System: articles reviewed. *CRC Critical Reviews in Clinical Laboratory Sciences, 5*(4), 387-412.

Mason, S. J., Miller, L. H., Shiroishi, T., Dvorak, J. A., & McGinniss, M. H. (1977). The Duffy blood group determinants: their role in the susceptibility of human and animal erythrocytes to *Plasmodium knowlesi* malaria. *British Journal of Haematology, 36*(3), 327-335.

McCutchan, T. F., Piper, R. C., & Makler, M. T. (2008). Use of malaria rapid diagnostic test to identify *Plasmodium knowlesi* infection. *Emerging Infectious Diseases, 14*(11), 1750-1752.

Meibalan, E., & Marti, M. (2017). Biology of malaria transmission. *Cold Spring Harbor Perspectives in Medicine, 7*(3), 25452.

Meny, G. M. (2010). The Duffy blood group system: a review. *Immunohematology, 26*(2), 51-56.

Meyer, E. V., Semenya, A. A., Okenu, D. M., Dluzewski, A. R., Bannister, L. H., Barnwell, J. W., & Galinski, M. R. (2009). The reticulocyte binding-like proteins of *Plasmodium knowlesi* locate to the micronemes of merozoites and define two new members of this invasion ligand family. *Molecular and Biochemical Parasitology, 165*(2), 111-121.

Michon, P., Fraser, T., & Adams, J. H. (2000). Naturally acquired and vaccine-elicited antibodies block erythrocyte cytoadherence of the *Plasmodium vivax* Duffy binding protein. *Infection and Immunity, 68*(6), 3164-3171.

Michon, P., Woolley, I., Wood, E. M., Kastens, W., Zimmerman, P. A., & Adams, J. H. (2001). Duffy-null promoter heterozygosity reduces DARC expression and abrogates adhesion of the *Plasmodium vivax* ligand required for blood-stage infection. *Federation of European Biochemical Societies Letters, 495*, 111-114.

Miller, L. H., Baruch, D. I., Marsh, K., & Doumbo, O. K. (2002). The pathogenic basis of malaria. *Nature, 415*(6872), 673-679.

Miller, L. H., Haynes, J. D., McAuliffe, F. M., Shiroishi, T., Durocher, J. R., & McGinniss, M. H. (1977). Evidence for differences in erythrocyte surface receptors for the malarial parasites, *Plasmodium falciparum* and *Plasmodium knowlesi. Journal of Experimental Medicine, 146*(1), 277-281.

Miller, L. H., Mason, S. J., Clyde, D. F., & McGinniss, M. H. (1976). The resistance factor to *Plasmodium vivax* in blacks. The Duffy-blood-group genotype, *FyFy*. *The New England Journal of Medicine, 295*(6), 302-304.

Miller, L. H., Mason, S. J., Dvorak, J. A., McGinniss, M. H., & Rothman, I. K. (1975). Erythrocyte receptors for (*Plasmodium knowlesi*) malaria: Duffy blood group determinants. *Science, 189*(4202), 561-563.

Min, H. M. K., Changrob, S., Soe, P. T., Han, J. H., Muh, F., Lee, S. K., . . . Han, E. T. (2017). Immunogenicity of the *Plasmodium vivax* merozoite surface protein 1 paralog in the induction of naturally acquired antibody and memory B cell responses. *Malaria Journal, 16*, 354.

Mishina, M., Kurosaki, T., Tobimatsu, T., Morimoto, Y., Noda, M., Yamamoto, T., . . . Kuno, M. (1984). Expression of functional acetylcholine receptor from cloned cDNAs. *Nature, 307*(5952), 604-608.

Mohandas, N., & Narla, A. (2005). Blood group antigens in health and disease. *Current Opinion in Hematology, 12*(2), 135-140.

Moon, R. W., Hall, J., Rangkuti, F., Ho, Y. S., Almond, N., Mitchell, G. H., . . . Blackman, M. J. (2013). Adaptation of the genetically tractable malaria pathogen *Plasmodium knowlesi* to continuous culture in human erythrocytes. *Proceedings of the National Academy of Sciences of the United States of America, 110*(2), 531-536.

Moon, R. W., Sharaf, H., Hastings, C. H., Ho, Y. S., Nair, M. B., Rchiad, Z., . . . Holder, A. A. (2016). Normocyte-binding protein required for human erythrocyte invasion by the zoonotic malaria parasite *Plasmodium knowlesi*. *Proceedings of the National Academy of Sciences of the United States of America, 113*(26), 7231-7236.

Napier, L. E., & Campbell, H. (1932). Observations on a *Plasmodium* infection which causes haemoglobinuria in certain species of monkey. *Indian Medical Gazette, 67*(5), 246-249.

Neote, K., Mak, J. Y., Kolakowski, L. F., Jr., & Schall, T. J. (1994). Functional and biochemical analysis of the cloned Duffy antigen: identity with the red blood cell chemokine receptor. *Blood, 84*(1), 44-52.

Ng, O. T., Ooi, E. E., Lee, C. C., Lee, P. J., Ng, L. C., Pei, S. W., . . . Leo, Y. S. (2008). Naturally acquired human *Plasmodium knowlesi* infection, Singapore. *Emerging Infectious Diseases, 14*(5), 814-816.

Nichols, M. E., Rubinstein, P., Barnwell, J., Rodriguez de Cordoba, S., & Rosenfield, R. E. (1987). A new human Duffy blood group specificity defined by a murine monoclonal antibody. Immunogenetics and association with susceptibility to *Plasmodium vivax. Journal of Experimental Medicine, 166*(3), 776-785.

Ntumngia, F. B., Thomson-Luque, R., de Menezes Torres, L., Gunalan, K., Carvalho, L. H., & Adams, J. H. (2016). A novel erythrocyte binding protein of *Plasmodium vivax* suggests an alternate invasion pathway into Duffy-Positive reticulocytes. *American Society for Microbiology, 7*(4), 1261-1216.

Olsson, M. L., Smythe, J. S., Hansson, C., Poole, J., Mallinson, G., Jones, J., . . . Daniels, G. (1998). The Fyx phenotype is associated with a missense mutation in the *Fyb* allele predicting Arg89Cys in the Duffy glycoprotein. *British Journal of Haematology, 103*(4), 1184-1191.

Ooi, C. H., Bujang, M. A., Tg Abu Bakar Sidik, T. M. I., Ngui, R., & Lim, Y. A. (2017). Over two decades of *Plasmodium knowlesi* infections in Sarawak: Trend and forecast. *Acta Tropica, 176*, 83-90.

Parasol, N., Reid, M., Rios, M., Castilho, L., Harari, I., & Kosower, N. S. (1998). A novel mutation in the coding sequence of the *FY*B* allele of the Duffy chemokine receptor gene is associated with an altered erythrocyte phenotype. *Blood, 92*(7), 2237-2243.

Paul, A. S., Egan, E. S., & Duraisingh, M. T. (2015). Host-parasite interactions that guide red blood cell invasion by malaria parasites. *Current Opinion in Hematology, 22*(3), 220-226.

Peiper, S. C., Wang, Z. X., Neote, K., Martin, A. W., Showell, H. J., Conklyn, M. J., . . . Horuk, R. (1995). The Duffy antigen/receptor for chemokines (DARC) is expressed in endothelial cells of Duffy negative individuals who lack the erythrocyte receptor. *Journal of Experimental Medicine, 181*(4), 1311-1317.

Pierce, M. M., Raman, C. S., & Nall, B. T. (1999). Isothermal Titration Calorimetry of protein-protein interactions. *Methods, 19*(2), 213-221.

Race, R. R., & Sanger, R. (1980). Blood Groups in Man. *Immunological Communications, 9*(4), 419-420.

Rahim, M. J. C., Mohammad, N., Besari, A. M., & Ghazali, W. S. W. (2017). Severe *Plasmodium knowlesi* with dengue coinfection. *British Medical Journal Case Reports*. 16(1), 2184.

Rajahram, G. S., Barber, B. E., William, T., Menon, J., Anstey, N. M., & Yeo, T. W. (2012). Deaths due to *Plasmodium knowlesi* malaria in Sabah, Malaysia: association with reporting as *Plasmodium malariae* and delayed parenteral artesunate. *Malaria Journal, 11*(1), 284.

Rajarathnam, K., & Rosgen, J. (2014). Isothermal Titration Calorimetry of membrane proteins - progress and challenges. *Biochimica et Biophysica Acta, 1838*(1), 69-77.

Ranjan, A., & Chitnis, C. E. (1999). Mapping regions containing binding residues within functional domains of *Plasmodium vivax* and *Plasmodium knowlesi* erythrocyte-binding proteins. *Proceedings of the National Academy of Sciences of United States of America, 96*(24), 14067-14072.

Riwom, S., Janvier, D., Navenot, J. M., Benbunan, M., Muller, J. Y., & Blanchard, D. (1994). Production of a new murine monoclonal antibody with Fy6 specificity and characterization of the immunopurified N-glycosylated Duffy-active molecule. *Vox Sanguinis, 66*(1), 61-67.

Ryan, B., & Henehan, G. (2013). Overview of approaches to preventing and avoiding proteolysis during expression and purification of proteins. *Current Protocols in Protein Science, 5*(5.25), 1-7.

Schumacher, R. F., & Spinelli, E. (2012). Malaria in children. *Mediterranean Journal of Hematology and Infectious Diseases, 4*(1), 2012073.

Sellami, M. H., Kaabi, H., Midouni, B., Dridi, A., Mojaat, N., Boukef, M. K., & Hmida, S. (2008). Duffy blood group system genotyping in an urban Tunisian population. *Annals of Human Biology, 35*(4), 406-415.

Semenya, A. A., Tran, T. M., Meyer, E. V., Barnwell, J. W., & Galinski, M. R. (2012). Two functional reticulocyte binding-like (RBL) invasion ligands of zoonotic *Plasmodium knowlesi* exhibit differential adhesion to monkey and human erythrocytes. *Malaria Journal, 11*, 228.

Sim, B. K., Chitnis, C. E., Wasniowska, K., Hadley, T. J., & Miller, L. H. (1994). Receptor and ligand domains for invasion of erythrocytes by *Plasmodium falciparum*. *Science, 264*(5167), 1941-1944.

Singh, A. P., Puri, S. K., & Chitnis, C. E. (2002). Antibodies raised against receptor-binding domain of *Plasmodium knowlesi* Duffy binding protein inhibit erythrocyte invasion. *Molecular and Biochemical Parasitology, 121*(1), 21-31.

Singh, B., & Daneshvar, C. (2010). *Plasmodium knowlesi* malaria in Malaysia. *Medical Journal of Malaysia, 65*(3), 166-172.

Singh, B., & Daneshvar, C. (2013). Human infections and detection of *Plasmodium knowlesi*. *Clinical Microbiology Reviews, 26*(2), 165-184.

Singh, B., Kim Sung, L., Matusop, A., Radhakrishnan, A., Shamsul, S. S., Cox-Singh, J., . . . Conway, D. J. (2004). A large focus of naturally acquired *Plasmodium knowlesi* infections in human beings. *Lancet, 363*(9414), 1017-1024.

Singh, S. K., Hora, R., Belrhali, H., Chitnis, C. E., & Sharma, A. (2006). Structural basis for Duffy recognition by the malaria parasite Duffy-binding-like domain. *Nature, 439*(7077), 741-744.

Singh, S. K., Singh, A. P., Pandey, S., Yazdani, S. S., Chitnis, C. E., & Sharma, A. (2003). Definition of structural elements in *Plasmodium vivax* and *Plasmodium knowlesi* Duffy-binding domains necessary for erythrocyte invasion. *Biochemical Journal, 374*(1), 193-198.

Sinton, J. A., & Mulligan, H. W. (1933). A critical review of the literature relating to the identification of the malarial parasites recorded from monkeys of the families *Circopithecidae* and *Colobidae*. *Records of the Malaria Survey of India, 3*(3), 381-444.

Smolarek, D., Hattab, C., Buczkowska, A., Kaczmarek, R., Jarzab, A., Cochet, S., . . . Czerwinski, M. (2015). Studies of a murine monoclonal antibody directed against DARC: reappraisal of its specificity. *PLOS One, 10*(2), 116472.

Snounou, G., Viriyakosol, S., Zhu, X. P., Jarra, W., Pinheiro, L., do Rosario, V., . . . Brown, K. N. (1993). High sensitivity of detection of human malaria parasites by the use of nested polymerase chain reaction. *Molecular and Biochemical Parasitology, 61*(2), 315-320.

Sri, K., Praveen, K. B., Himashu, S. C., Amreen, A., Rajesh, K., Puspendra, P. S., . . . Neeru, S. (2015). Detection of mixed infections with *Plasmodium* spp. by PCR, India, 2014. *Emerging Infectious Diseases, 21*(10), 1853-1857.

Sulistyaningsih, E., Fitri, L. E., Loscher, T., & Berens-Riha, N. (2010). Diagnostic difficulties with *Plasmodium knowlesi* infection in humans. *Emerging Infectious Diseases, 16*(6), 1033-1034.

Sutherland, C. J., Tanomsing, N., Nolder, D., Oguike, M., Jennison, C., Pukrittayakamee, S., . . . Polley, S. D. (2010). Two nonrecombining sympatric forms of the human malaria parasite *Plasmodium ovale* occur globally. *Journal of Infectious Diseases, 201*(10), 1544-1550.

Tanizaki, R., Ujiie, M., Kato, Y., Iwagami, M., Hashimoto, A., Kutsuna, S., . . . Ohmagari, N. (2013). First case of *Plasmodium knowlesi* infection in a Japanese traveller returning from Malaysia. *Malaria Journal, 12*, 128.

Tournamille, C., Colin, Y., Cartron, J. P., & Le Van Kim, C. (1995). Disruption of a GATA motif in the Duffy gene promoter abolishes erythroid gene expression in Duffy-negative individuals. *Nature Genetics, 10*(2), 224-228.

Tournamille, C., Filipe, A., Wasniowska, K., Gane, P., Lisowska, E., Cartron, J. P., . . . Le Van Kim, C. (2003). Structure-function analysis of the extracellular domains of the Duffy antigen/receptor for chemokines: characterization of antibody and chemokine binding sites. *British Journal of Haematology, 122*(6), 1014-1023.

Tournamille, C., Le-Van Kim, C., Gane, P., Le-Pennec, P. Y., Roubinet, F., Babinet, J., . . . Colin, Y. (1998). Arg89Cys substitution results in very low membrane expression of the Duffy antigen/receptor for chemokines in Fyx Individuals. *Blood, 92*(6), 2147-2156.

Van Hellemond, J. J., Rutten, M., Koelewijn, R., Zeeman, A.-M., Verweij, J. J., Wismans, P. J., . . . van Genderen, P. J. J. (2009). Human *Plasmodium knowlesi* infection detected by rapid diagnostic tests for malaria. *Emerging Infectious Diseases, 15*(9), 1478-1480.

Van Rooyen, C., & Pile, G. (1935). Observations on infection by *Plasmodium knowlesi* (ape malaria) in the treatment of general paralysis of the insane. *British Medical Journal, 2*(3901), 662.

VanBuskirk, K. M., Sevova, E., & Adams, J. H. (2004). Conserved residues in the *Plasmodium vivax* Duffy-binding protein ligand domain are critical for erythrocyte receptor recognition. *Proceedings of the National Academy of Sciences of the United States of America, 101*(44), 15754-15759.

Velazquez-Campoy, A., Leavitt, S. A., & Freire, E. (2015). Characterization of protein-protein interactions by Isothermal Titration Calorimetry. *Methods in Molecular Biology, 1278*, 183-204.

Verma, R., Boleti, E., & George, A. J. (1998). Antibody engineering: comparison of bacterial, yeast, insect and mammalian expression systems. *Journal of Immunological Methods, 216*(1-2), 165-181.

Vythilingam, I., Noorazian, Y. M., Huat, T. C., Jiram, A. I., Yusri, Y. M., Azahari, A. H., . . . Lokmanhakim, S. (2008). *Plasmodium knowlesi* in humans, macaques and mosquitoes in peninsular Malaysia. *Parasites & Vectors, 1*, 26.

Wagner-Jauregg, J. (1918). [On the effect of malaria on progressive paralysis] *Psychiatr Neurol Wochenschrift, 20*, 132-134.

Wang, B., Han, S. S., Cho, C., Han, J. H., Cheng, Y., Lee, S. K., . . . Han, E. T. (2014). Comparison of microscopy, nested-PCR, and real-time-PCR assays using high-throughput screening of pooled samples for diagnosis of malaria in asymptomatic carriers from areas of endemicity in Myanmar. *Journal of Clinical Microbiology, 52*(6), 1838-1845.

Warren, T. G., & Shields, D. (1984). Expression of preprosomatostatin in heterologous cells: biosynthesis, posttranslational processing, and secretion of mature somatostatin. *Cell, 39*(3), 547-555.

White, N. J. (2008). *Plasmodium knowlesi*: the fifth human malaria parasite. *Clinical Infectious Diseases, 46*(2), 172-173.

WHO. (2011). *Informal consultation on the public health importance of Plasmodium knowlesi.* Manila, Philippines: World Health Organization Western Pacific Regional Office.

WHO. (2017a). *World Malaria Report 2016*. Geneva, Switzerland: World Health Organization.

WHO. (2017b). *World Malaria Report 2017*. Geneva, Switzerland: World Health Organization.

William, T., Jelip, J., Menon, J., Anderios, F., Mohammad, R., Mohammad, T. A. A., . . . Barber, B. E. (2014). Changing epidemiology of malaria in Sabah, Malaysia: increasing incidence of *Plasmodium knowlesi*. *Malaria Journal, 13*, 390.

William, T., & Menon, J. (2014). A review of malaria research in malaysia. *Medical Journal of Malaysia, 69*, 82-87.

William, T., Menon, J., Rajahram, G., Chan, L., Ma, G., Donaldson, S., . . . Yeo, T. W. (2011). Severe *Plasmodium knowlesi* malaria in a tertiary care hospital, Sabah, Malaysia. *Emerging Infectious Diseases, 17*(7), 1248-1255.

William, T., Rahman, H. A., Jelip, J., Ibrahim, M. Y., Menon, J., Grigg, M. J., . . . Barber, B. E. (2013). Increasing incidence of *Plasmodium knowlesi* malaria following control of *Plasmodium falciparum* and *Plasmodium vivax* Malaria in Sabah, Malaysia. *PLOS Neglected Tropical Diseases, 7*(1), 2026.

Willmann, M., Ahmed, A., Siner, A., Wong, I. T., Woon, L. C., Singh, B., . . . Cox-Singh, J. (2012). Laboratory markers of disease severity in *Plasmodium knowlesi* infection: a case control study. *Malaria Journal, 11*, 363.

Wilson, M. L. (2012). Malaria rapid diagnostic tests. *Clinical Infectious Diseases, 54*(11), 1637-1641.

Yentur, D. N., Yildiz, Z. F., & Seyrek, A. (2016). Detection of *Plasmodium* using filter paper and nested PCR for patients with malaria in Sanliurfa, in Turkey. *Malaria Journal, 15*, 299.

Yusof, R., Lau, Y. L., Mahmud, R., Fong, M. Y., Jelip, J., Ngian, H. U., . . . Ali, M. M. (2014). High proportion of knowlesi malaria in recent malaria cases in Malaysia. *Malaria Journal, 13*, 168.

Zakeri, S., Kakar, Q., Ghasemi, F., Raeisi, A., Butt, W., Safi, N., . . . Djadid, N. D. (2010). Detection of mixed *Plasmodium falciparum* & *Plasmodium vivax* infections by nested-PCR in Pakistan, Iran & Afghanistan. *Indian Journal of Medical Research, 132*, 31-35.

Zhu, H. M., Li, J., & Zheng, H. (2006). [Human natural infection of *Plasmodium knowlesi*]. *Zhongguo Ji Sheng Chong Xue Yu Ji Sheng Chong Bing Za Zhi, 24*, 70-71.

Zimmerman, P. A., Ferreira, M. U., Howes, R. E., & Mercereau-Puijalon, O. (2013). Red blood cell polymorphism and susceptibility to *Plasmodium vivax*. *Advances in Parasitology, 81*, 27-76.

Zimmerman, P. A., Woolley, I., Masinde, G. L., Miller, S. M., McNamara, D. T., Hazlett, F., . . . Kazura, J. W. (1999). Emergence of *FY*A*(null) in a *Plasmodium vivax*-endemic region of Papua New Guinea. *Proceedings of the National Academy of Sciences of the United States of America, 96*(24), 13973-13977.